

# Bias-Variance Tradeoffs in Joint Spectral Embeddings

Benjamin Draves

Daniel Sussman

October 26, 2021

## Abstract

Latent position models and their corresponding estimation procedures offer a statistically principled paradigm for multiple network inference by translating multiple network analysis problems to familiar task in multivariate statistics. Latent position estimation is a fundamental task in this framework yet most work focus only on unbiased estimation procedures. We consider the ramifications of utilizing *biased* latent position estimates in subsequent statistical analysis in exchange for sizable variance reductions in finite networks. We establish an explicit bias-variance tradeoff for latent position estimates produced by the omnibus embedding of Levin et al. (2017) in the presence of heterogeneous network data. We reveal an analytic bias expression, derive a uniform concentration bound on the residual term, and prove a central limit theorem characterizing the distributional properties of these estimates. These explicit bias and variance expressions enable us to show that the omnibus embedding estimates are often preferable to comparable estimators with respect to mean square error, state sufficient conditions for exact recovery in community detection tasks, and develop a test statistic to determine whether two graphs share the same set of latent positions. These results are demonstrated in several experimental settings where community detection algorithms and hypothesis testing procedures utilizing the biased latent position estimates are competitive, and oftentimes preferable, to unbiased latent position estimates.

## 1 Introduction

Multiplex networks describe a set of entities, with multiple types of relationships among them, as a collection of networks over a common vertex set (Kivelä et al. 2014; Battiston, Nicosia, and Latora 2017). There is a growing demand for inferential frameworks for multiplex networks in a diverse variety of fields such as neuroscience (Battiston, Nicosia, Chavez, et al. 2016; De Domenico 2017; Ginestet et al. 2017), transportation systems (Cardillo et al. 2013; Kaluza et al. 2010), and the social sciences (Coscia et al. 2013; Goldblum et al. 2019; Takes et al. 2018; Szell and Thurner 2013; Stella, Beckage, and Brede 2017; Lazega and Snijders 2016). While developing a principled paradigm for random graph inference has been of great interest for individual networks (Kolaczyk 2009; Avanti Athreya et al. 2017), lesser attention has been given to multiplex networks. This data structure offers a more appropriate representation of complex systems by viewing the collection of networks as being drawn from a multivariate network distribution rather than a sample from one network distribution, yet poses novel challenges when developing a formal statistical framework that requires new insights.

Several recent works have focused on extending familiar descriptive statistics such as clustering coefficients (Battiston, Nicosia, and Latora 2014; Cozzo et al. 2015) and node centrality (Tudisco, Arrigo, and Gautier 2017; Taylor, Porter, and Mucha 2019), tools for network visualization (De Domenico, Porter, and Arenas 2014; Fatemi, Salehi, and Magnani 2016), and community detection algorithms (Ma et al. 2018; Hmimida and Kanawati 2015) to multilayer network data. Probabilistic models inspired by individual network models have been proposed in an attempt to capture multilayer network structure (Bianconi 2013; Nicosia and Latora 2015; Murase et al. 2014) and corresponding approaches to estimation and subsequence inference include likelihood approaches, tensor decompositions, and variational methods (Paez, Amini, and Lin 2019; Paul and Chen 2018; Gligorijević, Panagakis, and Zafeiriou 2019). While several of these frameworks are

constructed for general multilayer networks, we restrict our attention to multiplex networks; that is we study collections of node-aligned networks over a common vertex set.

A class of models that have seen success in capturing multiplex network phenomena, such as multilayer and time varying community structure, while remaining analytically tractable are latent position models (LPM) extended to multiplex data (Levin et al. 2017; S. Wang et al. 2017; Nielsen and Witten 2018; Arroyo et al. 2019). LPMs for single networks posit that the vertices are each associated to a point in a low dimensional space (Hoff, Raftery, and Handcock 2002; Young and Scheinerman 2007; Shalizi and Asta 2017; Rubin-Delanchy et al. 2017). One of the most ubiquitous random graph models of this type is the Random Dot Product Graph (RDPG) (Young and Scheinerman 2007). Under this model, each vertex in the network is associated with a *latent position* in a low dimensional Euclidean space and edge connection probabilities are given by the inner product of each vector-pair in this space. Estimates of these vectors, entitled *node embeddings*, are then amenable to statistical analysis using familiar techniques from multivariate statistics and machine learning (Luxburg 2007; Avanti Athreya et al. 2017; Vince Lyzinski et al. 2014). In characterizing the behavior of these estimates, one can derive guarantees on the statistical algorithms that utilize these node representations (Vince Lyzinski et al. 2014; M. Tang et al. 2017; A. Athreya et al. 2016; Levin et al. 2017).

In multiplex networks, we anticipate different layers of the network to share common structure. Recent works on multiplex extensions of the RDPG have incorporated this assumption and have focused on developing consistent estimators for this common structure as well as parameters specific to each layer (Nielsen and Witten 2018; S. Wang et al. 2017; Arroyo et al. 2019). These extensions are amenable to rigorous statistical analysis by studying the latent position estimation schemes. As estimation of the latent positions is a crucial task, the class of proposed estimators should extend beyond consistent estimators. Indeed, a *biased* latent position estimator may be preferable for certain inference tasks for finite networks. Latent position estimators that effectively borrow strength across layers of the multiplex may be biased due to layer specific variation, yet obtain sizable variance reductions by leveraging the common structure shared across layers. Moreover, if this incurred bias highlights an important network feature, the use of these biased latent position estimates may *aid* the performance of subsequent algorithms.

In what follows, we consider the omnibus embedding of Levin et al. (2017) as a method for latent position estimation. The omnibus embedding was proposed for inference under a multiplex network model where each random adjacency matrix is marginally distributed according to a RDPG with the same latent positions. Omnibus embedding estimates are biased for the latent positions in the presence of heterogeneous network data. Yet in Arroyo et al. (2019), empirical studies in the heterogeneous network regime show that community detection and graph classification algorithms that utilize the biased omnibus estimates are competitive and often preferable to algorithms that utilize unbiased estimates.

In this work we look to analytically establish the bias-variance tradeoff of the omnibus embedding estimates when confronted with heterogeneous network data. To that end, we propose the *Eigen-Scaling Random Dot Product Graph* (ESRDPG) as a model that extends the RDPG to multiplex network data. The ESRDPG is similar to models proposed by S. Wang et al. (2017) and Arroyo et al. (2019) and is asymptotically equivalent to the model proposed in Nielsen and Witten (2018). Under the ESRDPG, each vertex is associated with a latent position in a low dimensional Euclidean space where edge connection probabilities vary from graph to graph by altering the inner product between these latent positions. In particular, we consider diagonally weighted inner products of the form  $\mathbf{x}^T \mathbf{C}^{(g)} \mathbf{y}$  for some diagonal matrix  $\mathbf{C}^{(g)}$  that vary by layer. By requiring each vertex has a common latent position across each layer, the ESRDPG is able to capture shared structure across the multiplex network while describing layer specific variation.

In studying the omnibus embedding under the ESRDPG, we are able to extend the analysis completed in Levin et al. (2017) to the heterogeneous network setting. Under the ESRDPG, we provide an analytic expression for the bias in terms of the original latent positions the scaling matrices  $\mathbf{C}^{(g)}$ . In addition, we provide a uniform rate of convergence of the corresponding residual term that decays to zero as the network size increases. To further characterize the distributional properties of these estimates, we establish each embedded point converges in distribution to a mixture of normal distributions centered around this bias term. This bias and distributional result shed light on an implicit and often favorable bias-variance tradeoff

induced by the omnibus embedding for finite heterogeneous networks.

Next, we analyze the impact of the bias-variance tradeoff in subsequent statistical inference tasks such as multiplex community detection and network hypothesis testing. We theoretically and empirically demonstrate that applying common clustering techniques (e.g. k-means clustering, Gaussian Mixture Models) to the estimated latent positions produced by the omnibus embedding is competitive with state of the art methods for multiplex community detection. Moreover, we propose a pivotal test statistic that can be estimated directly from the data that allow for parametric testing procedures to be utilized in multiple network hypothesis testing. We empirically demonstrate that this approach to network hypothesis testing outperforms semi-parametric testing procedures proposed in Levin et al. (2017) that rely on unknown model parameters. These analyses establish that the bias-variance tradeoff induced by the omnibus embedding under the ESRDPG does not harm, and oftentimes aid, in downstream statistical inference.

This paper will be organized as follows. In Section 2, we introduce the ESRDPG model and discuss its properties. In addition, we revisit the omnibus embedding and consider a toy example that highlights the bias-variance tradeoff of various node embeddings. In Section 3, we provide theoretical results that establish the asymptotic bias and distributions of the rows of the omnibus estimator. In Section 4, we analyze the ramifications of these theoretical results on statistical tasks such as latent position estimation, multiplex community detection, and two-graph hypothesis testing, and empirically demonstrate these results in rigorous simulation settings. Finally, in Section 5 we discuss several extensions to the current work.

## 2 Background & the ESRDPG

In this section we review the Random Dot Product Graph (RDPG) for single-layer network data and introduce our extension to multiplex network data, the Eigen-Scaling RDPG (ESRDPG) for modeling heterogeneous network data. Next, we revisit the omnibus embedding as an approach to estimating the parameters of interest under the ESRDPG.

Throughout this work we will let  $n$  denote the number of nodes in the common vertex set,  $m$  denote the number of networks over this vertex set, and  $\mathbb{R}^d$  be the associated latent space of dimension  $d$ . Let  $\mathbf{M}_i$  denote the  $i$ -th row  $\mathbf{M}$  written as a column vector  $\mathbf{M}_i = (\mathbf{M}_{i \cdot})^T$

### 2.1 Eigen-Scaling RDPG

Under the RDPG, each vertex in the graph is associated with a latent position in Euclidean space. Conditional on these latent positions, edge connection probabilities are given by the inner product of the latent positions.

**Definition 2.1.** Suppose that  $\mathbf{x}_1, \mathbf{x}_2, \dots, \mathbf{x}_n \in \mathbb{R}^d$  have the property that  $\mathbf{x}_i^T \mathbf{x}_j \in [0, 1]$  for all  $i, j \in [n]$ . Then we say that a random adjacency matrix  $\mathbf{A} \in \mathbb{R}^{n \times n}$  follows a *Random Dot Product Graph* with latent positions  $\{\mathbf{x}_i\}_{i=1}^n$  if  $\{\mathbf{A}_{ij}\}_{i < j}$  are conditionally independent with  $\mathbf{A}_{ij} | \mathbf{x}_i, \mathbf{x}_j \sim \text{Bern}(\mathbf{x}_i^T \mathbf{x}_j)$  for  $i < j$ .

We will also assume that the latent positions are drawn i.i.d. from a distribution  $F$  over an appropriate subset of  $\mathbb{R}^d$ . The requisite properties of this distribution  $F$  are given in the following definition.

**Definition 2.2.** Let  $F$  be a distribution over  $\mathbb{R}^d$  with the property that for all  $\mathbf{x}, \mathbf{y} \in \text{supp}(F)$  has the property  $\mathbf{x}^T \mathbf{y} \in [0, 1]$ . If  $F$  satisfies these properties we say  $F$  is a *d-dimensional inner production distribution*.

In order to capture varying network structure, we extend this model to the multiplex graph setting by applying graph-specific weights to the inner products between each vector in the support of  $F$ . This inner product distribution induces a space of  $d \times d$ , diagonal weighting matrices  $\mathcal{C}_F$  that weight each component of this inner product while remaining in the unit interval.

**Definition 2.3.** Suppose that  $F$  is a  $d$ -dimensional inner product distribution. Then we say  $F$  induces a *diagonal weighting space*,  $\mathcal{C}_F$ , where  $\mathcal{C}_F$  is given by

$$\mathcal{C}_F = \{\mathbf{C} \in \mathbb{R}_{\geq 0}^{d \times d} : \mathbf{C} \text{ is diagonal, } \mathbf{x}^T \mathbf{C} \mathbf{y} \in [0, 1], \forall \mathbf{x}, \mathbf{y} \in \text{supp}(F)\}.$$

This leads us to our definition of the ESRPDG model.

**Definition 2.4.** Let  $F$  be a  $d$ -dimensional inner product distribution such that for  $\mathbf{y} \sim F$  the second moment matrix  $\Delta = \mathbb{E}[\mathbf{y}\mathbf{y}^T] \in \mathbb{R}^{d \times d}$  is diagonal and full rank. Let  $\mathbf{X}_1, \dots, \mathbf{X}_n \stackrel{i.i.d.}{\sim} F$  and organize these vectors in the rows of the matrix  $\mathbf{X} = [\mathbf{X}_1, \mathbf{X}_2, \dots, \mathbf{X}_n]^T$ . Let  $\mathbf{C}^{(1)}, \dots, \mathbf{C}^{(m)} \in \mathcal{C}_F$  with the property that  $\min_{i \in [d]} \max_{g \in [m]} \mathbf{C}_{ii}^{(g)} > 0$ . Then we say that the vertex-aligned, random adjacency matrices  $\{\mathbf{A}^{(g)}\}_{g=1}^m$  are distributed according to the *Eigen-Scale Random Dot Product Graph* and write  $(\{\mathbf{A}^{(g)}\}_{g=1}^m, \mathbf{X}) \sim \text{ESRDPG}(F, n, \{\mathbf{C}^{(g)}\}_{g=1}^m)$  if

$$\mathbb{P}[\mathbf{A}^{(1)}, \mathbf{A}^{(2)}, \dots, \mathbf{A}^{(m)} | \mathbf{X}] = \prod_{g=1}^m \prod_{i < j} (\mathbf{X}_i^T \mathbf{C}^{(g)} \mathbf{X}_j)^{\mathbf{A}_{ij}^{(g)}} (1 - \mathbf{X}_i^T \mathbf{C}^{(g)} \mathbf{X}_j)^{1 - \mathbf{A}_{ij}^{(g)}}$$

Under this model,  $\{\mathbf{A}^{(g)}\}_{g=1}^m$  are conditionally independent given  $\mathbf{X}$  with  $\mathbf{A}_{ij}^{(g)} | \mathbf{X} \sim \text{Bernoulli}(\mathbf{X}_i^T \mathbf{C}^{(g)} \mathbf{X}_j)$ .

By associating each network with a different weighting matrix in  $\mathcal{C}_F$ , we can flexibly capture variation between networks within the RDPG framework. Given  $\mathbf{X}$ , the probability of observing an edge between vertex  $i$  and vertex  $j$  in graph  $g$  is given by  $\mathbf{X}_i^T \mathbf{C}^{(g)} \mathbf{X}_j$ . We denote the matrix containing these probabilities as  $\mathbf{P}^{(g)} = \mathbf{X} \mathbf{C}^{(g)} \mathbf{X}^T$  for each graph  $g \in [m]$ , so that  $\mathbf{A}^{(g)} | \mathbf{X} \sim \text{Bern}(\mathbf{P}^{(g)})$ . See Figure 2.1 for a visual illustration of this model.

Heuristically, each dimension in the latent space can be interpreted as a principle direction capturing important features that govern the connectivity structure in the system. The diagonal elements of the weighting matrices  $\mathbf{C}_{ii}^{(g)}$  can then be interpreted as how influential the features captured by the  $i$ -th dimension are in determining the connectivity structure of graph  $g$ .

In the definition of the ESRDPG, we impose assumptions on the distribution  $F$  and weighting matrices  $\{\mathbf{C}^{(g)}\}_{g=1}^m$ . Similar assumptions on  $F$  are made in previous analysis (A. Athreya et al. 2016; Levin et al. 2017) but have somewhat different implications here. The assumption  $\text{rank}(\Delta) = d$  specifies the dimension of the latent space.  $\Delta$  being diagonal is an assumption made to ensure the weighting matrices  $\{\mathbf{C}^{(g)}\}_{g=1}^m$  are asymptotically scaling the eigenvalues of  $\{\mathbf{P}^{(g)}\}_{g=1}^m$  and enables analytic computation of the bias presented in Theorem 1. In addition, this assumption helps address the identifiability of the ESRDPG which we discuss in Remark 1. The assumption  $\min_{i \in [d]} \max_{g \in [m]} \mathbf{C}_{ii}^{(g)} > 0$  is a technical assumption to ensure that each latent dimension is given a nonzero weight in at least one graph.

We note that the ESRPDG includes settings where  $\mathbf{C}_{ii}^{(g)} = 0$ . Therefore, if certain principle directions in graph  $g$  are inconsequential in the connectivity structure of graph  $k$ , the ESRDPG can capture this relationship within a common probability model. Indeed, by adjusting  $d$  accordingly, the ESRDPG can capture a collection of conditionally independent RDPGs of differing dimension. We explore some of these distributions in the experiments section of this work.

The ESRDPG is similar to other multiple random graph models that extend the RDPG to multiplex network data. Nielsen and Witten (2018) propose the Multiple Random Dot Product Graph (MRDPG) in which the probability matrices take the form  $\mathbf{P}^{(g)} = \mathbf{U} \Lambda^{(g)} \mathbf{U}^T$  where  $\mathbf{U} \in \mathbb{R}^{n \times d}$  is orthogonal and  $\Lambda^{(g)} \in \mathbb{R}^{d \times d}$  is diagonal with positive entries for all  $g \in [m]$ . Under the ESRDPG, the probability matrices take the form  $\mathbf{P}^{(g)} = \mathbf{X} \mathbf{C}^{(g)} \mathbf{X}^T$  and due to the assumption that  $\Delta$  is diagonal, it can be shown that  $\mathbf{X}$  has orthogonal columns asymptotically. This observation and the fact that  $\mathbf{C}^{(g)}$  has strictly positive entries establishes asymptotic equivalence between the ESRDPG and the MRDPG.

Models that extend this paradigm include the Multiple Random Eigen Graphs (MREG) of S. Wang et al. (2017) and the Common Subspace Independent-Edge (COSIE) model of Arroyo et al. (2019). The

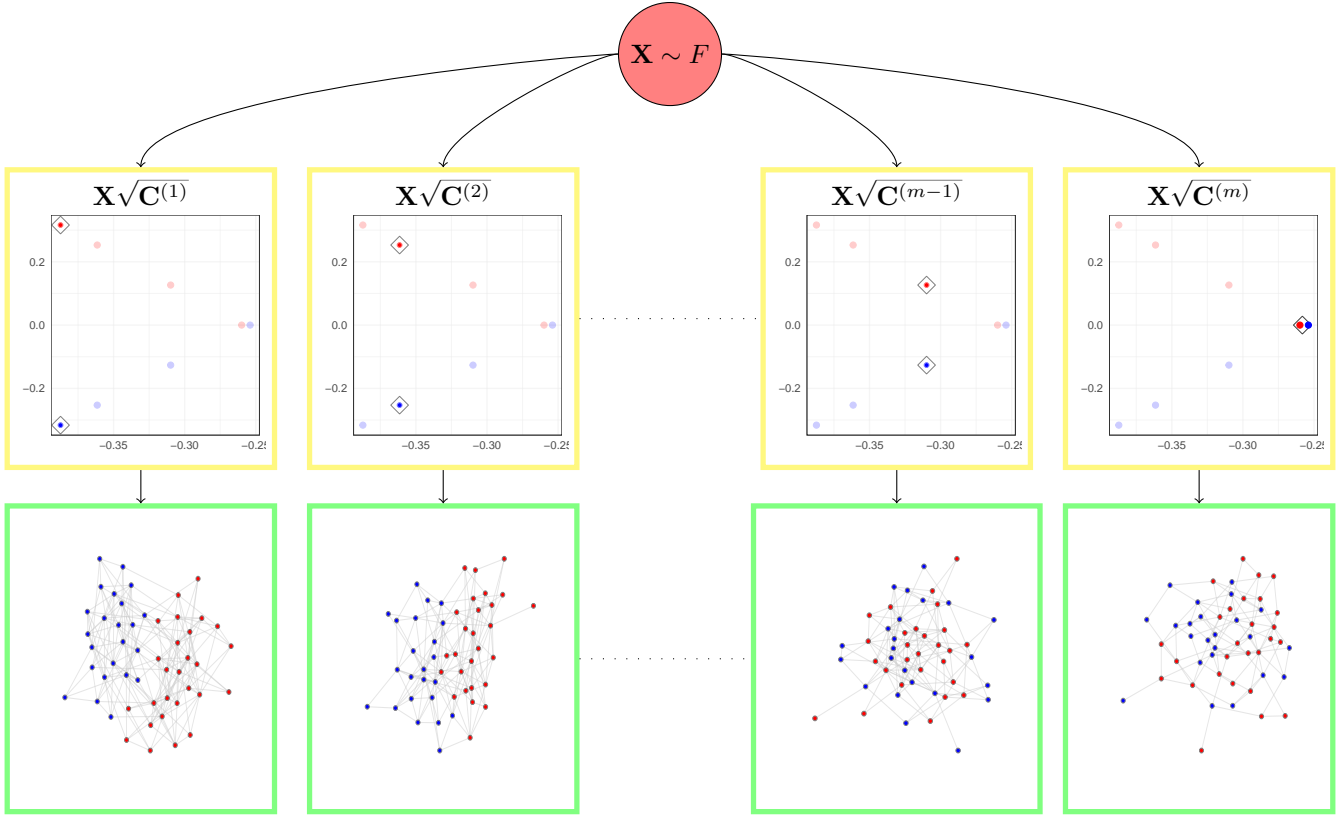


Figure 1: An illustration of the ESRPDG model's hierarchical structure. Latent positions are drawn from a common distribution  $F$ . From here each  $\mathbf{P}^{(g)}$  is defined as a function of the latent positions  $\mathbf{X}$  and weighting matrix  $\mathbf{C}^{(g)}$ . These scaled latent positions (yellow boxes) change the probability structure for each network. The random adjacency matrices (green boxes) are then drawn from  $\mathbf{A}^{(g)} \sim \text{Bern}(\mathbf{P}^{(g)})$ .

MREG model requires  $\mathbf{P}^{(g)} = \mathbf{U}\Lambda^{(g)}\mathbf{U}^T$  where the columns of  $\mathbf{U}$  have euclidean norm 1, but need not be orthogonal, and  $\Lambda^{(g)}$  be a diagonal matrix. The COSIE model assumes  $\mathbf{P}^{(g)} = \mathbf{U}\mathbf{R}^{(i)}\mathbf{U}^T$  where  $\mathbf{U} \in \mathbb{R}^{n \times d}$  has orthonormal columns and  $\mathbf{R}^{(g)} \in \mathbb{R}^{d \times d}$  is any symmetric matrix. These network models extend the class of potential probability matrices by allowing each  $\mathbf{P}^{(g)}$  to have different eigenvectors, while under the ESRDPG, each probability matrix shares a common eigenvectors asymptotically.

Notice that each method assumes the matrices  $\{\mathbf{P}^{(g)}\}_{g=1}^m$  share common structure through a vertex specific latent structure. Under the ESRDPG, the rows of the matrix  $\mathbf{X}$  are drawn i.i.d. from a common distribution  $F$ . In this way, the ESRDPG preserve the notion of an exchangeable latent position model in extending the RDPG to heterogeneous networks while asymptotically maintaining the shared latent structure of the probability matrices. This contrasts with MRDPG, COSIE, and MREG network models which make assumptions on the finite probability matrices  $\mathbf{P}^{(g)}$ . These assumptions make it less clear how to exploit the exchangeability structure of the RDPG.

**Remark 1** (Identifiability). In most latent position models, the model parameters are typically identifiable only within a larger equivalence class. Of note, the latent positions of the RDPG are only identifiable up to an orthogonal transformation as the edge probabilities are invariant under such transformation. Similar issues arise for the ESRDPG though the common structure among the graph somewhat limits the non-identifiability.

Generally, the latent positions and weighting matrices are only identifiable within the equivalence class

$$(\mathcal{X}, \mathcal{C}) = \{(\mathbf{X}\mathbf{M}, \{\mathbf{M}^{-1}\mathbf{C}^{(g)}\mathbf{M}^{-T}\}_{g=1}^m) : \mathbf{M} \in \mathcal{M}, \mathbf{X} \sim F\}.$$

where  $\mathcal{M}$  is the subset of  $d \times d$  invertible matrices such that  $\mathbf{M}^T \Delta \mathbf{M}$  and  $\{\mathbf{M}^{-1} \mathbf{C}^{(g)} \mathbf{M}^{-T}\}_{g=1}^m$  are diagonal and can be characterized more precisely by considering the co-multiplicities of the diagonal values of  $\Delta$  and  $\{\Delta \mathbf{C}^{(g)}\}_{g=1}^m$ . We can circumvent several of these identifiability issues by instead regarding the *scaled* latent  $\mathbf{X} \sqrt{\mathbf{C}^{(g)}}$  for all  $g \in [m]$  as the parameters of interest. While the scaled latent positions are identifiable within the equivalence class  $(\mathcal{X}, \mathcal{C})$ , in changing the estimand we introduce a new identifiability issue. Namely, for all  $g \in [m]$

$$\mathbf{P}^{(g)} = (\mathbf{X} \sqrt{\mathbf{C}^{(g)}} \mathbf{W}^{(g)}) (\mathbf{X} \sqrt{\mathbf{C}^{(g)}} \mathbf{W}^{(g)})^T$$

for some orthogonal matrix  $\mathbf{W}^{(g)} \in \mathcal{O}^{d \times d}$ .

For  $\mathbf{X} \sqrt{\mathbf{C}^{(g)}} \mathbf{W}^{(g)}$  to correspond to a ESRDPG, we further require the matrices  $\mathbf{W}^{(g)T} \mathbf{C}^{(g)} \Delta \mathbf{W}^{(g)}$  are also diagonal for all  $g \in [m]$ . Therefore the scaled latent positions are only identifiable within the equivalence class

$$\begin{aligned} \mathcal{L} &= \{\mathbf{L} = [\mathbf{X} \sqrt{\mathbf{C}^{(g)}} \mathbf{W}^{(g)}]_{g=1}^m \in \mathbb{R}^{nm \times d} : \mathbf{W}^{(g)} \in \mathcal{W}^{(g)}\} \\ \mathcal{W}^{(g)} &= \{\mathbf{W} \in \mathcal{O}^{d \times d} : \mathbf{W}^T \mathbf{C}^{(g)} \Delta \mathbf{W} \text{ is diagonal for all } g \in [m]\}. \end{aligned}$$

Therefore, our goal will be to estimate the scaled latent positions up to a rotation within the equivalence class. We note the size of  $\mathcal{W}^{(g)} \subseteq \mathcal{O}^{d \times d}$  is determined entirely by the matrices  $\mathbf{C}^{(g)} \Delta$ . Assuming  $\Delta = \delta \mathbf{I}$  and  $\mathbf{C}^{(g)} = \mathbf{I}$  then  $\mathcal{W}^{(g)} = \mathcal{O}^{d \times d}$ . However, if  $\mathbf{C}^{(g)} \Delta$  is of full rank with unique elements, then  $\mathcal{W}^{(g)} = \{\text{diag}(\mathbf{w}) : \mathbf{w} \in \{\pm 1\}^d\}$  and hence finite.

Based on these identifiability considerations, we now focus on the estimation of

$$\mathbf{L} = [\sqrt{\mathbf{C}^{(1)}} \mathbf{X}^T \ \sqrt{\mathbf{C}^{(2)}} \mathbf{X}^T \ \dots \ \sqrt{\mathbf{C}^{(m)}} \mathbf{X}^T]^T \in \mathbb{R}^{nm \times d},$$

the  $m$ -block matrix consisting of the scaled latent positions.

## 2.2 Omnibus Embedding

We focus on estimating  $\mathbf{L}$  using the *omnibus embedding* Levin et al. (2017), a method which simultaneously estimates the scaled latent positions for each graph.

**Definition 2.5.** Let  $\{\mathbf{A}^{(g)}\}_{g=1}^m \in \mathbb{R}^{n \times n}$  be a set of undirected, vertex-aligned, adjacency matrices. Let  $\tilde{\mathbf{A}} \in \mathbb{R}^{nm \times nm}$  be the omnibus matrix of  $\{\mathbf{A}^{(g)}\}_{g=1}^m$  given by

$$\tilde{\mathbf{A}} = \begin{bmatrix} \mathbf{A}^{(1)} & \frac{\mathbf{A}^{(1)} + \mathbf{A}^{(2)}}{2} & \dots & \frac{\mathbf{A}^{(1)} + \mathbf{A}^{(m)}}{2} \\ \frac{\mathbf{A}^{(2)} + \mathbf{A}^{(1)}}{2} & \mathbf{A}^{(2)} & \dots & \frac{\mathbf{A}^{(2)} + \mathbf{A}^{(m)}}{2} \\ \vdots & \vdots & \ddots & \vdots \\ \frac{\mathbf{A}^{(m)} + \mathbf{A}^{(1)}}{2} & \frac{\mathbf{A}^{(m)} + \mathbf{A}^{(2)}}{2} & \dots & \mathbf{A}^{(m)} \end{bmatrix}.$$

Denote the eigendecomposition of  $\tilde{\mathbf{A}}$  as

$$\tilde{\mathbf{A}} = [\mathbf{U}_{\tilde{\mathbf{A}}} | \tilde{\mathbf{U}}_{\tilde{\mathbf{A}}}] [\mathbf{S}_{\tilde{\mathbf{A}}} \oplus \tilde{\mathbf{S}}_{\tilde{\mathbf{A}}}] [\mathbf{U}_{\tilde{\mathbf{A}}} | \tilde{\mathbf{U}}_{\tilde{\mathbf{A}}}]^T$$

where the columns of  $\mathbf{U}_{\tilde{\mathbf{A}}} \in \mathbb{R}^{nm \times d}$  are the  $d$  eigenvectors of  $\tilde{\mathbf{A}}$  corresponding to the  $d$  largest positive eigenvalues of  $\tilde{\mathbf{A}}$  and  $\mathbf{S}_{\tilde{\mathbf{A}}} \in \mathbb{R}^{d \times d}$  is a diagonal matrix containing these  $d$  eigenvalues in decreasing order. Then the  $d$ -dimensional *omnibus embedding* of  $\{\mathbf{A}^{(g)}\}_{g=1}^m$ , denoted as  $\text{Omni}(\{\mathbf{A}^{(g)}\}_{g=1}^m, d)$ , is given by the  $d$ -dimensional spectral embedding of  $\tilde{\mathbf{A}}$ . That is

$$\text{Omni}(\{\mathbf{A}^{(g)}\}_{g=1}^m, d) = \mathbf{U}_{\tilde{\mathbf{A}}} \mathbf{S}_{\tilde{\mathbf{A}}}^{1/2} \in \mathbb{R}^{nm \times d}$$

Note that the omnibus embedding is of dimension  $nm \times d$  yielding  $m$  separate latent position estimates for each vertex in the vertex set.

The omnibus embedding was introduced as a method for the simultaneous embedding of multiple networks and was analyzed in the case of i.i.d. networks. Under the ESRDPG, the graphs are i.i.d. if  $\mathbf{C}^{(g)} = \mathbf{I}$  for all  $g \in [m]$ . In this setting, the omnibus embedding provides an asymptotically unbiased estimate of the latent positions in each graph. Moreover, the authors produce a  $2 \rightarrow \infty$  norm bound on the residual term and prove a central limit theorem for the estimated latent positions.

Under the ESRDPG the networks are not i.i.d. and we therefore expect the omnibus embedding to produce biased estimates of the scaled latent positions. In turn, we will demonstrate that this bias is offset by a favorable variance reduction in the estimation of the scaled latent positions. As an illustrative toy example, consider the following simulation experiment which we will use as a running example in the next sections.

**Example 1.** Consider  $m = 2$  networks over  $n = 100$  vertices. Suppose that the first network is distributed according to the Erdős-Rényi model with parameter  $p = 1/2$  and the second network is an Erdős-Rényi with parameter  $c^2 p$  for some constant  $c \in [0, \sqrt{2}]$ . This model falls under the ESRDPG with  $\mathbf{X} = \sqrt{p}\mathbf{1}_n$ ,  $\mathbf{C}^{(1)} = \mathbf{I}$ , and  $\mathbf{C}^{(2)} = c^2\mathbf{I}$  and gives rise to the probability matrices  $\mathbf{P}^{(1)} = p\mathbf{1}_n\mathbf{1}_n^T$  and  $\mathbf{P}^{(2)} = c^2p\mathbf{1}_n\mathbf{1}_n^T$ .

In this experiment we look to estimate the scaled latent positions,  $p\mathbf{1}_n$  and  $cp\mathbf{1}_n$ , using three different methods. Following the adjacency spectral embedding (ASE) of Sussman et al. (2012), we first embed the networks separately, ignoring their common structure to attain the estimates  $\hat{\mathbf{X}}_{\text{ASE}}^{(1)}$  and  $\hat{\mathbf{X}}_{\text{ASE}}^{(2)}$  of  $p\mathbf{1}_n$  and  $cp\mathbf{1}_n$  respectively. Second, we embed the the average of the two observed adjacency matrices  $\bar{\mathbf{A}} = \frac{1}{2}(\mathbf{A}^{(1)} + \mathbf{A}^{(2)})$  as proposed in R. Tang et al. (2019), a method that assumes the network structures are the same to attain a global estimate  $\hat{\mathbf{X}}_{\text{Abar}}$  of both sets of latent positions. Lastly, we jointly embed the networks using the omnibus embedding to attain the estimates  $\hat{\mathbf{X}}_{\text{Omni}}^{(1)}$  and  $\hat{\mathbf{X}}_{\text{Omni}}^{(2)}$  of  $p\mathbf{1}_n$  and  $cp\mathbf{1}_n$  respectively. Note that none of these estimators would be optimal if the Erdős-Rényi structure were known but instead illustrate the behavior of these varying embeddings under the ESRDPG.

For values of  $c$  spaced from 0.1 to 1.4, we sample adjacency matrices for each model and produce the estimates described above. We replicate this process  $T = 1000$  times and denote each estimate as  $\hat{\mathbf{X}}_E^{(g),t}$  for each estimator  $E \in \{\text{ASE}, \text{Abar}, \text{Omni}\}$ , each graph  $g \in \{1, 2\}$ , and each Monte Carlo replicate  $t \in [T]$ . With these estimates, we estimate MSE for each vertex  $i \in [n]$  in each graph  $g \in \{1, 2\}$  as

$$\text{MSE}_E^{(1),i} = \frac{1}{T} \sum_{t=1}^T (\hat{\mathbf{X}}_E^{(1),t} - p\mathbf{1}_n)_i^2 \quad \text{MSE}_E^{(2),i} = \frac{1}{T} \sum_{t=1}^T (\hat{\mathbf{X}}_E^{(2),t} - cp\mathbf{1}_n)_i^2.$$

The results of this simulation can be found in Figure 2. The values  $\{\text{MSE}_E^{(g),i}\}$  are plotted on a log scale along the vertical axis against varying values of  $c$  on the horizontal axis. As each vertex has the same latent position under the Erdős-Rényi model, each point is estimating the same mean square error. In the left panel are the MSE plots for Graph 1 and in the right panel are the MSE plots for Graph 2. The lines are theoretical mean squared error curves calculated *a priori* based on the expressions given in Table 1. While these lines are based on asymptotic distributional results, they match very closely with finite sample networks (i.e.  $n = 100$ ). As network size increases, these differences diminish to zero.

This simulation highlights the ability of the omnibus estimator to robustly estimate the scaled latent positions of heterogeneous networks under the ESRDPG. At  $c = 1$ , the network connectivity structures are the same and  $\hat{\mathbf{X}}_{\text{Abar}}$  (red) has the lowest MSE followed by the omnibus embedding (blue) and lastly the ASE (green). This is not surprising as the embedding of  $\bar{\mathbf{A}}$  correctly assumes that the networks are identically distributed which substantially reduces variance. As  $c$  varies away from 1, however, the bias of this method increases the MSE significantly.

For  $c$  values far from this 1 (networks with very different edge probabilities) the individual embeddings given by the ASE have the lowest MSE followed by the omnibus estimates and then the Abar estimates. Again, this should not be surprising as this method assumed that the networks shared no joint structure. For

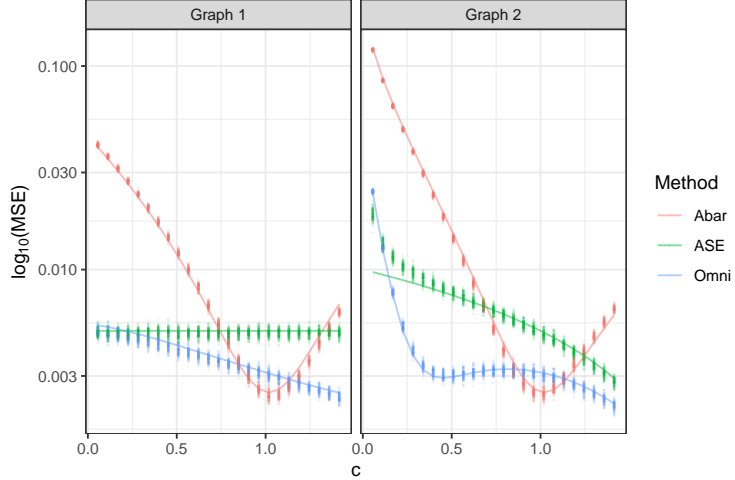


Figure 2: Comparing the MSE of three estimators; the individual adjacency spectral embedding (green), the embedding of the sample average of the adjacency matrices (red), and the omnibus embedding (blue). It appears that the omnibus embedding is the most robust estimator for networks with similar connectivity structure.

$c$  values larger than  $\approx .25$  however, it appears that the omnibus embedding is the most robust estimator. This relationship is not symmetric around  $c = 1$  suggesting that the omnibus embedding is borrowing strength from the denser network for more accurate estimation in the sparser network.  $\square$

As this simulation demonstrates, the omnibus approach offers a favorable bias-variance tradeoff for classes of  $\{\mathbf{C}^{(g)}\}_{g=1}^m$  that do not vary too far from  $\mathbf{I}$ . In the following section, we analytically quantify the asymptotic bias and variance of the omnibus embedding estimator for scaled latent positions under the ESRDPG.

### 3 Main Results

In this section we present the main theoretical analysis of the asymptotic bias and variance of the omnibus embedding under the ESRDPG. Theorem 1 provides the asymptotic bias of the omnibus embedding for estimating the scaled latent positions. Theorem 1 also provides a uniform bound of the residual term, supporting our bias result. Theorem 2 states a central limit theorem for the rows of the omnibus embedding, showing that the rows of the omnibus embedding converge to a mixture of normal random variables. We then provide a corollary that characterizes the asymptotic joint distribution of the rows of the omnibus embedding which will be useful in the analysis of subsequent statistical applications.

Before we state these results, we provide relevant notation necessary in the presentation of Theorem 1 and Theorem 2. We say a sequence of events  $\{E_n\}_{n=1}^\infty$  occurs with high probability if  $\mathbb{P}(E_n^C) \leq n^{-2}$ . Next, we define a set of diagonal matrices we call *scaling matrices* with entries that are nonlinear transformation of the weighting matrices  $\{\mathbf{C}^{(g)}\}_{g=1}^m$ .

**Definition 3.1.** Define the vector  $\mathbf{v}_i \in \mathbb{R}^m$  as  $\mathbf{v}_i = \left[ \mathbf{C}_{ii}^{(1)} \ \mathbf{C}_{ii}^{(2)} \dots \mathbf{C}_{ii}^{(m)} \right]^T$  and let  $\mathbf{H}(\mathbf{x}) = 2^{-1}(\mathbf{x}\mathbf{1}_m^T + \mathbf{1}_m\mathbf{x}^T) \in \mathbb{R}^{m \times m}$ . Let  $\alpha^{(i)} = \text{ASE}(\mathbf{H}(\mathbf{v}_i), 1) \in \mathbb{R}_{\geq 0}^m$  for  $i \in [d]$  chosen such that  $\alpha^{(i)}$  has strictly positive entries. Define the scaling matrices  $\mathbf{S}^{(g)} \in \mathbb{R}^{d \times d}$  for  $g \in [m]$  by

$$\mathbf{S}^{(g)} = \text{diag} \left( \alpha_g^{(1)}, \alpha_g^{(2)}, \dots, \alpha_g^{(d)} \right)$$

Finally, define the  $nm \times d$  block matrix  $\mathbf{L}_S$  as

$$\mathbf{L}_S = [\mathbf{S}^{(1)} \mathbf{X}^T \ \mathbf{S}^{(2)} \mathbf{X}^T \ \dots \ \mathbf{S}^{(m)} \mathbf{X}^T]^T \in \mathbb{R}^{nm \times d}$$

These scaling matrices will be central to our bias result stated in Theorem 1. As stated Proposition B.1 in Appendix B, the Perron-Frobenius theorem for irreducible matrices allows us to choose the entries of  $\alpha^{(i)}$  to be strictly positive. We also show the mapping from the weighting matrices  $\{\mathbf{C}^{(g)}\}_{g=1}^m$  to the scaling matrices  $\{\mathbf{S}^{(g)}\}_{g=1}^m$  is one-to-one. Moreover, as  $\{\mathbf{S}^{(g)}\}_{g=1}^m$  are constructed through the leading eigenvector of the matrices  $\mathbf{H}(\mathbf{v}_i)$ , the  $\{\mathbf{S}^{(g)}\}_{g=1}^m$  are nonlinear, smooth functions of the weighting matrices  $\{\mathbf{C}^{(g)}\}_{g=1}^m$ . Therefore, the weighting matrices uniquely determine the scaling matrices  $\{\mathbf{S}^{(g)}\}_{g=1}^m$ . In two-graph settings, such as Example 1, we can directly analyze the behavior of the entries of  $\{\mathbf{S}^{(g)}\}_{g=1}^m$  as a function of the scaling matrices  $\{\mathbf{C}^{(g)}\}_{g=1}^m$ .

**Example 1. (continued)** Under this simulation  $d = 1$  so the weighting matrices  $\mathbf{C}^{(1)}, \mathbf{C}^{(2)}$  take on scalar values. Moreover,  $\mathbf{S}^{(1)}, \mathbf{S}^{(2)} \in \mathbb{R}$  are real, positive numbers. From  $\mathbf{C}^{(1)} = 1, \mathbf{C}^{(2)} = c$  we construct  $\mathbf{v}_1 = (1, c)^T$  and the matrix

$$\mathbf{H}(\mathbf{v}_1) = \begin{bmatrix} 1 & \frac{1+c}{2} \\ \frac{1+c}{2} & c \end{bmatrix}.$$

By definition,  $(\mathbf{S}^{(1)}, \mathbf{S}^{(2)})^T = \text{ASE}(\mathbf{H}(\mathbf{v}_1), 1)$ . The Taylor expansions of these values around  $c = 1$  results in the approximations

$$\begin{aligned} \mathbf{S}^{(1)} &\simeq 1 + O((c-1)^2) \\ \mathbf{S}^{(2)} &\simeq \frac{c+1}{2} + O((c-1)^2) \end{aligned}$$

Near  $c = 1$ , the scaling of the first network is nearly flat at 1,  $\mathbf{S}^{(1)} \simeq 1$ . In the second network, the linear scaling is given by  $\mathbf{S}^{(2)} \simeq \frac{1+c}{2}$ , indicating the second network's embedding is subject to a linear scaling bias of  $\frac{1-c}{2}$ . As  $\frac{1+c}{2}$  is the mean of the scaling in the first and second network, we can interpret this scaling bias as the omnibus embedding shrinking the latent position scaling towards the matrix  $(\frac{1+c}{2}) \mathbf{I}$ .  $\square$

This example highlights how the elements of the scaling matrices  $\{\mathbf{S}^{(g)}\}_{g=1}^m$  are combining elements of the weighting matrices  $\{\mathbf{C}^{(g)}\}_{g=1}^m$  in each dimension of the latent space. Our first result identifies the bias of the omnibus embedding under the ESRDPG.

**Theorem 1.** Suppose that  $(\{\mathbf{A}\}_{g=1}^m, \mathbf{X}) \sim \text{ESRDPG}(F, n, \{\mathbf{C}^{(g)}\}_{g=1}^m)$  for some  $d$ -dimensional inner product distribution  $F$ . Let  $\hat{\mathbf{L}} = \text{Omni}(\{\mathbf{A}\}_{g=1}^m, d)$  and  $\mathbf{L}$  be given as above. Let  $h = n(g-1) + i$  for some  $g \in [m]$  and  $i \in [n]$  denote some row of  $\hat{\mathbf{L}}$ . Then there exists a sequence of orthogonal matrices  $\{\tilde{\mathbf{W}}_n\}_{n=1}^\infty$  depending on  $\tilde{\mathbf{A}}$  and  $\tilde{\mathbf{P}}$  such that

$$(\hat{\mathbf{L}} \tilde{\mathbf{W}}_n - \mathbf{L})_h = (\mathbf{S}^{(g)} - \sqrt{\mathbf{C}^{(g)}}) \mathbf{X}_i + \mathbf{R}_h \quad (\text{A})$$

where  $\mathbf{R}_h$  is a residual term that with high probability satisfies

$$\max_{h \in [nm]} \|\mathbf{R}_h\|_2 \leq Cm^{3/2} \frac{\log nm}{\sqrt{n}} \quad (\text{B})$$

*Proof.* The proof can be found in Appendix B.  $\square$

The essence of this result is that the estimated scaled latent positions  $\hat{\mathbf{L}}$  do not concentrate around the scaled latent positions  $\mathbf{L} = [\mathbf{X} \sqrt{\mathbf{C}^{(g)}}]_{g=1}^m$  but instead around  $\mathbf{L}_S = [\mathbf{X} \mathbf{S}^{(g)}]_{g=1}^m$ . Therefore, the omnibus embedding introduces a row-wise asymptotic bias of  $(\mathbf{S}^{(g)} - \sqrt{\mathbf{C}^{(g)}}) \mathbf{X}_i$ . The second portion of this theorem provides a uniform rate for this concentration.

The rate  $O(m^{3/2}n^{-1/2} \log nm)$  is reminiscent of those given in Levin et al. (2017) with an additional factor of  $m$  due to permitting  $\mathbf{C}_{ii}^{(g)} = 0$  for all but one  $g \in [m]$ . If all  $\mathbf{C}_{ii}^{(g)}$  are positive then the uniform bound is instead  $O(\sqrt{m/n} \log(nm))$ .

Uncovering this asymptotic bias completes the first stage in characterizing the bias-variance tradeoff of the estimates provided by the omnibus embedding. The result allows for rigorous analysis of community detection methods for individual and multiplex networks which we discuss in Section 4. In order to more precisely characterize the behavior of this residual term, we uncover its limiting distributional behavior in Theorem 2.

**Theorem 2.** Suppose that  $(\{\mathbf{A}\}_{g=1}^m, \mathbf{X}) \sim \text{ESRDPG}(F, n, \{\mathbf{C}^{(g)}\}_{g=1}^m)$  for some  $d$ -dimensional inner product distribution  $F$ . Let  $\mathbf{S}^2 = \sum_{g=1}^m (\mathbf{S}^{(g)})^2$  and  $h = n(g-1) + i$  for some  $g \in [m]$  and  $i \in [n]$ . Then in the context of Theorem 1 we have

$$\lim_{n \rightarrow \infty} \mathbb{P} [\sqrt{n} \mathbf{R}_h \leq \mathbf{x}] = \int_{\text{supp}(F)} \Phi(\mathbf{x}; \mathbf{0}, \Sigma_g(\mathbf{y})) dF(\mathbf{y}) \quad (1)$$

where  $\Phi(\mathbf{x}; \mu, \Sigma)$  is the multivariate normal cumulative distribution function with mean  $\mu$  and covariance matrix  $\Sigma$ . Moreover, the covariance matrix can be written as

$$\Sigma_g(\mathbf{y}) = \frac{1}{4} (\mathbf{S}^2 \Delta)^{-1} \left[ (\mathbf{S}^{(g)} + m\bar{\mathbf{S}}) \tilde{\Sigma}_g(\mathbf{y}) (\mathbf{S}^{(g)} + m\bar{\mathbf{S}}) + \sum_{k \neq g} \mathbf{S}^{(k)} \tilde{\Sigma}_k(\mathbf{y}) \mathbf{S}^{(k)} \right] (\Delta \mathbf{S}^2)^{-1}$$

and  $\tilde{\Sigma}_\ell(\mathbf{y})$  is given by

$$\tilde{\Sigma}_\ell(\mathbf{y}) = \mathbb{E} \left[ (\mathbf{y}^T \mathbf{C}^{(\ell)} \mathbf{X}_j - (\mathbf{y}^T \mathbf{C}^{(\ell)} \mathbf{X}_j)^2) \mathbf{X}_j \mathbf{X}_j^T \right]$$

*Proof.* The proof can be found in the Appendix C. □

Similar results were achieved in A. Athreya et al. (2016) and Levin et al. (2017) using a combination of perturbation arguments. These arguments largely study the differences in eigenstructure between  $\hat{\mathbf{A}}$  and its expectation  $\hat{\mathbf{P}} = \mathbb{E}[\hat{\mathbf{A}}|\mathbf{X}]$ . In previous work, under the assumption that the  $m$  graphs are iid, the rank of this matrix was equal to that of the latent space, i.e.  $\text{rank}(\hat{\mathbf{P}}) = d$ . However, under the ESRDPG the rank of  $\tilde{\mathbf{P}}$  could be as great as  $2d$  and we must characterize how these eigenvalues relate to model parameters.

This result establishes that the rows of omnibus embedding when centered by the bias term given in Theorem 1 converges in distribution to a mixture of mean zero normal random variables. Moreover, the variance of this random variable, while complicated, is a function of the weighting matrices  $\{\mathbf{C}^{(g)}\}_{g=1}^m$ , and the latent position distribution  $F$ . Together with Theorem 1, these results show the weighting matrices  $\{\mathbf{C}^{(g)}\}_{g=1}^m$  are central in the bias-variance tradeoff of the omnibus embedding under the ESRDPG.

In statistical applications of these estimates, it will often be necessary to consider linear combinations of the rows of  $\hat{\mathbf{L}}$ . Our next corollary establishes the asymptotic joint distribution of any two rows  $\hat{\mathbf{L}}$  and can be easily extended to study any finite collection of rows.

**Corollary 1.** Let  $r_i = i + n(g-1)$  and  $r_j = j + n(k-1)$  for  $i, j \in [n]$  and  $g, k \in [m]$ . Define the vector  $\mathbf{V} = (\mathbf{R}_{r_i}^T \mathbf{R}_{r_j}^T)^T \in \mathbb{R}^{2d}$  and let  $\mathbf{v} \in \mathbb{R}^{2d}$ . Then in the context of Theorem 2 we have

$$\lim_{n \rightarrow \infty} \mathbb{P} [\sqrt{n} \mathbf{V} \leq \mathbf{v}] = \int_{\text{supp}(F)} \Phi(\mathbf{v}; \mathbf{0}, \Omega_{r_i r_j}(\mathbf{y})) dF(\mathbf{y})$$

where  $\Omega_{r_i r_j}(\mathbf{y}) \in \mathbb{R}^{2d \times 2d}$  is given by

$$\Omega_{r_i r_j}(\mathbf{y}) = \begin{bmatrix} \Sigma_g(\mathbf{y}) & \Sigma_{gk}^{(ij)}(\mathbf{y}) \\ \Sigma_{kg}^{(ij)}(\mathbf{y}) & \Sigma_k(\mathbf{y}) \end{bmatrix}$$

where  $\Sigma_g(\mathbf{y})$  and  $\Sigma_k(\mathbf{y})$  are as in Theorem 2 and  $\Sigma_{gk}^{(ij)}(\mathbf{y}) = \Sigma_{kg}(\mathbf{y})^{(ij)T}$ . For  $g \neq k$ , if  $i \neq j$  then  $\Sigma_{gk}^{(ij)}(\mathbf{y}) = \mathbf{0}$  and if  $i = j$  the covariance can be written as

$$\Sigma_{gk}^{(ii)}(\mathbf{y}) = \frac{1}{4}(\mathbf{S}^2\Delta)^{-1} \left[ (\mathbf{S}^{(g)} + m\bar{\mathbf{S}})\tilde{\Sigma}_g(\mathbf{y})(\mathbf{S}^{(g)}) + (\mathbf{S}^{(k)})\tilde{\Sigma}_k(\mathbf{y})(\mathbf{S}^{(k)} + m\bar{\mathbf{S}}) + 2 \sum_{\ell \neq g, k} \mathbf{S}^{(\ell)}\tilde{\Sigma}_\ell(\mathbf{y})\mathbf{S}^{(\ell)} \right] (\mathbf{S}^2\Delta)^{-1}.$$

For  $g = k$ , if  $i \neq j$  then  $\Sigma_{gg}^{(ij)}(\mathbf{y}) = \mathbf{0}$  and if  $i = j$  then  $\Sigma_{gg}^{(ii)}(\mathbf{y}) = \Sigma_g(\mathbf{y})$ .

This result establishes that the asymptotic covariances of the rows of  $\hat{\mathbf{L}}$  is zero for rows corresponding to a different vertex and provides an explicit expression for the covariance of rows of  $\hat{\mathbf{L}}$  corresponding to a common vertex across graphs.

## 4 Statistical Consequences

Having characterized the large-graph properties of the rows of the omnibus embedding under the ESRDPG, we turn to analyzing the statistical consequences of this bias-variance tradeoff both analytically and in experimental settings. We first analyze the mean squared error for estimation of the latent position of the omnibus embedding under the ESRDPG and compare this error to other embedding techniques. Next, we rigorously analyze the ability of various clustering algorithms to detect community structure in individual and multiplex networks when applied to the rows of the omnibus embedding estimates. Finally, we develop a two graph hypothesis test which exploits the distributional results for the estimated latent positions found in Corollary 1.

### 4.1 Latent Position Estimation

To support the theoretical findings discussed in Section 3, we consider a simulation of a three-layer multiplex graph and show that (i) the estimates produced by the omnibus embedding are biased, (ii) they concentrate around the unique rows of  $\mathbf{L}_S$  at the rate given in Theorem 1, and (iii) each unique latent position has a unique, graph-specific variance.

Consider the two-group stochastic block model parameterized by prior class probabilities  $\pi = (0.5, 0.5)$  and block probability matrix  $\mathbf{B} \in \mathbb{R}^{2 \times 2}$ . Under this model,  $F$  is a discrete distribution over two latent positions each with probability  $\frac{1}{2}$ . The specific parameterization we consider is  $\mathbf{x}_1 = (-0.39, 0.32)^T$  and  $\mathbf{x}_2 = (-0.39, -0.32)^T$ . Suppose  $F$  describes this discrete distribution and consider  $(\{\mathbf{A}^{(g)}\}_{g=1}^3, \mathbf{X}) \sim \text{ESRDPG}(F, n, \{\mathbf{C}^{(g)}\}_{g=1}^3)$ . Let  $\mathbf{B}$  and  $\{\mathbf{C}^{(g)}\}_{g=1}^3$  be given by

$$\mathbf{B} = \begin{bmatrix} 0.25 & 0.05 \\ 0.05 & 0.25 \end{bmatrix} \quad \mathbf{C}^{(1)} = \begin{bmatrix} 0.75 & 0 \\ 0 & 0.5 \end{bmatrix} \quad \mathbf{C}^{(2)} = \begin{bmatrix} 0.5 & 0 \\ 0 & 0.75 \end{bmatrix} \quad \mathbf{C}^{(3)} = \begin{bmatrix} 1 & 0 \\ 0 & 0 \end{bmatrix} \quad (2)$$

Marginally,  $\mathbf{A}^{(1)}$  is a down weighted two-group SBM,  $\mathbf{A}^{(2)}$  is a disconnected SBM, and  $\mathbf{A}^{(3)}$  is an Erdős-Rényi network model with parameter 3/20.

We sample each  $\mathbf{A}^{(1)}, \mathbf{A}^{(2)}, \mathbf{A}^{(3)}$  from this ESRDPG for  $n \in \{250, 500, 1000\}$ . For each sample, we construct the omnibus matrix  $\tilde{\mathbf{A}}$  and calculate the omnibus embedding  $\hat{\mathbf{L}}$  in  $d = 2$  dimensions. We look to compare  $\hat{\mathbf{L}}$  to the scaled latent positions  $\mathbf{L}$  as well as the matrix  $\mathbf{L}_S$ . We compare these three quantities in the left panel of Figure 3. The xs represent the points  $\mathbf{S}^{(g)}\mathbf{x}_i$  and the +s represent the points  $\sqrt{\mathbf{C}^{(g)}}\mathbf{x}_i$  for each  $i = 1, 2$  and  $g = 1, 2, 3$ . The colored points are the estimated latent positions. The confidence ellipses are calculated *a priori* from known model parameters and expressions given in Theorem 2. Theorem 1 provides a uniform bound on the rows of  $\hat{\mathbf{L}} - \mathbf{L}_S$ . The right panel of Figure 3, compares the  $\log(nm)/\sqrt{n}$  rate of this bound to the observed residuals from the simulation study.

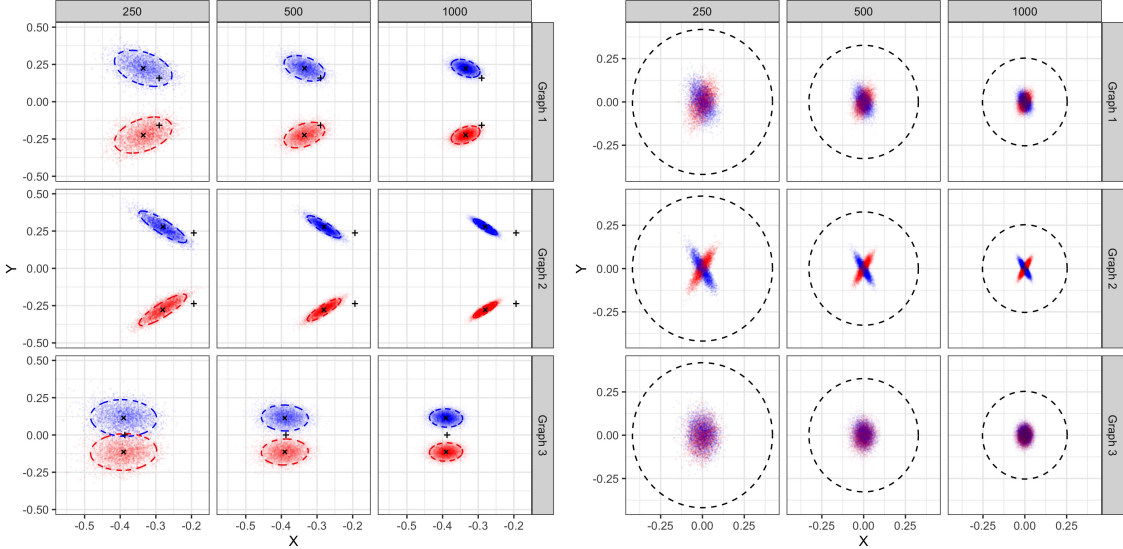


Figure 3: Left panel: Estimated scaled latent positions produced by the omnibus embedding for the ESRDPG in Eq. (2). Rows correspond to each network  $\mathbf{A}^{(1)}, \mathbf{A}^{(2)}, \mathbf{A}^{(3)}$  while columns represent network size. Points correspond to vertices and are colored by community labels. The  $x$ s correspond to the biased estimands  $\mathbf{L}_S$  and the  $+$ s correspond to the original scaled latent positions  $\mathbf{L}$ . Right panel: Centered scaled latent positions  $\hat{\mathbf{L}} - \mathbf{L}_S$ . The dashed balls are of radius  $n^{-1/2} \log 3n$  corresponding to the bound provided in Theorem 1.

The results from Section 3 along with previous results for other embeddings (A. Athreya et al. 2016) allow us to analytically compare the MSE of the omnibus estimator to similar estimators. Namely, we consider the three embedding techniques used in Example 1; the adjacency spectral embedding (ASE) of Sussman et al. (2012), the Abar estimator of R. Tang et al. (2019), and the omnibus estimator as introduced by Levin et al. (2017). As the the omnibus embedding provides  $m$  distinct points in  $\mathbb{R}^d$  corresponding to each vertex  $i \in [n]$ , Levin et al. 2017 propose estimating the scaled latent positions using the rows of the so called *omnibar* matrix

$$\hat{\mathbf{X}}_{\text{Omnibar}} = \frac{1}{m} \sum_{g=1}^m \hat{\mathbf{X}}_{\text{Omnibar}}^{(g)} \quad (3)$$

where  $\hat{\mathbf{X}}_{\text{Omnibar}}^{(g)}$  is the  $g$ -th,  $n \times d$  block matrix of  $\hat{\mathbf{L}}$ . While the distributional properties of the ASE and Abar estimates can be derived from results in A. Athreya et al. (2016), the distribution of the omnibar estimate has not been established. The results of Section 3 allow us to readily derive the asymptotic bias and variance of this estimator.

**Corollary 2.** Let  $\bar{\mathbf{X}} = m^{-1} \sum_{g=1}^m \hat{\mathbf{X}}_{\text{Omnibar}}^{(g)}$  be the omnibar matrix. Let  $\{\mathbf{W}_n\}_{n=1}^\infty$  be as in Theorem 2 and let  $\bar{\mathbf{S}} = m^{-1} \sum_{g=1}^m \mathbf{S}^{(g)}$ . Then the  $i$ -th row of this matrix satisfies

$$\lim_{n \rightarrow \infty} \mathbb{P} [\sqrt{n} (\bar{\mathbf{X}} \mathbf{W}_n - \mathbf{X} \bar{\mathbf{S}})_i \leq \mathbf{x}] = \int_{\text{supp}(F)} \Phi(\mathbf{x}; \mathbf{0}, \Sigma_{\text{OB}}(\mathbf{y})) dF(\mathbf{y})$$

where the variance is given by

$$\Sigma_{\text{OB}}(\mathbf{x}_i) = \frac{1}{4} (\mathbf{S}^2 \Delta)^{-1} \sum_{g=1}^m \left( \bar{\mathbf{S}} + \mathbf{S}^{(g)} \right) \tilde{\Sigma}_g(\mathbf{x}_i) \left( \bar{\mathbf{S}} + \mathbf{S}^{(g)} \right) (\Delta \mathbf{S}^2)^{-1}$$

This result will be helpful in selecting appropriate clustering algorithms for multiplex community detection discussed in the Section 4 as well as facilitate our mean squared error comparisons here. This result

Method	Bias	Variance
ASE	$\mathbf{0}$	$(\sqrt{\mathbf{C}^{(g)}}\Delta)^{-1}\tilde{\Sigma}_g(\mathbf{x}_i)(\Delta\sqrt{\mathbf{C}^{(g)}})^{-1}/n$
Abar	$(\sqrt{\bar{\mathbf{C}}}-\sqrt{\mathbf{C}^{(g)}})\mathbf{x}_i$	$(\sqrt{\bar{\mathbf{C}}}\Delta)^{-1}\sum_{g=1}^m\tilde{\Sigma}_g(\mathbf{x}_i)(\Delta\sqrt{\bar{\mathbf{C}}})^{-1}/m^2n$
Omni	$(\mathbf{S}^{(g)}-\sqrt{\mathbf{C}^{(g)}})\mathbf{x}_i$	$\Sigma_g(\mathbf{x}_i)/n$
Omnibar	$(\bar{\mathbf{S}}-\sqrt{\mathbf{C}^{(g)}})\mathbf{x}_i$	$\Sigma_{OB}(\mathbf{x}_i)/n$

Table 1: The asymptotic bias and variance of the ASE, Abar, omnibus, and omnibar embedding techniques under the ESRDPG.

serves as an example for how Corollary 1 can be used to derive asymptotic distributions of finite linear combinations of rows of  $\hat{\mathbf{L}}$ .

Equipped with asymptotic distributions for all four estimates, we can now compare their the mean squared error for estimating the scaled latent positions. The bias and asymptotic variance of each estimator can be found in Table 1.

The ASE is the only asymptotically unbiased estimator of the scaled latent positions. This method, however, ignores common structure among the networks and as a consequence suffers higher variance than the other methods. The remaining methods all incur bias in the direction of the true latent position  $\mathbf{x}_i$ , but are unbiased when  $\mathbf{C}^{(g)} = \mathbf{I}$ .

The comparison of variances under the ESRDPG is a more complicated undertaking. The variance introduced in Theorem 2 and Corollary 2 can be interpreted as linear combinations of the individual network variances  $\tilde{\Sigma}_g(\mathbf{x}_i)$  with weights given by the scaling matrices  $\{\mathbf{S}^{(g)}\}_{g=1}^m$ . This interpretation becomes more clear for the omnibar estimator where we see each  $\mathbf{S}^{(g)}$  is included in the scaling of each  $\tilde{\Sigma}_g(\mathbf{x}_i)$ . The variance of ASE and Abar can be seen as a normalization of the graph variance  $\tilde{\Sigma}_g(\mathbf{x}_i)$  by pre and post multiplying either  $(\sqrt{\mathbf{C}^{(g)}})^{-1}$  or  $(\sqrt{\bar{\mathbf{C}}})^{-1}$ . In the i.i.d. setting,  $\tilde{\Sigma}_g(\mathbf{x}_i) = \tilde{\Sigma}(\mathbf{x}_i)$  for all  $g \in [m]$  and the Abar variance reduces to  $\Delta^{-1}\tilde{\Sigma}(\mathbf{x}_i)\Delta^{-1}/mn$ . This expression was presented in Theorem C.1 of R. Tang et al. 2019 and highlights the variance reduction enjoyed by the Abar embedding.

As the MSE of each estimator is somewhat difficult to interpret for general model parameters, we turn to a simulation study, as in Figure 2, to demonstrate the relative performance of these methods and the accuracy of the asymptotic bias-variance results.

**Example 2.** Suppose that  $F$  corresponds to the two-group SBM introduced in Figure 3. Next assume that  $(\{\mathbf{A}^{(g)}\}_{g=1}^2, \mathbf{X}) \sim \text{ESRDPG}(F, n = 100, \{\mathbf{C}^{(g)}\}_{g=1}^2)$  where  $\mathbf{C}^{(1)} = \mathbf{I}$  and  $\mathbf{C}^{(2)}$  is given by

$$\mathbf{C}^{(2)} = \mathbf{C}(t) = \begin{bmatrix} t+1 & 0 \\ 0 & 1-t \end{bmatrix} \quad t \in [0, 1]. \quad (4)$$

For  $t = 0$ ,  $\mathbf{C}^{(2)} = \mathbf{I}$  and hence  $\mathbf{A}^{(1)}$  and  $\mathbf{A}^{(2)}$  follow the same marginal distribution. When  $t = 1$ ,  $\mathbf{A}^{(2)}$  follows an Erdős-Rényi with parameter  $p = 0.3$ . Under this model, we look to estimate four latent positions; one for each community in each network. As in Example 1, we compare the mean squared error of the ASE, Abar, and Omni estimators as well as the Omnibar estimator for different values of  $t \in [0, 1]$  for  $T = 500$  Monte Carlo replicates. For each replicate, we plot the average empirical vertex-level mean square error as a point in Figure 4. The lines represent the theoretical mean square error computed via the asymptotic distributions.

This figure is consistent with Example 1. For  $t$  near zero, the networks share near identical marginal distributions and the Abar and the Omnibar estimators outperform the ASE and Omni estimators in estimating the latent positions for each community in each graph. The omnibus embedding becomes the preferred estimator in Graph 1 for  $t \geq 0.3$  and in Graph 2 for  $t \geq 0.55$  due to its favorable bias-variance tradeoff. Moreover, these figures suggest that the Omni estimator is the most robust estimator of the four embedding techniques considered here. Note that embedding the networks individually (ASE) is never the optimal estimator for these graph parameters.

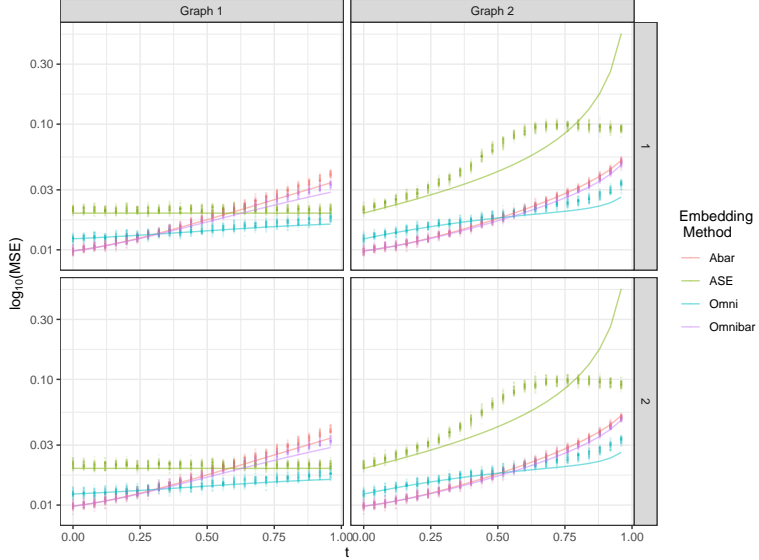


Figure 4: Comparing the MSE of four estimators as a function of  $t$ . At  $t = 0$  the  $\mathbf{A}^{(1)}$  and  $\mathbf{A}^{(2)}$  have the same marginal distribution - a two group SBM. At  $t = 1$ ,  $\mathbf{A}^{(1)}$  is a two group SBM and  $\mathbf{A}^{(2)}$  is an Erdős-Rényi graph. Columns correspond to the two networks and rows to the different communities within each network.

For latent position in Graph 1, the MSE of the ASE method does not depend on  $t$  and has better performance than Abar and Omnibar for  $t \geq 0.5$  where the bias dominates the MSE of the  $\bar{\mathbf{A}}$  embedding when the graphs have very different structure. For latent positions in Graph 2, the MSE of the ASE method is growing as a function of  $t$ . As  $t$  nears 1,  $\mathbf{A}^{(2)}$  is approximately distributed according to an Erdős-Rényi random graph with parameter  $p = 0.3$ . As this model can be captured by a one dimensional RDPG, this increased MSE and the deviation away from the theoretical line can be explained by the fact that we are embedding  $\mathbf{A}^{(2)}$  into a  $d = 2$  dimensional space which adds additional noise to this estimate. Moreover, as the size of each community is  $n = 50$ , the effective sample size for each ASE estimate is small. However, in general, these finite sample MSE's match closely with our theoretical results derived from asymptotic distributional results.  $\square$

The omnibus embedding can robustly estimate latent positions under a heterogeneous network structure due to its favorable bias-variance tradeoff. This tradeoff will further benefit the performance of downstream statistical analysis.

## 4.2 Community Detection

The omnibus embedding provides  $m$  separate node embeddings in  $\mathbb{R}^d$  corresponding to each vertex. With a Euclidean representation of each network, familiar techniques from statistics and machine learning can be employed to complete multiple network inference. For example, by applying clustering techniques for Euclidean data to the node embeddings produced by the omnibus embedding, we can readily complete community detection tasks. Our results enable a rigorous analysis of the performance of these clustering techniques when applied to the omnibus node embeddings. In this section we consider the performance of the k-means and Gaussian Mixture Model (GMM) clustering algorithms. We analyze these methods both theoretically and in simulation studies and highlight the ramifications of the bias-variance tradeoff of the omnibus embedding. In Section 4.2.1 we consider individual network community detection (i.e. identifying community structure for each layer separately) and in Section 4.2.2 we consider multiplex community detection (i.e. identifying community structure shared across layers).

### 4.2.1 Individual Network Performance

In this section we focus on identifying communities in individual networks for each  $g \in [m]$  by clustering the rows of  $\hat{\mathbf{X}}_{\text{Ommi}}^{(g)}$ . In particular, we consider community detection under Stochastic Block Model (SBM) where  $F$  is a discrete distribution over  $\{\mathbf{x}_k\}_{k=1}^K \subset \mathbb{R}^d$  with respective probabilities  $\{\pi_k\}_{k=1}^K \subset (0, 1)$  with  $\sum_{k=1}^K \pi_k = 1$ . Under the RDPG, vertices  $i, j \in [n]$  belong to the same community if and only if  $\mathbf{X}_i = \mathbf{X}_j$ . Recall, Theorem 1 established that the rows of  $\hat{\mathbf{X}}_{\text{Ommi}}^{(g)}$  concentrate around the scaled cluster centers  $\{\mathbf{S}^{(g)}\mathbf{x}_k\}_{k=1}^K$ . For k-means to achieve exact recovery of community labels in finite sample networks, these scaled cluster centers must be sufficiently separated. That is, provided

$$\|\mathbf{S}^{(g)}(\mathbf{x}_i - \mathbf{x}_j)\|_2 > \beta(m, n, \pi),$$

where  $\beta(m, n, \pi)$  is a constant depending on model parameters that satisfies  $\beta = \omega(m^{3/2}n^{-1/2} \log nm)$ , for fixed  $\{\mathbf{x}_i\}_{i=1}^K$  and  $\pi$ , then k-means attains exact recovery with high probability when applied to the rows of the matrix  $\hat{\mathbf{X}}_{\text{Ommi}}^{(g)}$ . An analogous analysis of k-means applied to the rows of  $\hat{\mathbf{X}}_{\text{ASE}}^{(g)}$  was completed in Vince Lyzinski et al. (2014). As the rows of the matrix  $\hat{\mathbf{X}}_{\text{ASE}}^{(g)}$  concentrate around the vectors  $\{\mathbf{x}_k\}_{k=1}^K$ , exact recovery is achieved provided the points  $\{\mathbf{x}_k\}_{k=1}^K$  are sufficiently separated. As the argument here follows *mutatis mutandis* from Theorem 2.6 of Vince Lyzinski et al. (2014) with the application of Theorem 1, we refer the reader to this analysis and and remark these results can similarly be extended to the Degree Corrected Stochastic Block Model (DCSBM). These different separation requirements highlight the ramifications the bias introduced by the omnibus embedding plays in the analysis of individual community detection.

We next consider alternative clustering techniques to identify community structure. Suppose again that  $F$  corresponds to a SBM. Then under the RDPG parameterization of the SBM, conditioning on a vertex's community assignment is equivalent to conditioning on its latent position  $\{\mathbf{X}_i = \mathbf{x}_i\}$  which gives rise to the distributional result in Corollary 3.

**Corollary 3.** In the context of Theorem 2, suppose that  $\mathbf{x} \in \text{supp}(F)$  such that  $\mathbb{P}(\mathbf{X}_i = \mathbf{x}) > 0$ . Then conditional on  $\{\mathbf{X}_i = \mathbf{x}\}$

$$\lim_{n \rightarrow \infty} \mathbb{P} \left[ \sqrt{n}(\hat{\mathbf{L}}\mathbf{W}_n - \mathbf{L}_S)_h \leq \mathbf{z} | \mathbf{X}_i = \mathbf{x} \right] = \Phi(\mathbf{z}; \mathbf{0}, \Sigma_g(\mathbf{x}_k)) \quad (5)$$

The community specific covariance  $\Sigma_g(\mathbf{x}_k)$  in Corollary 3 suggests the use of GMM fit using the EM algorithm as this algorithm can flexibly incorporate differing variance structures between communities. To further understand the ramifications of this graph specific variance, we investigate the Mahalanobis distance between cluster centers for each embedding method considered; ASE, Abar, Omni, and Omnibar. Optimal embedding methods will both separate the centroids sufficiently and reduce dispersion around these centroids as both contribute to clustering performance. By analyzing the Mahalanobis distance between centroids, we can quantify the difficulty of the community detection task with respect to both centroid separation and the node embeddings' dispersion imposed by each method.

**Example 2. (continued)** In the context of Example 2, for a grid of values in  $t \in [0, 1]$  we estimate  $\{\hat{\mathbf{X}}_{\text{Ommi}}^{(g)}, \hat{\mathbf{X}}_{\text{ASE}}^{(g)}, \hat{\mathbf{X}}_{\text{Abar}}^{(g)}, \hat{\mathbf{X}}_{\text{Omnibar}}^{(g)}\}$  and then perform GMM clustering on the rows of each matrix. Using these community assignment estimates, we then estimate the Mahalanobis distance between the first and second community centroid for each network. To estimate these distances we calculate

$$d(\bar{\mathbf{x}}_1, \bar{\mathbf{x}}_2) = (\bar{\mathbf{x}}_1 - \bar{\mathbf{x}}_2)^T \hat{\Sigma}^{-1} (\bar{\mathbf{x}}_1 - \bar{\mathbf{x}}_2)$$

where  $\bar{\mathbf{x}}_i$  is mean of the rows of  $\hat{\mathbf{X}}$  classified to community  $i$  and  $\hat{\Sigma}^{-1}$  is the standard pooled variance estimate. We visualize these distances as a function of  $t$  in Figure 5.

As  $t$  increases, the estimated distance between cluster centers decreases for all methods save  $\hat{\mathbf{X}}_{\text{ASE}}^{(1)}$  as this embedding method is independent of  $t$ . As  $t$  approaches 1,  $\mathbf{A}^{(2)}$  is approaching an Erdős-Rényi graph and we therefore expect the community detection task to become more difficult. This increased difficulty

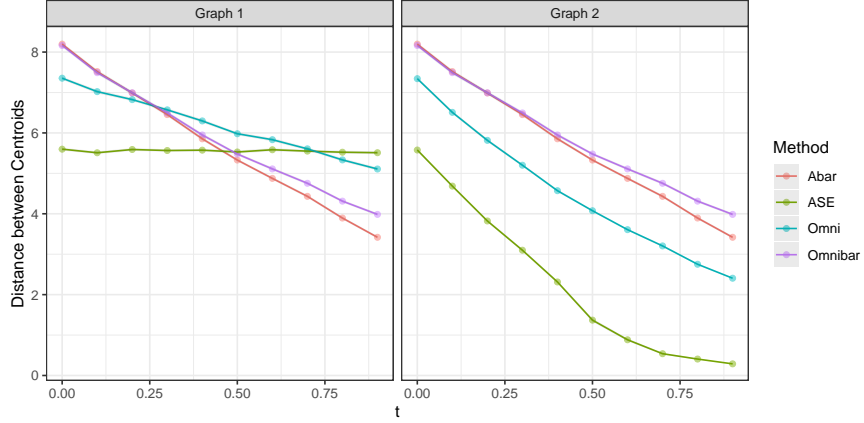


Figure 5: Estimated Mahalanobis distance between cluster centers as a function of  $t$ . As  $t$  increases, the distance between clusters decrease.

is captured by the decrease in distance between centroids. In Graph 1, for  $t \leq 0.25$  the distance between centers of  $\hat{\mathbf{X}}_{\text{Abar}}$  and  $\hat{\mathbf{X}}_{\text{Omnibar}}$  are the greatest. As the networks become more heterogeneous however, these distances quickly become smaller than the distances corresponding to  $\hat{\mathbf{X}}_{\text{Omni}}$  ( $t \in [.25, .75]$ ) and  $\hat{\mathbf{X}}_{\text{ASE}}$  ( $t \in [.75, 1]$ ). In Graph 2, the distance corresponding to  $\hat{\mathbf{X}}_{\text{Omnibar}}$  is the greatest for all  $t$  followed by  $\hat{\mathbf{X}}_{\text{Abar}}$ ,  $\hat{\mathbf{X}}_{\text{Omni}}$ , and then  $\hat{\mathbf{X}}_{\text{ASE}}$ . These distances demonstrate that the optimal embedding technique for individual network community detection greatly depends on the level of heterogeneity between the two networks.  $\square$

Corollary 3 gives an exact limiting distribution but this distribution is only approximate for finite  $n$ . Moreover, while Corollary 1 establishes asymptotic independence between  $(\hat{\mathbf{X}}_{\text{Omni}}^{(g)})_i$  and  $(\hat{\mathbf{X}}_{\text{Omni}}^{(g)})_j$  for  $i \neq j$ , for finite  $n$  these estimates are correlated. Nonetheless, these results motivate the use of a pseudo-likelihood method that assume the rows of  $\hat{\mathbf{X}}_{\text{Omni}}^{(g)}$  are independent, normally distributed vectors. Let  $\mathbf{Z} \in [K]^n$  be a vector in which  $\mathbf{Z}_i$  is the community assignment of vertex  $i$ . Then the pseudo-likelihood has the form of a GMM and is defined as

$$\mathcal{PL}(\hat{\mathbf{X}}_{\text{Omni}}^{(g)}, \mathbf{Z}) = \prod_{i=1}^n p((\hat{\mathbf{X}}_{\text{Omni}}^{(g)})_i | \mathbf{Z}_i) p(\mathbf{Z}_i) = \prod_{i=1}^n \prod_{k=1}^K \pi_k^{I(\mathbf{Z}_i=k)} \phi(\mathbf{S}^{(g)} \mathbf{x}_k, n^{-1} \Sigma_g(\mathbf{x}_k))^{I(\mathbf{Z}_i=k)}$$

where  $\phi(\mu, \Sigma)$  is the density function of a normal random variable with mean  $\mu$  and covariance  $\Sigma$ .

The maximization step is slightly more complex than that of a standard in GMM as the variance is mean dependent and hence represent a curved sub-family of the multivariate normal model. However, to avoid difficulty, we implement the traditional GMM algorithm to derive estimates for the model parameters  $(\pi, \mathbf{S}^{(g)} \mathbf{x}_k, n^{-1} \Sigma_g(\mathbf{x}_k))$  and community assignment vector  $\mathbf{Z}$ .

Having introduced and analyzed two approaches to individual network community detection, we now analyze their performance in a simulation setting. As the GMM is equipped to utilize community specific variance structures, we compare the clustering performance of GMM clustering using the estimated latent positions  $\{\hat{\mathbf{X}}_{\text{Omni}}^{(g)}, \hat{\mathbf{X}}_{\text{ASE}}^{(g)}, \hat{\mathbf{X}}_{\text{Abar}}^{(g)}, \hat{\mathbf{X}}_{\text{Omnibar}}^{(g)}\}$ .

**Example 2. (continued)** For  $t = 0.5$  and a grid of network sizes between 25 and 250, we estimate  $\{\hat{\mathbf{X}}_{\text{Omni}}^{(g)}, \hat{\mathbf{X}}_{\text{ASE}}^{(g)}, \hat{\mathbf{X}}_{\text{Abar}}^{(g)}, \hat{\mathbf{X}}_{\text{Omnibar}}^{(g)}\}$  and then perform GMM clustering on the rows of each matrix. From here we calculate the misclassification rate for each method. Finally, we complete 200 Monte Carlo replicates. Figure 6 compares the misclassification rate of each method as a function to the network size.

As network size increases, the performance of each method improves. For vertices in Graph 1, it appears that all methods behave almost identically with the clustering on the rows of  $\hat{\mathbf{X}}_{\text{Omni}}^{(1)}$  perhaps being the preferable method. For vertices in Graph 2, it is clear that clustering performance on the rows of  $\hat{\mathbf{X}}_{\text{ASE}}^{(2)}$  is

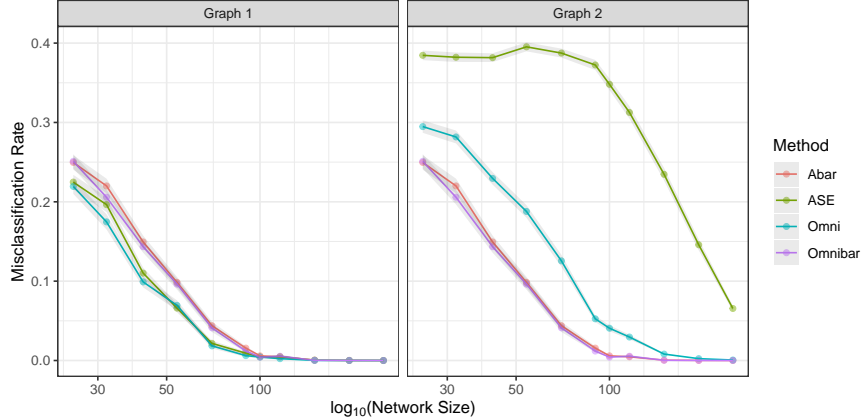


Figure 6: For  $t = 0.5$ , a plot of the misclassification rate for each method as a function of network size. As network size increases, each method approaches exact recovery.

poor in comparison to other methods. This is not surprising as  $\mathbf{A}^{(2)}$  is approaching an Erdős-Rényi model. The methods that combine the structure of  $\mathbf{A}^{(1)}$ ,  $\mathbf{A}^{(2)}$  are preferable in this setting. In particular, clustering on the rows of  $\hat{\mathbf{X}}_{\text{Omnibar}}$  or  $\hat{\mathbf{X}}_{\text{Abar}}$  appear to be the optimal methods in this setting. Clustering on the rows of  $\hat{\mathbf{X}}_{\text{Omni}}$  lags behind these approaches as it more accurately reflects the changes in the latent positions in Graph 2. We note that the distances corresponding to  $t = 0.5$  in Figure 5 almost perfectly corresponds with the clustering performance as seen in the Figure 6.  $\square$

#### 4.2.2 Multiplex Network Performance

To this point, we have only considered the ability of the omnibus embedding to detect community structure within individual layers. To broaden this analysis, we consider the ability of this method to recover communities shared across layers, the multiplex community detection task. In an attempt to use the representation of all  $m$  networks, following Levin et al. (2017) one could apply clustering algorithms to the rows of the Omnibar matrix,  $\bar{\mathbf{X}}$ , to estimate a global community assignment vector. Recall that Corollary 2 gives an asymptotic distributional characterization of the rows of  $\bar{\mathbf{X}}$ , enabling a similar analysis of these multiplex clustering algorithms as was completed in the individual network setting. By an identical argument as presented in the individual network setting, with high probability,  $k$ -means clustering applied to the rows of  $\bar{\mathbf{X}}$  achieves error free classification provided the unique rows of  $\bar{\mathbf{X}}\mathbf{S}$  are sufficiently separated. Moreover, under the SBM, the rows of  $\bar{\mathbf{X}}$  are distributed according to a finite mixture of normal distributions motivating the use of the GMM for independent, normally distributed data.

Having summarized two approaches to multiplex community detection that utilize the omnibus embedding, we compare their performance to competing methods in the following simulation studies. In these settings, we only consider the GMM approach as it uniformly outperformed  $k$ -means. We compare the performance of this algorithm when applied to the omnibus embedding, Multiple Adjacency Spectral Embedding (MASE) of Arroyo et al. (2019), the Multiple Random Dot Product Graph (MRDPG) of Nielsen and Witten (2018), and the Joint Embedding of Graphs (JE) of S. Wang et al. (2017). We refer the reader to Section 2.1 for an overview of these models.

**Example 2. (continued)** In the context of Example 2, we consider the task recovering the community labels for different values of  $t$ . We attain estimates of the community assignment for each method described above by training the GMM clustering algorithm on the rows of  $\hat{\mathbf{U}}_{\text{JE}}$ ,  $\hat{\mathbf{U}}_{\text{MRDPG}}$ ,  $\hat{\mathbf{U}}_{\text{MASE}}$ , and  $\hat{\mathbf{X}}_{\text{Omnibar}}$ . In addition, we consider the GMM trained to the rows of  $\hat{\mathbf{X}}_{\text{ASE}}^{(1)}$  and  $\hat{\mathbf{X}}_{\text{ASE}}^{(2)}$ , and denote these methods as ASE1 and ASE2, respectively. We sample networks of size  $n = 100$  and attain these estimated community labels for each method for 500 Monte Carlo iterations. The results of this simulation can be found in Figure 7.

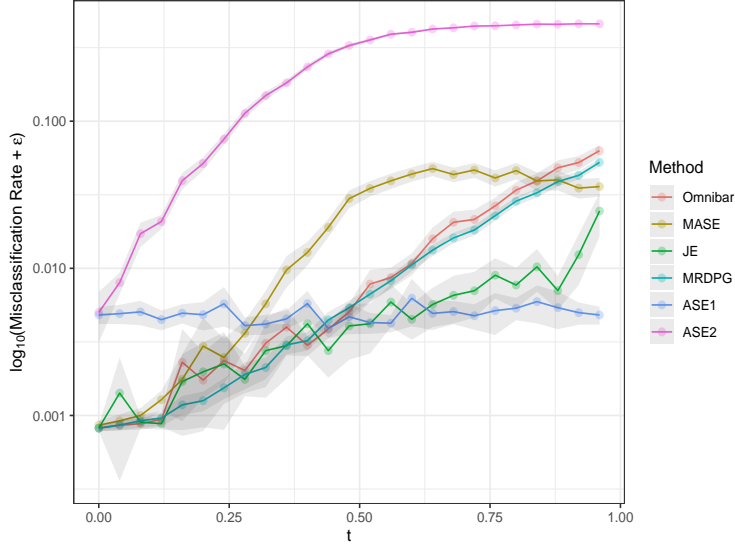


Figure 7: Comparing misclassification rates of multiple network community detection methods. As  $t$  increases, the second network's community structure is less pronounced, resulting in a more difficult community detection task.

From Figure 7 it is clear that as the second network begins to lose its community structure the performance of each method, save ASE1, declines. As  $\hat{\mathbf{X}}_{\text{ASE}}^{(1)}$  is independent of  $t$ , the misclassification rate is constant with respect to  $t$ . In contrast, as the rows of  $\hat{\mathbf{X}}_{\text{ASE}}^{(2)}$  concentrate around a single point for both communities as  $t$  approaches 1 and as a result the misclassification rate approaches that of random chance 1/2.

For small values of  $t$ ,  $t \in [0, 0.25]$ , it appears that each multiplex community detection method achieves similar misclassification rates and improves that of the individual network approaches ASE1 and ASE2. As  $t$  increases to moderate sizes,  $t \in [0.25, 0.5]$ , the JE method appears to become the preferred method, followed by Omnibar and MRDPG. Indeed, the JE is optimal for almost all values of  $t$  except for those near 1, where no multiplex approach improves on simply clustering the first graph. The Omnibar and MRDPG demonstrate similar performance and are preferable over the individual network performance of ASE1 for  $t \leq 0.5$ . The MASE community detection method is the least preferable multiplex method considered in this simulation yet offers improvement over the individual network approaches for  $t \leq 0.3$ .  $\square$

Example 2 establishes that multiplex community detection methods may be preferable to individual network algorithms for two networks with similar structure. As  $m$  increases, however, we expect multiplex community detection methods to outperform individual network algorithms even when the networks have much different edge probabilities. To that end, consider following simulation study.

Suppose that  $(\{\mathbf{A}^{(g)}\}_{g=1}^4, \mathbf{X}) \sim \text{ESRDPG}(F, n = 100, \{\mathbf{C}^{(g)}\}_{g=1}^4)$  where  $F$  corresponds to a SBM with  $K = 3$  groups. Let  $\mathbf{B}$  be the block probability matrix given by

$$\mathbf{B} = \begin{bmatrix} 0.3 & 0.1 & 0.1 \\ 0.1 & 0.25 & 0.15 \\ 0.1 & 0.15 & 0.25 \end{bmatrix}.$$

corresponding to latent positions  $\mathbf{x}_1 = (0.41, -0.37, 0)^T$ ,  $\mathbf{x}_2 = (0.41, 0.18 - 0.23)^T$ , and  $\mathbf{x}_3 = (0.41, 0.18, 0.23)^T$ . Moreover, suppose the four weighting matrices are given by

$$\mathbf{C}^{(1)} = \mathbf{I} \quad \mathbf{C}^{(2)}(t) = \begin{bmatrix} 1 & 0 & 0 \\ 0 & 1 & 0 \\ 0 & 0 & 1-t \end{bmatrix} \quad \mathbf{C}^{(3)}(t) = \begin{bmatrix} 1 & 0 & 0 \\ 0 & 1-t & 0 \\ 0 & 0 & 1 \end{bmatrix} \quad \mathbf{C}^{(4)}(t) = \begin{bmatrix} 1 & 0 & 0 \\ 0 & 1-t & 0 \\ 0 & 0 & 1-t \end{bmatrix}$$

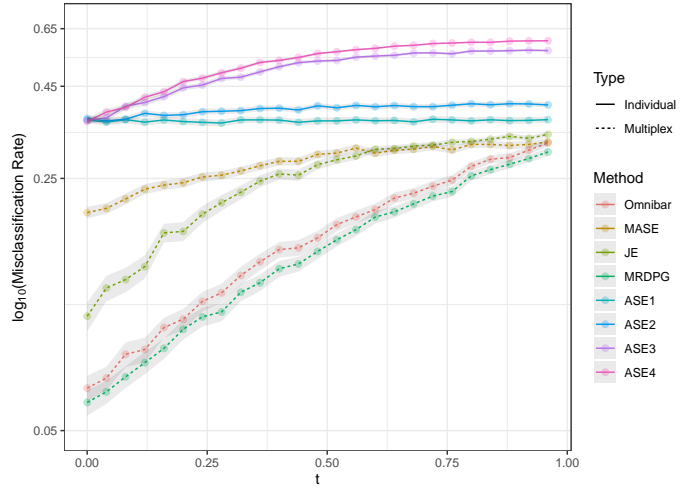


Figure 8: Comparing misclassification rates of multiple network community detection methods. As  $t$  increases, the networks become more heterogeneous and resulting in a more difficult community detection task. The MRDPG or Omni method offer the best performance for all values of  $t$ .

for  $t \in [0, 1]$ . As above,  $t$  parameterizes the distance from homogeneity. At  $t = 1$ ,  $\mathbf{A}^{(2)}|\mathbf{X}$  corresponds to a  $K = 2$  group SBM,  $\mathbf{A}^{(3)}|\mathbf{X}$  corresponds a  $K = 3$  group SBM with different connectivity structure, and  $\mathbf{A}^{(4)}|\mathbf{X}$  corresponds to an Erdős-Rényi graph. We sample networks of size  $n = 100$  and attain estimated community labels from the GMM for each method 500 times. The results of this simulation can be found in Figure 8.

From Figure 8 it is clear as the networks become more heterogeneous the performance of each multiplex method declines. However, each multiplex method outperforms every individual network algorithm for every value of  $t \in [0, 1]$ . For small to moderate values of  $t$ ,  $t \in [0, 0.6]$  it appears that the MRDPG methods is preferable followed closely by the Omnibar method. In contrast to Example 2, the JE clustering technique never appears to be competitive in this setting possibly suggesting this approach is able to effectively pool information across few networks but not across many networks with similar structure. The MASE technique suffers the worst misclassification rate for homogeneous networks (i.e.  $t = 0$ ) but appears to be relatively stable with respect to  $t$ . This could suggest that MASE, while effective at modeling a larger class of heterogeneous networks, does not integrate information shared across networks under the ESRDPG as readily as the MRDPG or Omnibar approaches.

### 4.3 Hypothesis Testing

Under the ESRDPG, we parameterize network differences through the graph specific weighting matrices  $\{\mathbf{C}^{(g)}\}_{g=1}^m$ . In this section, we consider the task of testing the hypothesis that two networks drawn from the ESRDPG share the same scaling matrix:

$$H_0 : \mathbf{C}^{(1)} = \mathbf{C}^{(2)} \quad H_A : \mathbf{C}^{(1)} \neq \mathbf{C}^{(2)}.$$

Recall, as the scaling matrices  $\mathbf{S}^{(1)}$  and  $\mathbf{S}^{(2)}$  are one-to-one functions of  $\mathbf{C}^{(1)}$  and  $\mathbf{C}^{(2)}$ , we see that  $\mathbf{C}^{(1)} = \mathbf{C}^{(2)}$  if and only if  $\mathbf{S}^{(1)} = \mathbf{S}^{(2)}$ . Furthermore, as  $\mathbf{X}$  is full rank,  $\mathbf{S}^{(1)} = \mathbf{S}^{(2)}$  if and only if  $\mathbf{X}\mathbf{S}^{(1)} = \mathbf{X}\mathbf{S}^{(2)}$ . That is, an equivalent hypothesis test is given by

$$H_0 : \mathbf{X}\mathbf{S}^{(1)} = \mathbf{X}\mathbf{S}^{(2)} \quad H_A : \mathbf{X}\mathbf{S}^{(1)} \neq \mathbf{X}\mathbf{S}^{(2)}.$$

Theorem 1 probabilistically ensures that the matrix  $\hat{\mathbf{D}} = \hat{\mathbf{X}}_{\text{Omnibar}}^{(1)} - \hat{\mathbf{X}}_{\text{Omnibar}}^{(2)}$  will reflect differences in  $\mathbf{C}^{(1)}$  and  $\mathbf{C}^{(2)}$ . For this reason, it will be useful to derive the asymptotic distribution of the rows of  $\hat{\mathbf{D}}$  which in turn

will help uncover asymptotic distributions of global asymptotic test statistics that rely on these row-wise differences.

**Corollary 4.** Let  $i \in [n]$  be some row of  $\hat{\mathbf{D}}$  and let  $\{\mathbf{W}_n\}_{n=1}^\infty$  be as in Theorem 2. Then we have the distributional result

$$\lim_{n \rightarrow \infty} \mathbb{P} \left[ \sqrt{n} (\hat{\mathbf{D}} \mathbf{W}_n - \mathbf{X}(\mathbf{S}^{(1)} - \mathbf{S}^{(2)}))_i \leq \mathbf{x} \right] = \int_{\text{supp}(F)} \Phi(\mathbf{x}; \mathbf{0}, \Sigma_D(\mathbf{y})) dF(\mathbf{y})$$

where the variance is given by

$$\Sigma_D(\mathbf{y}) = (\mathbf{S}^2 \Delta)^{-1} \bar{\mathbf{S}}(\tilde{\Sigma}_1(\mathbf{y}) + \tilde{\Sigma}_2(\mathbf{y})) \bar{\mathbf{S}}(\mathbf{S}^2 \Delta)^{-1}$$

The proof of this Theorem is a straightforward application of Corollary 1. Notice that this variance is not simply  $\Sigma_1(\mathbf{y}) + \Sigma_2(\mathbf{y})$  again illustrating that the rows of  $\hat{\mathbf{L}}$  corresponding to the same vertex are asymptotically correlated. This additional covariance will slightly complicate the analysis of our test statistic but provides an explicit covariance useful in construction of Wald statistics to detect vertex level differences.

Levin et al. (2017) compare the test statistic  $T = \|\hat{\mathbf{D}}\|_F^2$  to a reference distribution constructed through Monte Carlo iterations under the null hypothesis. In simulation settings, this test statistic demonstrates higher empirical power than a Procrustes based test introduced by M. Tang et al. (2017) that utilizes individual network embeddings. We stress that this statistic does not correct for row-wise correlation in  $\hat{\mathbf{D}}$  and relies on a reference distribution that is constructed with prior knowledge of the latent positions  $\mathbf{X}$ . In an attempt to remedy these issues, we propose a test statistic that does not rely on unknown model parameters and utilizes the covariance expressions presented in Corollary 4. As the test statistic  $T$  is computed based on Euclidean rather than Mahalanobis distances, we expect our test statistic will offer improvements in practice over that of  $T$ . We propose a Wald statistic for each row of  $\hat{\mathbf{D}}$  which we present in Theorem 3.

**Theorem 3.** Let  $\mathbf{D}(\mathbf{x}) = (\mathbf{S}^{(1)} - \mathbf{S}^{(2)})\mathbf{x}$  and let  $F_{\chi_d^2}(x)$  be the cumulative distribution function of a  $\chi^2$  random variable with  $d$  degrees of freedom. The asymptotic distribution of the statistic  $W_i = \hat{\mathbf{D}}_i^T \Sigma_D^{-1}(\mathbf{X}_i) \hat{\mathbf{D}}_i$  under both hypotheses is given by

$$\begin{aligned} H_0 : \lim_{n \rightarrow \infty} \mathbb{P}[nW_i \leq x] &= F_{\chi_d^2}(x) \\ H_A : \lim_{n \rightarrow \infty} \mathbb{P} \left[ \sqrt{n}[W_i - \mathbf{D}(\mathbf{X}_i)^T \Sigma_D^{-1}(\mathbf{X}_i) \mathbf{D}(\mathbf{X}_i)] \leq x \right] &= \int_{\text{supp}F} \Phi(\mathbf{x}; \mathbf{0}, 4\mathbf{D}(\mathbf{y})^T \Sigma_D^{-1}(\mathbf{y}) \mathbf{D}(\mathbf{y})) dF(\mathbf{y}) \end{aligned}$$

This statistic is only constructed for each row of  $\hat{\mathbf{D}}$  but suggests a global test statistic to test the full network hypothesis  $H_0 : \mathbf{X}\mathbf{S}^{(1)} = \mathbf{X}\mathbf{S}^{(2)}$ . We propose using the statistic  $W = \sum_{i=1}^n W_i$  for this network wide testing task. Notice that if each  $W_i$  were independent for finite  $n$ , under the null  $W$  would follow a  $\chi_{nd}^2$  distribution. However, as the rows of  $\hat{\mathbf{D}}$  are not independent, we assume  $W$  is *approximately* distributed as  $\chi_{nd}^2$  as a principled approach to testing  $H_0 : \mathbf{C}^{(1)} = \mathbf{C}^{(2)}$ . This assumption is similar to that made in the application of the GMM for community detection and has minimal effects in practice for moderate network sizes as demonstrated in our simulation study.

To this point, the test statistics  $W$  still relies on unknown model parameters,  $\Sigma_D(\mathbf{X}_i)$ , which will need to be estimated in practice. We propose a combination of method of moments estimators to estimate  $\Sigma_D(\mathbf{X}_i)$  under  $H_0$ . Under the null hypothesis,  $\Sigma_D(\mathbf{X}_i)$  takes the form

$$\Sigma_D(\mathbf{X}_i) = \frac{\Delta^{-1} \tilde{\Sigma}(\mathbf{X}_i) \Delta^{-1}}{2}$$

where  $\tilde{\Sigma}(\mathbf{X}_i) = \mathbb{E}[(\mathbf{X}_i^T \mathbf{X}_j - (\mathbf{X}_i^T \mathbf{X}_j)^2) \mathbf{X}_j \mathbf{X}_j^T]$ . Due to Theorem 1, under the null hypothesis  $\hat{\mathbf{L}}$  concentrates around  $\mathbf{L}_S \mathbf{W}_n^T = \mathbf{1}_m \otimes \mathbf{X}$ . Moreover  $(nm)^{-1} \mathbf{L}^T \mathbf{L} = m^{-1} \sum_{g=1}^m n^{-1} \mathbf{X}^T \mathbf{X} \xrightarrow{a.s.} \Delta$ . Therefore we use  $((nm)^{-1} \hat{\mathbf{L}}^T \hat{\mathbf{L}})^{-1}$  as an estimator for  $\Delta^{-1}$ . By Corollary 2, under the null  $\bar{\mathbf{X}}_j$  concentrates around  $\mathbf{X}_j$ . Using

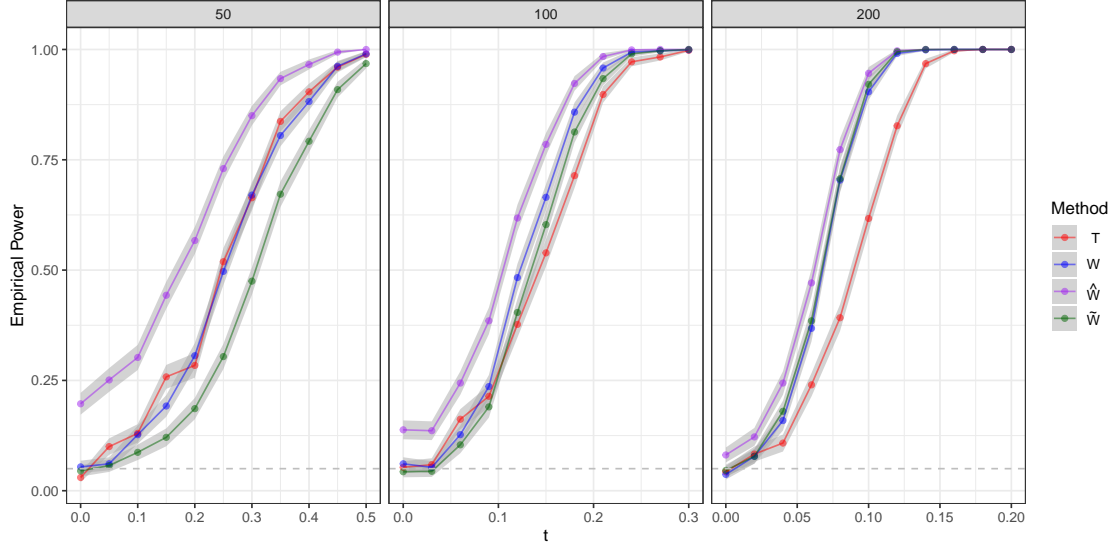


Figure 9: The empirical power of  $T$ ,  $W$ ,  $\hat{W}$ , and  $\tilde{W}$  for testing  $H_0 : \mathbf{I} = \mathbf{C}(t)$  in the context of Example 2 for differing values of  $t$ .

this result we can estimate  $\hat{\Sigma}(\mathbf{X}_i)$  by

$$\hat{\Sigma}(\mathbf{x}_i) = \frac{1}{n-1} \sum_{j \neq i} (\bar{\mathbf{X}}_i^T \bar{\mathbf{X}}_j - (\bar{\mathbf{X}}_i^T \bar{\mathbf{X}}_j)^2) \bar{\mathbf{X}}_j \bar{\mathbf{X}}_j^T$$

Combining these estimates, the covariance estimate can be written as

$$\hat{\Sigma}_D(\mathbf{X}_i) = \frac{1}{2} \left( \frac{1}{nm} \hat{\mathbf{L}}^T \hat{\mathbf{L}} \right)^{-1} \left( \frac{1}{n-1} \sum_{j \neq i} (\bar{\mathbf{X}}_i^T \bar{\mathbf{X}}_j - (\bar{\mathbf{X}}_i^T \bar{\mathbf{X}}_j)^2) \bar{\mathbf{X}}_j \bar{\mathbf{X}}_j^T \right) \left( \frac{1}{nm} \hat{\mathbf{L}}^T \hat{\mathbf{L}} \right)^{-1}.$$

To ensure that this estimate is positive semi-definite, we then project this matrix onto the p.s.d. cone, denoted  $\hat{\Sigma}_D(\mathbf{X}_i)^+$ . Given our estimates for  $\Sigma_D(\mathbf{X}_i)$ , we define our estimates  $\hat{W}_i$  as

$$\hat{W}_i = n^{-1} \hat{\mathbf{D}}_i^T (\hat{\Sigma}_D^+(\mathbf{X}_i))^{\dagger} \hat{\mathbf{D}}_i$$

and our estimate of  $W$  as  $\hat{W} = \sum_{i=1}^n \hat{W}_i$ . Using this test statistic, we reject  $H_0$  when  $\hat{W} > F_{\chi_{nd}^2}^{-1}(1-\alpha)$  where  $F_{\chi_{nd}^2}^{-1}$  is the quantile function of a  $\chi_{nd}^2$  random variable and  $\alpha$  is the predetermined significance level. We note that  $\hat{W}$  is purely a function of the data and can be estimated after having computed the omnibus embedding of  $\mathbf{A}^{(1)}$  and  $\mathbf{A}^{(2)}$ . We also consider a level-corrected version of the  $\hat{W}$  statistic,  $\tilde{W}$ . These corrections are completed by choosing  $c_n \in \mathbb{N}_0$  such that the critical value  $\chi_{nd+c_n}^2$  achieves an  $\alpha$ -level rejection under  $H_0$  for each value of  $n$ . We compare the empirical power of  $T$ ,  $W$ ,  $\hat{W}$ , and  $\tilde{W}$  in the following simulation setting.

**Example 2. (continued)** In the context of example 2, we look to test the hypothesis  $H_0 : \mathbf{I} = \mathbf{C}(t)$  where  $t = 0$  corresponds to  $H_0$  and  $t \in (0, 1]$  corresponds to  $H_A$ . We sample networks of size  $n \in \{50, 100, 200\}$  and test  $H_0$  using  $T$ ,  $W$ ,  $\hat{W}$ , and  $\tilde{W}$ . We complete 1000 Monte Carlo replicates and calculate the empirical power of each testing procedure. The results of this simulations study can be found in Figure 9.

First, as  $t$  increases the power of each method achieves perfect power. Moreover, as  $n$  increases, each method achieves perfect power for smaller values of  $t$ . For networks of size  $n = 50$ , there appears to be no difference between the  $T$  and  $W$  test statistics but as the networks increase to moderate size, ( $n = 100, 200$ ), our proposed test statistic  $W$  outperforms the  $T$  statistic. Indeed,  $W$  offers an average relative improvement in empirical power over  $T$  of  $\{1\%, 7\%, 21\%\}$  for networks of size  $\{50, 100, 200\}$ , respectively. Both  $T$  and

$W$  achieve the correct level for each value of  $n$  but the test statistic  $\hat{W}$  is overpowered for small network sizes. This is due to the under estimation of the variance matrix  $\Sigma_D(\mathbf{x}_i)$ . As  $n$  increases, our proposed estimator  $\hat{\Sigma}_D(\mathbf{x}_i)$  improves and  $\hat{W}$  begins to achieve level. The corrected version of the  $\hat{W}$  statistic,  $\tilde{W}$ , achieves similar level of power as that of  $T$  for networks of size  $n = 100$  and outperforms this statistic for networks of size  $n = 200$ . The degree of freedom correction for  $\tilde{W}$  was  $(c_{50}, c_{100}, c_{200}) = (19, 13, 10)$ .  $\square$

The  $\hat{W}$  test statistic is a fully data-dependent approach to testing the hypothesis  $H_0 : \mathbf{C}^{(1)} = \mathbf{C}^{(2)}$  yet does not achieve level for moderate network sizes. The level corrected test statistic,  $\tilde{W}$ , offers comparable empirical power to semi-parametric testing approaches for moderate network sizes but relies on unknown model parameters. An estimation scheme for the degrees of freedom of the critical value for the level-correction of  $\hat{W}$  will offer an improved fully data-dependent, parametric testing framework that achieves comparable empirical power to semi-parametric approaches.

## 5 Discussion

In this work we establish an explicit bias-variance tradeoff for latent position estimates provided by the omnibus embedding in the presence of heterogeneous network data. We reveal an analytic bias expression introduced by the omnibus embedding, derive a uniform concentration bound on the residual term at a rate of  $O(m^{3/2}n^{-1/2} \log nm)$ , and prove a central limit theorem which characterizes the distributional properties of the estimator. By deriving an analytic bias and variance for the estimated latent positions, we show that the omnibus embedding is a robust estimator for a wide variety of multiplex networks and is often a preferable estimator when compared to similar estimators with respect to mean squared error. These explicit bias and variance expressions enable us to state sufficient conditions for exact recovery in community detection tasks, determine appropriate clustering algorithms for community detection, and develop a test statistic to determine whether two graphs drawn from the ESRDPG share the same weighting matrices. This analysis underscores the benefits of using *biased* latent position estimators that effectively pool strength across networks in multiplex network analysis.

In what follows we provide remarks on possible extensions of Theorem 1 and Theorem 2 beyond the ESRDPG. Specifically, we consider the possibility of reducing our assumptions on the scaling matrices  $\mathbf{C}^{(g)}$  and the implications of asymptotics in the number of graphs  $m$ .

In Definition 2.4, it is required that the  $\{\mathbf{C}^{(g)}\}_{g=1}^m$  are diagonal and nonnegative. This is an assumption needed to identify the  $d$  most positive eigenvalues of the expected omnibus matrix  $\tilde{\mathbf{P}} = \mathbb{E}[\tilde{\mathbf{A}}|\mathbf{X}]$  as the  $d$  dimensions best for estimating the latent positions. Under certain graph models, our analysis would need to be generalized to settings where these weighting matrices contain negative values. In particular, the *Generalized Random Dot Product Graph* (GRDPG) of Rubin-Delanchy et al. (2017) is an extension of the RDPG that captures both assortative and disassortative community structure. By allowing for the weighting matrices to contain negative eigenvalues, the ESRDPG can model multiplex networks with widely varying community structures across different layers. By enriching the model class, however,  $\tilde{\mathbf{P}}$  isn't guaranteed to have  $d$  positive eigenvalues which obfuscates the proper embedding dimension. A further analysis of the positive definite part of  $\tilde{\mathbf{P}}$  and the proper embedding dimension will yield similar results as those presented here. Additionally, following the approach of Rubin-Delanchy et al. (2017) and embedding  $\tilde{\mathbf{P}}$  into  $\mathbb{R}^{2d}$  by considering the largest eigenvalues of  $\tilde{\mathbf{P}}$  in magnitude will yield similar results.

Further extending the ESRDPG to include non-diagonal weighting matrices is a more complicated undertaking. Assuming the scaling matrices are diagonal allowed us to exploit a dimension-wise Kronecker product structure of  $\tilde{\mathbf{P}}$ . This structure allowed for us to analyze the eigenvectors of  $\tilde{\mathbf{P}}$  in terms of the latent positions  $\mathbf{X}$  and the weighting matrices  $\{\mathbf{C}^{(g)}\}_{g=1}^m$ . In extending the ESRPDG to non-diagonal matrices, this dimension-wise Kronecker product structure is lost and relating the eigenstructure of  $\tilde{\mathbf{P}}$  to these model parameters will require a modified approach to those considered here.

Throughout, we assumed that the number of networks  $m$  was of fixed size but we can readily extend the

results an asymptotic analysis in the number of networks,  $m$ . Considering the convergence rate presented in Theorem 1,  $O(m^{3/2}n^{-1/2} \log nm)$  by letting  $n = \omega(m^{3/2+\xi})$  for  $\xi > 0$  we still achieve asymptotic concentration. If the number of nonzero  $\{\mathbf{C}_{ii}^{(g)}\}_{g=1}^m$  grows as  $\omega(m)$ , for instance if each weighting matrix has strictly positive entries, then concentration presented in Theorem 1 occurs at the rate consistent with Levin et al. (2017),  $O(m^{1/2}n^{-1/2} \log nm)$ . Hence, provided  $n = \omega(m^{1/2+\xi})$  for  $\xi > 0$  concentration will occur asymptotically in  $m$

$$\max_{h \in [nm]} \|\mathbf{R}_h\|_2 \leq C \frac{\log m^{5/2+\xi}}{m^\xi}.$$

This result is of particular interest as we establish that the number of networks can dominate the number of vertices while still achieving concentration of the rows of the omnibus embedding. This result suggests that the omnibus embedding may be useful in dynamical network applications where the weighting matrices are a discrete time stochastic process  $\{\mathbf{C}^{(t)}\}_{t=1}^T$ . This stochastic process could impose a dependence structure among edges across layers or among the scaling matrices  $\{\mathbf{S}^{(t)}\}_{t=1}^T$ . Characterizing this dependency structure for different stochastic processes models will result in a wide array of new theoretical questions as well as potential methodological developments for dynamical network models.

Finally, a full power analysis of the test statistic introduced in Section 4 will provide further insight into the proposed testing paradigm. Deriving guarantees on the covariance estimator  $\hat{\Sigma}_D(\mathbf{x}_i)$  will help in establishing the asymptotic distribution of  $\hat{W}_i$  and by extension  $\hat{W}$ . These asymptotic distributions could lead to a power analysis for this test statistic and offer insights into a data dependent choice of the finite sample corrected test statistic  $\tilde{W}$ . A full analysis of this statistic would suggest it is possible to develop and analyze test statistics for testing the hypothesis  $H_0 : \mathbf{C}^{(i)} = \mathbf{C}^{(j)}$  for  $i \neq j$  which will lead to a MANOVA framework for heterogeneous network data. Further developing a testing framework with the alternative hypothesis falling outside the ESRDPG will further enrich the hypothesis testing framework supported by these theoretical findings.

## References

Arroyo, Jesús et al. (2019). “Inference for multiple heterogeneous networks with a common invariant subspace”. In: arXiv preprint: 1906.10026.

Athreya, Avanti et al. (2017). “Statistical inference on random dot product graphs: A survey”. In: *Journal of Machine Learning Research* 18, 226:1–226:92.

Athreya, A. et al. (2016). “A Limit Theorem for Scaled Eigenvectors of Random Dot Product Graphs”. In: *Sankhya A* 78.1, pp. 1–18.

Battiston, Federico, Vincenzo Nicosia, Mario Chavez, et al. (2016). “Multilayer motif analysis of brain networks”. In: *Chaos: An Interdisciplinary Journal of Nonlinear Science* 27, p. 047404.

Battiston, Federico, Vincenzo Nicosia, and Vito Latora (2014). “Structural measures for multiplex networks”. In: *Phys. Rev. E* 89 (3), p. 032804.

— (2017). “The new challenges of multiplex networks: Measures and models”. In: *The European Physical Journal Special Topics* 226.3, pp. 401–416.

Bianconi, Ginestra (2013). “Statistical mechanics of multiplex networks: Entropy and overlap”. In: *Phys. Rev. E* 87 (6), p. 062806.

Cardillo, Alessio et al. (2013). “Emergence of network features from multiplexity”. In: *Sci Rep* 3, p. 1344.

Coscia, Michele et al. (2013). “You know Because I Know’: A multidimensional network approach to human resources problem”. In: *2013 IEEE/ACM International Conference on Advances in Social Networks Analysis and Mining (ASONAM 2013)*, pp. 434–441.

Cozzo, Emanuele et al. (2015). “Structure of triadic relations in multiplex networks”. In: *New Journal of Physics* 17.7, p. 073029.

De Domenico, Manlio (2017). “Multilayer modeling and analysis of human brain networks”. In: *GigaScience* 6.5.

De Domenico, Manlio, Mason A. Porter, and Alex Arenas (2014). “MuxViz: a tool for multilayer analysis and visualization of networks”. In: *Journal of Complex Networks* 3.2, pp. 159–176.

Fatemi, Zahra, Mostafa Salehi, and Matteo Magnani (2016). “A simple multiforce layout for multiplex networks”. In: arXiv preprint: [arXiv:1607.03914](https://arxiv.org/abs/1607.03914).

Ginestet, Cedric E. et al. (2017). “Hypothesis testing for network data in functional neuroimaging”. In: *Ann. Appl. Stat.* 11.2, pp. 725–750.

Gligorijević, V., Y. Panagakis, and S. Zafeiriou (2019). “Non-Negative Matrix Factorizations for Multiplex Network Analysis”. In: *IEEE Transactions on Pattern Analysis and Machine Intelligence* 41.4, pp. 928–940.

Goldblum, Bethany L. et al. (2019). “The nuclear network: multiplex network analysis for interconnected systems”. In: *Applied Network Science* 4.1, p. 36.

Hmimida, Manel and Rushed Kanawati (2015). “Community detection in multiplex networks: A seed-centric approach”. In: *Networks and Heterogeneous Media* 10, pp. 71–85.

Hoff, Peter D, Adrian E Raftery, and Mark S Handcock (2002). “Latent Space Approaches to Social Network Analysis”. In: *Journal of the American Statistical Association* 97.460, pp. 1090–1098.

Horn, Roger A. and Charles R. Johnson (2012). *Matrix Analysis*. 2nd. New York, NY, USA: Cambridge University Press.

Kaluza, Pablo et al. (2010). “The complex network of global cargo ship movements”. In: *J. R. Soc. Interface* 7, pp. 1093–1103.

Kivelä, Mikko et al. (2014). “Multilayer networks”. In: *Journal of Complex Networks* 2.3, pp. 203–271.

Kolaczyk, Eric D. (2009). *Statistical Analysis of Network Data: Methods and Models*. 1st. Springer Publishing Company, Incorporated.

Lazega, Emmanuel and Tom Snijders (2016). *Multilevel Network Analysis for the Social Sciences : Theory, Methods and Applications*. 1st. Springer International Publishing, Incorporated.

Levin, Keith et al. (2017). “A central limit theorem for an omnibus embedding of multiple random graphs and implications for multiscale network inference”. In: arXiv preprint: [1705.09355](https://arxiv.org/abs/1705.09355).

Luxburg, Ulrike von (2007). “A tutorial on spectral clustering”. In: *Statistics and Computing* 17, pp. 395–416.

Lyzinski, Vince et al. (2014). “Perfect clustering for stochastic blockmodel graphs via adjacency spectral embedding”. In: *Electron. J. Statist.* 8.2, pp. 2905–2922.

Lyzinski, V. et al. (2017). “Community Detection and Classification in Hierarchical Stochastic Blockmodels”. In: *IEEE Transactions on Network Science and Engineering* 4.1, pp. 13–26.

Ma, Lijia et al. (2018). “Detecting composite communities in multiplex networks: A multilevel memetic algorithm”. In: *Swarm and Evolutionary Computation* 39, pp. 177–191.

Murase, Yohsuke et al. (2014). “Multilayer weighted social network model”. In: *Phys. Rev. E* 90 (5), p. 052810.

Nicosia, Vincenzo and Vito Latora (2015). “Measuring and modeling correlations in multiplex networks”. In: *Physical Review E* 92, p. 032805.

Nielsen, Agnes Martine and Daniela Witten (2018). “The Multiple Random Dot Product Graph Model”. In: arXiv preprint: [1811.12172](https://arxiv.org/abs/1811.12172).

Paez, Marina S., Arash A. Amini, and Lizhen Lin (2019). “Hierarchical Stochastic Block Model for Community Detection in Multiplex Networks”. In: arXiv preprint: [arXiv:1904.05330](https://arxiv.org/abs/1904.05330).

Paul, Subhadeep and Yuguo Chen (2018). “A random effects stochastic block model for joint community detection in multiple networks with applications to neuroimaging”. In: arXiv preprint: [arXiv:1805.02292](https://arxiv.org/abs/1805.02292).

Rubin-Delanchy, Patrick et al. (2017). “A statistical interpretation of spectral embedding: the generalised random dot product graph”. In: arXiv preprint: [arXiv:1709.05506](https://arxiv.org/abs/1709.05506).

Shalizi, Cosma Rohilla and Dena Asta (2017). “Consistency of Maximum Likelihood for Continuous-Space Network Models”. In: arXiv preprint: [1711.02123](https://arxiv.org/abs/1711.02123).

Stella, Massimo, Nicole M. Beckage, and Markus Brede (2017). “Multiplex lexical networks reveal patterns in early word acquisition in children”. In: *Scientific Reports* 7.1. ISSN: 2045-2322.

Sussman, Daniel L. et al. (2012). “A Consistent Adjacency Spectral Embedding for Stochastic Blockmodel Graphs”. In: *Journal of the American Statistical Association* 107.499, pp. 1119–1128.

Szell, Michael and Stefan Thurner (2013). “How women organize social networks different from men”. In: *Scientific Reports* 3.1, p. 1214.

Takes, Frank W. et al. (2018). “Multiplex network motifs as building blocks of corporate networks”. In: *Applied Network Science* 3.1, p. 39.

Tang, Minh et al. (2017). “A Semiparametric Two-Sample Hypothesis Testing Problem for Random Graphs”. In: *Journal of Computational and Graphical Statistics* 26.2, pp. 344–354.

Tang, Runze et al. (2019). “Connectome Smoothing via Low-Rank Approximations”. In: *IEEE Transactions on Medical Imaging* 38, pp. 1446–1456.

Taylor, Dane, Mason A. Porter, and Peter J. Mucha (2019). “Tunable Eigenvector-Based Centralities for Multiplex and Temporal Networks”. In: arXiv preprint: [arXiv:1904.02059](https://arxiv.org/abs/1904.02059).

Tudisco, Francesco, Francesca Arrigo, and Antoine Gautier (2017). “Node and Layer Eigenvector Centralities for Multiplex Networks”. In: *SIAM Journal on Applied Mathematics* 78.2, pp. 853–876.

Wang, Shangsi et al. (2017). “Joint Embedding of Graphs”. In: arXiv preprint: [1703.03862](https://arxiv.org/abs/1703.03862).

Young, Stephen J. and Edward R. Scheinerman (2007). “Random Dot Product Graph Models for Social Networks”. In: WAW’07, pp. 138–149.

Yu, Y., T. Wang, and R. J. Samworth (2014). “A useful variant of the Davis–Kahan theorem for statisticians”. In: *Biometrika* 102.2, pp. 315–323.

Zhu, Peizhen and Andrew Knyazev (2013). “Angles between subspaces and their tangents”. In: *Journal of Numerical Mathematics* 21, pp. 325–340.

## A Analysis Layout

Our main focus is on the rows of the matrix  $\hat{\mathbf{L}}\mathbf{W} - \mathbf{L}$  for some orthogonal matrix  $\mathbf{W}$ . We propose that  $\mathbf{W} = \tilde{\mathbf{V}}^T \tilde{\mathbf{W}}^T$  where  $\tilde{\mathbf{V}}$  and  $\tilde{\mathbf{W}}$  are rotation matrices to be introduced. Define  $\mathbf{L}_S$  the  $nm \times d$  block matrix whose  $g$ -th,  $n \times d$  block is  $\mathbf{X}\mathbf{S}^{(g)}$ . Then by adding and subtracting this term, we arrive at our first moment expansion

$$\hat{\mathbf{L}}\mathbf{W} - \mathbf{L} = (\hat{\mathbf{L}}\mathbf{W} - \mathbf{L}_S) + (\mathbf{L}_S - \mathbf{L}) \quad (6)$$

From here we will prove the following.

1. *Theorem 1 (A)*: The second term in (6) captures the asymptotic bias of the omnibus embedding  $\mathbf{B} = (\mathbf{L}_S - \mathbf{L})$  where  $\mathbf{B}$  is a known matrix that is a smooth, one-to-one function of the weighting matrices  $\{\mathbf{C}^{(g)}\}_{g=1}^m$  and the latent positions  $\mathbf{X}$ .
2. *Theorem 1 (B)*: Defining  $\mathbf{R}^{(1)} = \hat{\mathbf{L}}\mathbf{W} - \mathbf{L}_S$  we intend to show

$$\|\mathbf{R}^{(1)}\|_{2,\infty} \leq O\left(m^{3/2}n^{-1/2} \log nm\right)$$

We establish Theorem 1 (A) directly by uniquely constructing the  $\{\mathbf{S}^{(g)}\}_{g=1}^m$  from only  $\{\mathbf{C}^{(g)}\}_{g=1}^m$ . Then, we prove Theorem 1 (B) through a series of perturbation arguments. Moving to the second moment, we adopt the expansion of  $(\hat{\mathbf{L}}\mathbf{W} - \mathbf{L}_S) = (\hat{\mathbf{L}} - \mathbf{Z}\tilde{\mathbf{V}})\tilde{\mathbf{V}}^T \tilde{\mathbf{W}}^T$  introduced by Levin et al. (2017). In particular, we consider

$$\begin{aligned} \hat{\mathbf{L}} - \mathbf{Z}\tilde{\mathbf{V}} &= (\tilde{\mathbf{A}} - \tilde{\mathbf{P}})\mathbf{U}_{\tilde{\mathbf{P}}}\mathbf{S}_{\tilde{\mathbf{P}}}^{-1/2}\tilde{\mathbf{V}} \\ &\quad + (\tilde{\mathbf{A}} - \tilde{\mathbf{P}})\mathbf{U}_{\tilde{\mathbf{P}}} \left( \tilde{\mathbf{V}}\mathbf{S}_{\tilde{\mathbf{A}}}^{-1/2} - \mathbf{S}_{\tilde{\mathbf{P}}}^{-1/2}\tilde{\mathbf{V}} \right) \\ &\quad - \mathbf{U}_{\tilde{\mathbf{P}}}\mathbf{U}_{\tilde{\mathbf{P}}}^T(\tilde{\mathbf{A}} - \tilde{\mathbf{P}})\mathbf{U}_{\tilde{\mathbf{P}}}\tilde{\mathbf{V}}\mathbf{S}_{\tilde{\mathbf{A}}}^{-1/2} \\ &\quad + (\mathbf{I} - \mathbf{U}_{\tilde{\mathbf{P}}}\mathbf{U}_{\tilde{\mathbf{P}}}^T)(\tilde{\mathbf{A}} - \tilde{\mathbf{P}})\mathbf{R}_3\mathbf{S}_{\tilde{\mathbf{A}}}^{-1/2} \\ &\quad + \mathbf{R}_1\mathbf{S}_{\tilde{\mathbf{A}}}^{1/2} + \mathbf{U}_{\tilde{\mathbf{P}}}\mathbf{R}_2 \\ &\quad - \tilde{\mathbf{U}}_{\tilde{\mathbf{P}}}\tilde{\mathbf{S}}_{\tilde{\mathbf{P}}}\tilde{\mathbf{U}}_{\tilde{\mathbf{P}}}^T\mathbf{U}_{\tilde{\mathbf{A}}}\mathbf{S}_{\tilde{\mathbf{A}}}^{-1/2} \end{aligned}$$

where each matrix introduced above will be introduced throughout. We will show that the last five lines, which we denote by  $\mathbf{R}^{(2)}$ , will converge in probability to zero after scaled by  $\sqrt{n}$ . For this first term, we will consider the following decomposition

$$(\tilde{\mathbf{A}} - \tilde{\mathbf{P}})\mathbf{U}_{\tilde{\mathbf{P}}}\mathbf{S}_{\tilde{\mathbf{P}}}^{-1/2}\tilde{\mathbf{V}} = (\tilde{\mathbf{A}} - \tilde{\mathbf{P}})\mathbf{Z}\mathbf{S}_{\tilde{\mathbf{P}}}^{-1}\tilde{\mathbf{V}} = (\tilde{\mathbf{A}} - \tilde{\mathbf{P}})\mathbf{L}_S\tilde{\mathbf{W}}\mathbf{S}_{\tilde{\mathbf{P}}}^{-1}\tilde{\mathbf{V}}.$$

Reapplying the rotations  $\tilde{\mathbf{V}}^T\tilde{\mathbf{W}}^T$  we arrive at  $(\tilde{\mathbf{A}} - \tilde{\mathbf{P}})\mathbf{L}_S\tilde{\mathbf{W}}\mathbf{S}_{\tilde{\mathbf{P}}}^{-1}\tilde{\mathbf{W}}^T$  from which scaling the  $h = n(g-1) + i$  row by  $\sqrt{n}$  gives

$$\sqrt{n} \left[ (\tilde{\mathbf{A}} - \tilde{\mathbf{P}})\mathbf{L}_S\tilde{\mathbf{W}}\mathbf{S}_{\tilde{\mathbf{P}}}^{-1}\tilde{\mathbf{W}}^T \right]_h = n \left( \tilde{\mathbf{W}}\mathbf{S}_{\tilde{\mathbf{P}}}^{-1}\tilde{\mathbf{W}}^T \right) * \frac{1}{\sqrt{n}} \left[ (\tilde{\mathbf{A}} - \tilde{\mathbf{P}})\mathbf{L}_S \right]_h$$

We will analyze this term similarly as A. Athreya et al. (2016) and Levin et al. (2017). For concreteness we consider the expansion

$$\hat{\mathbf{L}}\mathbf{W} - \mathbf{L}_S = (\tilde{\mathbf{A}} - \tilde{\mathbf{P}})\mathbf{L}_S\tilde{\mathbf{W}}\tilde{\mathbf{S}}_{\tilde{\mathbf{P}}}^{-1}\tilde{\mathbf{W}}^T + \mathbf{R}^{(2)}$$

from which we intend to prove the following.

1. *Theorem 2:* Following an analysis technique closely related to the power method, we intend to show

$$\sqrt{n}[(\tilde{\mathbf{A}} - \tilde{\mathbf{P}})\mathbf{L}_S\tilde{\mathbf{W}}\tilde{\mathbf{S}}_{\tilde{\mathbf{P}}}^{-1}\tilde{\mathbf{W}}^T]_h | \{\mathbf{X}_i = \mathbf{x}_i\} \xrightarrow{D} N(0, \Sigma_g(\mathbf{x}_i)).$$

2. *Theorem 2:* We provide a residual bound  $\sqrt{n}\mathbf{R}_h^{(2)} \xrightarrow{\mathbb{P}} 0$ .

Having established the asymptotic bias and variance of the omnibus embedding estimates, we can use these results to prove corollaries and useful in subsequent statistical procedures.

## B First Moment

To begin, we first relate the form of  $\mathbf{Z} = \text{ASE}(\tilde{\mathbf{P}}, d)$  to that of the latent positions  $\mathbf{X}$ . In doing so, we can analyze the difference between the rows of  $\mathbf{Z}$ , properly rotated, and those of the scaled latent positions  $\mathbf{L}$ . This analysis, summarized in Theorem 1 (A), will capture the bias of the omnibus embedding under the ESRDPG. Secondly, we establish bounds on the corresponding residual term,  $\mathbf{R}^{(1)}$ . Namely, we establish a uniform concentration rate of the rows of  $\hat{\mathbf{L}} = \text{ASE}(\tilde{\mathbf{A}}, d)$  to those of  $\mathbf{Z}$ . This is the focus Theorem 1 (B). To this end, we provide Lemma 1 and Lemma 2 which establish the analytic form of  $\mathbf{Z}$ .

**Lemma 1.** Let  $\mathbf{x} \in \mathbb{R}_{\geq 0}^m$  such that  $\max_{i \in [m]} \mathbf{x}_i > 0$ . Define the matrix  $\mathbf{H}(\mathbf{x}) = \frac{1}{2}(\mathbf{x}\mathbf{1}_m^T + \mathbf{1}_m\mathbf{x}^T)$ . Then  $\mathbf{H}(\mathbf{x})$  is at most rank two and

$$\lambda_{\min}(\mathbf{H}(\mathbf{x})) = \frac{1}{2}(\|\mathbf{x}\|_1 - \sqrt{m}\|\mathbf{x}\|_2) \leq 0 < \frac{1}{2}(\|\mathbf{x}\|_1 + \sqrt{m}\|\mathbf{x}\|_2) = \lambda_{\max}(\mathbf{H}(\mathbf{x}))$$

*Proof.* Recall a matrix  $\mathbf{A} \in \mathbb{R}^{n \times n}$  with  $\text{rank}(\mathbf{A}) = 2$  satisfies  $\text{tr}(\mathbf{A}) = \lambda_{\min} + \lambda_{\max}$  and  $\text{tr}(\mathbf{A}^2) = \lambda_{\min}^2 + \lambda_{\max}^2$ . Notice

$$\text{tr}[\mathbf{H}(\mathbf{x})] = \sum_{i=1}^m x_i = \|\mathbf{x}\|_1 \quad \text{tr}[\mathbf{H}(\mathbf{x})^2] = \frac{\|\mathbf{x}\|_1^2 + m\|\mathbf{x}\|_2^2}{2}$$

and the proposed eigenvalues satisfy

$$\lambda_{\min} + \lambda_{\max} = \|\mathbf{x}\|_1, \quad \lambda_{\min}^2 + \lambda_{\max}^2 = \frac{\|\mathbf{x}\|_1^2 + m\|\mathbf{x}\|_2^2}{2}.$$

Moreover, by the Cauchy-Schwarz inequality  $\|\mathbf{x}\|_1 \leq \sqrt{m}\|\mathbf{x}\|_2$ . Hence,  $\lambda_{\min} = \frac{\|\mathbf{x}\|_1 - \sqrt{m}\|\mathbf{x}\|_2}{2} \leq 0$  and  $\lambda_{\max} = \frac{\|\mathbf{x}\|_1 + \sqrt{m}\|\mathbf{x}\|_2}{2} > 0$ .  $\square$

**Lemma 2.** Suppose that  $\mathbf{L}_S \in \mathbb{R}^{nm \times d}$  with its  $g$ -th block given by  $\mathbf{X}\mathbf{S}^{(g)}$  and  $\mathbf{Z} = \text{ASE}(\tilde{\mathbf{P}}, d)$ . Then there exists an orthogonal matrix  $\tilde{\mathbf{W}} \in \mathcal{O}^{d \times d}$  such that  $\mathbf{Z}\tilde{\mathbf{W}}^T = \mathbf{L}_S$ .

*Proof.* Suppose that  $(\{\mathbf{A}^{(g)}\}_{g=1}^m, \mathbf{X}) \sim \text{ESRDPG}(F, n, \{\mathbf{C}^{(g)}\}_{g=1}^m)$ . We wish to understand the expected omnibus matrix  $\tilde{\mathbf{P}} = \mathbb{E}[\tilde{\mathbf{A}}|\mathbf{X}]$ . Recall from Definition 3.1,  $\mathbf{v}_i = (\mathbf{C}_{ii}^{(g)})_{g=1}^m \in \mathbb{R}^m$ . Notice that we can express  $\tilde{\mathbf{P}}$  in terms of the matrices  $\mathbf{H}(\mathbf{v}_i)$  as

$$\tilde{\mathbf{P}} = (\mathbf{I}_{m \times m} \otimes \mathbf{X}) \left( \sum_{i=1}^d \mathbf{H}(\mathbf{v}_i) \otimes \mathbf{e}_i \mathbf{e}_i^T \right) (\mathbf{I}_{m \times m} \otimes \mathbf{X})^T.$$

Using this expression can bound the rank of  $\tilde{\mathbf{P}}$  as follows.

$$\begin{aligned} \text{rank}(\tilde{\mathbf{P}}) &\leq \min \left\{ \text{rank}(\mathbf{I}_{m \times m} \otimes \mathbf{X}), \text{rank} \left( \sum_{i=1}^d \mathbf{H}(\mathbf{v}_i) \otimes \mathbf{e}_i \mathbf{e}_i^T \right), \text{rank}(\mathbf{I}_{m \times m} \otimes \mathbf{X})^T \right\} \\ &\leq \min \{md, 2d, md\} \\ &= 2d \end{aligned}$$

Moreover, by the assumption that  $\Delta = \mathbb{E}[\mathbf{X}_1 \mathbf{X}_1^T]$  is full rank and the Sylvester rank inequality, the rank of  $\tilde{\mathbf{P}}$  is also bounded from below  $d \leq \text{rank}(\tilde{\mathbf{P}})$ . Next, consider the following decomposition of  $\tilde{\mathbf{P}}$ .

$$\tilde{\mathbf{P}} = \sum_{j=1}^d \mathbf{H}(\mathbf{v}_j) \otimes \mathbf{X}_{\cdot j} \mathbf{X}_{\cdot j}^T$$

Lemma 1 establishes  $\text{rank}(\mathbf{H}(\mathbf{v}_j)) = 2$  with  $\lambda_{\min}(\mathbf{H}(\mathbf{v}_j)) \leq 0 < \lambda_{\max}(\mathbf{H}(\mathbf{v}_j))$ . Therefore, we can factor  $\mathbf{H}(\mathbf{v}_j)$  into a positive definite and negative semidefinite matrix as  $\mathbf{H}(\mathbf{v}_j) = \mathbf{H}^+(\mathbf{v}_j) - \mathbf{H}^-(\mathbf{v}_j)$ . With this we write

$$\tilde{\mathbf{P}} = \sum_{j=1}^d \mathbf{H}^+(\mathbf{v}_j) \otimes \mathbf{X}_{\cdot j} \mathbf{X}_{\cdot j}^T - \sum_{j=1}^d \mathbf{H}^-(\mathbf{v}_j) \otimes \mathbf{X}_{\cdot j} \mathbf{X}_{\cdot j}^T$$

Define  $\tilde{\mathbf{P}}^+ = \sum_{j=1}^d \mathbf{H}^+(\mathbf{v}_j) \otimes \mathbf{X}_{\cdot j} \mathbf{X}_{\cdot j}^T$  and  $\tilde{\mathbf{P}}^- = \sum_{j=1}^d \mathbf{H}^-(\mathbf{v}_j) \otimes \mathbf{X}_{\cdot j} \mathbf{X}_{\cdot j}^T$  so that  $\tilde{\mathbf{P}} = \tilde{\mathbf{P}}^+ - \tilde{\mathbf{P}}^-$ . Seeing  $\mathbf{H}^+(\mathbf{v}_j)$  and  $\mathbf{X}_{\cdot j} \mathbf{X}_{\cdot j}^T$  are both positive definite and rank 1, we see that  $\tilde{\mathbf{P}}^+$  is positive definite with  $\text{rank}(\tilde{\mathbf{P}}^+) = d$ . Similarly,  $\tilde{\mathbf{P}}^-$  is negative semidefinite with  $\text{rank}(\tilde{\mathbf{P}}^-) \leq d$ . With these observations, and  $d \leq \text{rank}(\tilde{\mathbf{P}}) \leq 2d$ ,  $\tilde{\mathbf{P}}$  has  $d$  positive eigenvalues that will come from the matrix  $\tilde{\mathbf{P}}^+$  (Horn and Johnson 2012, Proposition 4.1.13 and 4.1.P22). Therefore, for  $\mathbf{Z} = \text{ASE}(\tilde{\mathbf{P}}, d)$  we have

$$\tilde{\mathbf{P}}^+ = \mathbf{Z} \mathbf{Z}^T = \sum_{j=1}^d \begin{bmatrix} [\mathbf{H}^+(\mathbf{v}_j)]_{11} \mathbf{X}_{\cdot j} \mathbf{X}_{\cdot j}^T & \dots & [\mathbf{H}^+(\mathbf{v}_j)]_{1m} \mathbf{X}_{\cdot j} \mathbf{X}_{\cdot j}^T \\ \vdots & \ddots & \vdots \\ [\mathbf{H}^+(\mathbf{v}_j)]_{m1} \mathbf{X}_{\cdot j} \mathbf{X}_{\cdot j}^T & \dots & [\mathbf{H}^+(\mathbf{v}_j)]_{mm} \mathbf{X}_{\cdot j} \mathbf{X}_{\cdot j}^T \end{bmatrix}$$

Define the diagonal matrices  $\mathbf{D}$  by  $\mathbf{D}_{ij} = \mathbf{D}_{ji} = \text{diag}[(\mathbf{H}^+(\mathbf{v}_k))_{ij}]_{k=1}^d$ . Then

$$\mathbf{Z} \mathbf{Z}^T = \begin{bmatrix} \mathbf{X} \mathbf{D}_{11} \mathbf{X}^T & \dots & \mathbf{X} \mathbf{D}_{1m} \mathbf{X}^T \\ \vdots & \ddots & \vdots \\ \mathbf{X} \mathbf{D}_{m1} \mathbf{X}^T & \dots & \mathbf{X} \mathbf{D}_{mm} \mathbf{X} \mathbf{X}^T \end{bmatrix}$$

Now, consider  $\mathbf{L}_S \mathbf{L}_S^T$ .

$$\mathbf{L}_S \mathbf{L}_S^T = \begin{bmatrix} \mathbf{X} (\mathbf{S}^{(1)})^2 \mathbf{X}^T & \dots & \mathbf{X} \mathbf{S}^{(1)} \mathbf{S}^{(m)} \mathbf{X}^T \\ \vdots & \ddots & \vdots \\ \mathbf{X} \mathbf{S}^{(1)} \mathbf{S}^{(m)} \mathbf{X}^T & \dots & \mathbf{X} (\mathbf{S}^{(m)})^2 \mathbf{X}^T \end{bmatrix}$$

Now recall that  $\mathbf{S}^{(g)} = \text{diag}(\alpha_g^{(1)}, \dots, \alpha_g^{(d)})$  where  $\alpha^{(k)} = \text{ASE}(\mathbf{H}(\mathbf{v}_k), 1)$ . Notice that  $\alpha^{(k)}(\alpha^{(k)})^T = \mathbf{H}^+(\mathbf{v}_k)$  so  $[\alpha^{(k)}(\alpha^{(k)})^T]_{ij} = \alpha_i^{(k)}\alpha_j^{(k)} = [\mathbf{H}^+(\mathbf{v}_k)]_{ij}$  and therefore

$$\mathbf{S}^{(k)}\mathbf{S}^{(\ell)} = \text{diag}\left(\alpha_k^{(1)}\alpha_\ell^{(1)}, \alpha_k^{(2)}\alpha_\ell^{(2)}, \dots, \alpha_k^{(d)}\alpha_\ell^{(d)}\right) = \text{diag}([\mathbf{H}^+(\mathbf{v}_r)]_{k\ell})_{r=1}^d = \mathbf{D}_{k\ell}$$

Therefore, we see that  $\mathbf{Z}\mathbf{Z}^T = \mathbf{L}_S\mathbf{L}_S^T$ . With this we conclude that there exists some orthogonal matrix  $\tilde{\mathbf{W}} \in \mathcal{O}^{d \times d}$  such that  $\mathbf{Z} = \mathbf{L}_S\tilde{\mathbf{W}}$ .  $\square$

Having established the analytic expression for  $\mathbf{Z}$  we now turn to analyzing the mapping from  $\{\mathbf{C}^{(g)}\}_{g=1}^m$  to  $\{\mathbf{S}^{(g)}\}_{g=1}^m$ . In doing so, we demonstrate the scaling matrices' impact on the bias introduced by the omnibus embedding.

**Proposition B.1.** The map from the scaling matrices  $\{\mathbf{C}^{(g)}\}_{g=1}^m$  to the set  $\{\mathbf{S}^{(g)}\}_{g=1}^m$ ,  $\{\mathbf{C}^{(g)}\}_{g=1}^m \mapsto \{\mathbf{S}^{(g)}\}_{g=1}^m$ , is one-to-one.

*Proof of Proposition B.1.* By definition,  $\mathbf{S}^{(g)} = \text{diag}(\alpha_g^{(1)}, \alpha_g^{(2)}, \dots, \alpha_g^{(d)})$  where  $\alpha^{(i)} = \text{ASE}(\mathbf{H}(\mathbf{v}_i), 1)$  for  $i \in [d]$ . Under the ESRDPG, there exists a  $j \in [m]$  such that  $(\mathbf{v}_i)_j > 0$ . Therefore,  $\mathbf{H}(\mathbf{v}_i)$  has positive entries in its  $j$ -th row and  $j$ -th column. Hence,  $\mathbf{H}(\mathbf{v}_i)$  is an irreducible matrix. By the Perron-Frobenius Theorem,  $\mathbf{H}(\mathbf{v}_i)$  has a largest positive eigenvalue of multiplicity one that corresponds to a unique eigenvector with strictly positive entries. As  $\alpha^{(i)}$  is a product of the square root of this positive eigenvalue and this eigenvector, we can always choose it to be positive valued. Moreover, as this eigenvalue-eigenvector pair were unique, then  $\alpha^{(i)}$  is also unique with respect to  $\mathbf{v}_i$ . That is  $\mathbf{v}_i \mapsto \alpha^{(i)}$  is one-to-one. As the scaling matrices  $\{\mathbf{C}^{(g)}\}_{g=1}^m$  uniquely determine  $\{\mathbf{v}_i\}_{i=1}^d$  and the  $\{\alpha^{(i)}\}_{i=1}^d$  uniquely determine the  $\{\mathbf{S}^{(g)}\}_{g=1}^m$ , the map from  $\{\mathbf{C}^{(g)}\}_{g=1}^m \mapsto \{\mathbf{S}^{(g)}\}_{g=1}^m$  is one-to-one.  $\square$

Having successfully related the form of  $\mathbf{Z}$  to the latent positions and characterized the scaling matrices  $\{\mathbf{S}^{(g)}\}_{g=1}^m$  as a smooth, one-to-one function the weighting matrices  $\{\mathbf{C}^{(g)}\}_{g=1}^m$  we are ready to prove Theorem 1 (A).

*Proof of Theorem 1 (A).* Suppose that  $\tilde{\mathbf{W}} \in \mathcal{O}^{d \times d}$  given in Lemma 2. Then we see that  $\mathbf{Z}\tilde{\mathbf{W}}^T = \mathbf{L}_S$ . Recall for a matrix  $\mathbf{M}$  we denote  $\mathbf{M}_i = (\mathbf{M}_i)^T$  and letting  $h = n(g-1) + i$  denote the row corresponding to node  $i$  in graph  $g$ , we have

$$(\mathbf{L}_S - \mathbf{L})_h = (\mathbf{X}\mathbf{S}^{(g)} - \mathbf{X}\sqrt{\mathbf{C}^{(g)}})_i = (\mathbf{S}^{(g)} - \sqrt{\mathbf{C}^{(g)}})\mathbf{X}_i.$$

As a consequence of Proposition B.1 the  $\{\mathbf{S}^{(g)}\}_{g=1}^m$  are smooth functions of the weighting matrices. Therefore, the bias matrix  $\mathbf{L}_S - \mathbf{L}$  is a known smooth, one-to-one function of the weighting matrices  $\{\mathbf{C}^{(g)}\}_{g=1}^m$  and the latent position matrix  $\mathbf{X}$ .  $\square$

The proof of Theorem 1 (A) reveals that the bias is given by coordinate scaling of the matrix  $\mathbf{X}$ . To affirm that this term captures the asymptotic bias of the omnibus embedding, we establish a concentration rate of the corresponding residual term. We follow the approach introduced by Levin et al. (2017) *mutatis mutandis*. For this reason, we only include proofs in which the argument was fundamentally changed by the ESRDPG model. Other results we state without proof and refer the reader to Levin et al. (2017). To begin, we prove the bound in Theorem 1 (B) and highlight results used therein that will be subsequently stated.

*Proof of Theorem 1 (B).* Suppose that  $\tilde{\mathbf{V}}$  is defined as in Lemma 5 and  $\mathbf{R}_1, \mathbf{R}_2$ , and  $\mathbf{R}_3$  as in Lemma 8.

Consider the following decomposition

$$\begin{aligned}
\hat{\mathbf{L}} - \mathbf{Z}\tilde{\mathbf{V}} &= (\tilde{\mathbf{A}} - \tilde{\mathbf{P}})\mathbf{U}_{\tilde{\mathbf{P}}}\mathbf{S}_{\tilde{\mathbf{P}}}^{-1/2}\tilde{\mathbf{V}} + (\tilde{\mathbf{A}} - \tilde{\mathbf{P}})\mathbf{U}_{\tilde{\mathbf{P}}}(\tilde{\mathbf{V}}\mathbf{S}_{\tilde{\mathbf{A}}}^{-1/2} - \mathbf{S}_{\tilde{\mathbf{P}}}^{-1/2}\tilde{\mathbf{V}}) \\
&\quad - \mathbf{U}_{\tilde{\mathbf{P}}}\mathbf{U}_{\tilde{\mathbf{P}}}^T(\tilde{\mathbf{A}} - \tilde{\mathbf{P}})\mathbf{U}_{\tilde{\mathbf{P}}}\tilde{\mathbf{V}}\mathbf{S}_{\tilde{\mathbf{A}}}^{-1/2} \\
&\quad + (\mathbf{I} - \mathbf{U}_{\tilde{\mathbf{P}}}\mathbf{U}_{\tilde{\mathbf{P}}}^T)(\tilde{\mathbf{A}} - \tilde{\mathbf{P}})\mathbf{R}_3\mathbf{S}_{\tilde{\mathbf{A}}}^{-1/2} \\
&\quad + \mathbf{R}_1\mathbf{S}_{\tilde{\mathbf{A}}}^{1/2} + \mathbf{U}_{\tilde{\mathbf{P}}}\mathbf{R}_2 \\
&\quad - \tilde{\mathbf{U}}_{\tilde{\mathbf{P}}}\tilde{\mathbf{S}}_{\tilde{\mathbf{P}}}\tilde{\mathbf{U}}_{\tilde{\mathbf{P}}}^T\mathbf{U}_{\tilde{\mathbf{A}}}\mathbf{S}_{\tilde{\mathbf{A}}}^{-1/2}.
\end{aligned}$$

Using the supporting Lemmas to be developed it holds with high probability that

$$\begin{aligned}
\|(\tilde{\mathbf{A}} - \tilde{\mathbf{P}})\mathbf{U}_{\tilde{\mathbf{P}}}(\tilde{\mathbf{V}}\mathbf{S}_{\tilde{\mathbf{A}}}^{-1/2} - \mathbf{S}_{\tilde{\mathbf{P}}}^{-1/2}\tilde{\mathbf{V}})\| &\leq \frac{Cm^{3/4}d^{1/2}\log^{3/2}nm}{n} & (\text{Lemma 6, 7}) \\
\|\mathbf{U}_{\tilde{\mathbf{P}}}\mathbf{U}_{\tilde{\mathbf{P}}}^T(\tilde{\mathbf{A}} - \tilde{\mathbf{P}})\mathbf{U}_{\tilde{\mathbf{P}}}\tilde{\mathbf{V}}\mathbf{S}_{\tilde{\mathbf{A}}}^{-1/2}\|_F &\leq Cd\sqrt{\frac{\log nm}{n}} & (\text{Lemma 6}) \\
\|\mathbf{R}_1\mathbf{S}_{\tilde{\mathbf{A}}}^{1/2} + \mathbf{U}_{\tilde{\mathbf{P}}}\mathbf{R}_2\|_F &\leq \frac{Cm^{3/2}\log nm}{\sqrt{n}} & (\text{Lemma 8}) \\
\|(\mathbf{I} - \mathbf{U}_{\tilde{\mathbf{P}}}\mathbf{U}_{\tilde{\mathbf{P}}}^T)(\tilde{\mathbf{A}} - \tilde{\mathbf{P}})\mathbf{R}_3\mathbf{S}_{\tilde{\mathbf{A}}}^{-1/2}\|_F &\leq \frac{Cm^{5/4}\log nm}{\sqrt{n}} & (\text{Lemma 8}) \\
\|\tilde{\mathbf{U}}_{\tilde{\mathbf{P}}}\tilde{\mathbf{S}}_{\tilde{\mathbf{P}}}\tilde{\mathbf{U}}_{\tilde{\mathbf{P}}}^T\mathbf{U}_{\tilde{\mathbf{A}}}\mathbf{S}_{\tilde{\mathbf{A}}}^{-1/2}\|_F &\leq C\frac{dm^{3/2}\log nm}{\sqrt{n}} & (\text{Lemma 9})
\end{aligned}$$

Therefore, we with high probability, we can write

$$\|\hat{\mathbf{L}} - \mathbf{Z}\tilde{\mathbf{V}}\|_F = \|(\tilde{\mathbf{A}} - \tilde{\mathbf{P}})\mathbf{U}_{\tilde{\mathbf{P}}}\mathbf{S}_{\tilde{\mathbf{P}}}^{-1/2}\|_F + O\left(\frac{m^{3/2}\log nm}{\sqrt{n}}\right)$$

and note

$$\|(\tilde{\mathbf{A}} - \tilde{\mathbf{P}})\mathbf{U}_{\tilde{\mathbf{P}}}\mathbf{S}_{\tilde{\mathbf{P}}}^{-1/2}\|_{2,\infty} \leq \|(\tilde{\mathbf{A}} - \tilde{\mathbf{P}})\mathbf{U}_{\tilde{\mathbf{P}}}\|_{2,\infty}\|\mathbf{S}_{\tilde{\mathbf{P}}}^{-1/2}\|.$$

Let  $\mathbf{u}_j$  be the  $j$ -th column of  $\tilde{\mathbf{P}}$ . Then we have

$$\|(\tilde{\mathbf{A}} - \tilde{\mathbf{P}})\mathbf{U}_{\tilde{\mathbf{P}}}\|_{2,\infty} \leq \sqrt{d} \max_{j \in [d]} \|(\tilde{\mathbf{A}} - \tilde{\mathbf{P}})\mathbf{u}_j\|_\infty = \sqrt{d} \max_{j \in [d]} \max_{h \in [nm]} |(\tilde{\mathbf{A}} - \tilde{\mathbf{P}})\mathbf{u}_j|_h$$

An application of Hoeffding's inequality as in Lemma 6 shows that  $|(\tilde{\mathbf{A}} - \tilde{\mathbf{P}})\mathbf{u}_j|_h \leq Cm^{1/4}\sqrt{c\log nm}$  with probability at least  $1 - (nm)^{-c}$ . Changing  $c$  only changes the constant  $C$  for this element-wise bound. Hence, choosing  $c$  sufficiently large and a union bound shows

$$\sqrt{d} \max_{j \in [d]} \max_{h \in [nm]} |(\tilde{\mathbf{A}} - \tilde{\mathbf{P}})\mathbf{u}_j|_h \leq Cdm^{1/4}\sqrt{\log nm}$$

with high probability. Lastly, as  $\|\mathbf{S}_{\tilde{\mathbf{P}}}^{-1/2}\| \leq C(n\sqrt{m})^{-1/2}$  and integrating over  $\mathbf{X}$  then establishes the bound

$$\|(\tilde{\mathbf{A}} - \tilde{\mathbf{P}})\mathbf{U}_{\tilde{\mathbf{P}}}\mathbf{S}_{\tilde{\mathbf{P}}}^{-1/2}\|_{2,\infty} \leq Cd\sqrt{\frac{\log nm}{n}}.$$

Finally, we have with high probability

$$\|\hat{\mathbf{L}}\mathbf{W} - \mathbf{L}_S\|_{2,\infty} = \|(\hat{\mathbf{L}} - \mathbf{Z}\tilde{\mathbf{V}})\tilde{\mathbf{V}}^T\tilde{\mathbf{W}}^T\|_{2,\infty} \leq \|\hat{\mathbf{L}} - \mathbf{Z}\tilde{\mathbf{V}}\|_{2,\infty} \leq O\left(\frac{m^{3/2}\log nm}{\sqrt{n}}\right).$$

□

To support this result, we begin by stating two key Lemmas, Lemma 3 and Lemma 4. Lemma 3 gives spectral norm control on the difference between  $\tilde{\mathbf{A}}$  and  $\tilde{\mathbf{P}}$ . This will allow us to use tools from perturbation theory including Weyl's inequality to show the eigenvalues of  $\tilde{\mathbf{A}}$  are close to those of  $\tilde{\mathbf{P}}$ . Lemma 4 gives a lower bound on the growth of the eigenvalues of  $\mathbf{P}$  at a rate of  $O(n\sqrt{m})$  from which an application of the Davis-Kahan Theorem (Yu, T. Wang, and Samworth 2014) will allow us to relate the eigenvectors of  $\tilde{\mathbf{A}}$  to those of  $\tilde{\mathbf{P}}$ .

**Lemma 3.** (Adapted from Levin et al. 2017, Lemma 2) Let  $\tilde{\mathbf{A}} \in \mathbb{R}^{nm \times nm}$  be the omnibus matrix of  $\{\mathbf{A}^{(g)}\}_{g=1}^m$  where  $\{\mathbf{A}^{(g)}\}_{g=1}^m \sim \text{ESRDPG}(F, n, \{\mathbf{C}^{(g)}\}_{g=1}^m)$ . Then w.h.p.  $\|\tilde{\mathbf{A}} - \tilde{\mathbf{P}}\| \leq Cm\sqrt{n \log mn}$

**Lemma 4.** (Adapted from Levin et al. 2017, Observation 2) Let  $F$  be an inner product distribution on  $\mathbb{R}^d$  and let  $\mathbf{X}_1, \dots, \mathbf{X}_n \stackrel{i.i.d.}{\sim} F$ . Define  $\mathbf{S}^2 = \sum_{k=1}^m (\mathbf{S}^{(k)})^2$ . With probability  $1 - d^2/(nm)^2$  for all  $i \in [d]$  it holds that  $|\lambda_i(\tilde{\mathbf{P}}) - n\lambda_i(\mathbf{S}^2\Delta)| \leq Cd^2m\sqrt{n \log mn}$ . Moreover, for all  $i \in [d]$ ,  $\lambda_i(\tilde{\mathbf{P}}) \geq C\delta\sqrt{mn}$ .

*Proof.* Let  $\lambda_1 \geq \lambda_2 \geq \dots \geq \lambda_d > 0$  be the positive  $d$  eigenvalues of  $\tilde{\mathbf{P}}$ . Then  $\lambda_i(\tilde{\mathbf{P}}) = \lambda_i$  for  $i \in [d]$ . Moreover,  $\lambda_d(\tilde{\mathbf{P}}) = \lambda_d(\mathbf{L}_S \mathbf{L}_S^T) = \lambda_d(\mathbf{L}_S^T \mathbf{L}_S)$ . Notice that  $\mathbf{L}_S^T \mathbf{L}_S$  takes the form

$$\mathbf{L}_S^T \mathbf{L}_S = \sum_{k=1}^m \mathbf{S}^{(k)} \mathbf{X}^T \mathbf{X} \mathbf{S}^{(k)}$$

Next, consider

$$\left\| \sum_{k=1}^m \mathbf{S}^{(k)} [\mathbf{X}^T \mathbf{X} - n\Delta] \mathbf{S}^{(k)} \right\|_F \leq \sum_{k=1}^m \|\mathbf{S}^{(k)}\|^2 \|\mathbf{X}^T \mathbf{X} - n\Delta\|_F$$

First notice,  $(\mathbf{X}^T \mathbf{X} - n\Delta)_{ij} = \sum_{k=1}^n (\mathbf{X}_{ki} \mathbf{X}_{kj} - \Delta_{ij})$  which is a sum of bounded, i.i.d random variables. Applying Hoeffding's inequality yields

$$\mathbb{P} \left[ |\mathbf{X}^T \mathbf{X} - n\Delta|_{ij} \geq 2\sqrt{n \log mn} \right] \leq \frac{2}{n^2 m^2}$$

Therefore, applying a union bound over the matrix we have  $\|\mathbf{X}^T \mathbf{X} - n\Delta\|_F \leq 2d^2\sqrt{n \log mn}$  with high probability. Moreover, as  $\{\mathbf{S}^{(k)}\}_{k=1}^m$  is independent of  $n$  we see that  $\|\mathbf{S}^{(k)}\|^2 \leq C$ . Therefore, with high probability

$$\left\| \sum_{k=1}^m \mathbf{S}^{(k)} [\mathbf{X}^T \mathbf{X} - n\Delta] \mathbf{S}^{(k)} \right\|_F \leq \sum_{k=1}^m \|\mathbf{S}^{(k)}\|^2 \|\mathbf{X}^T \mathbf{X} - n\Delta\|_F \leq Cd^2m\sqrt{n \log mn}$$

Let  $\mathbf{S}^2 = \sum_{k=1}^m (\mathbf{S}^{(k)})^2$ . Using Weyl's inequality and bounding the spectral norm by the Frobenius norm, we have for  $i \in [d]$

$$|\lambda_i(\tilde{\mathbf{P}}) - \lambda_i(n\mathbf{S}^2\Delta)| = |\lambda_i(\mathbf{L}_S^T \mathbf{L}_S) - \lambda_i(n\mathbf{S}^2\Delta)| \leq \|\mathbf{L}_S^T \mathbf{L}_S - n\mathbf{S}^2\Delta\|_F \leq Cmd^2\sqrt{n \log mn}$$

Using this result with the reverse triangle inequality, we see that for sufficiently large  $n$

$$\lambda_i(\tilde{\mathbf{P}}) = \lambda_i(\mathbf{L}_S^T \mathbf{L}_S) \geq |n\lambda_d(\mathbf{S}^2\Delta) - Cmd^2\sqrt{n \log mn}| \geq Cn\delta \min_{i \in [d]} \mathbf{S}_{ii}^2$$

where  $\delta = \min_i \Delta_{ii} > 0$ . Notice that  $\mathbf{S}_{ii}^2 = \sum_{k=1}^m [\mathbf{S}_{ii}^{(k)}]^2$  and recall  $\alpha^{(i)} = (\mathbf{S}_{ii}^{(1)}, \dots, \mathbf{S}_{ii}^{(m)}) = \text{ASE}(\mathbf{H}(\mathbf{v}_i), 1)$ . Therefore,  $\mathbf{S}_{ii}^2 = \|\alpha^{(i)}\|_2^2$ . Recall, as  $\alpha^{(i)}$  is rank 1 adjacency spectral embedding of  $\mathbf{H}(\mathbf{v}_i)$  we have

$$\mathbf{S}_{ii}^2 = \|\alpha^{(i)}\|_2^2 = \lambda_{\max}(\mathbf{H}(\mathbf{v}_i)) = \frac{\|\mathbf{v}_i\|_1 + \sqrt{m}\|\mathbf{v}_i\|_2}{2}$$

Defining  $\lambda_* = \min_{i \in [d]} 2^{-1}(\|\mathbf{v}_i\|_1 + \sqrt{m}\|\mathbf{v}_i\|_2)$  and the fact  $\lambda_* \geq C\sqrt{m}$  and we see with high probability for  $i \in [d]$

$$\lambda_i(\tilde{\mathbf{P}}) \geq C\delta n\lambda_* \geq C\delta n\sqrt{m}$$

□

We note that this rate is slower than that presented in Levin et al. (2017) by a factor of  $\sqrt{m}$ . However, if  $\|\mathbf{v}_i\|_2 = \omega(\sqrt{m})$  then the this rate is improved to that of  $O(nm)$  consistent with that of Levin et al. (2017). A setting where this occurs is when the diagonal elements of  $\mathbf{C}^{(g)}$  are strictly positive. By allowing  $\mathbf{C}_{ii} = 0$  for all but one  $g \in [m]$ , this slower rate  $O(n\sqrt{m})$  is a direct consequence in extending the model class of the ESRDPG.

The next two results are cited directly in the proof of Theorem 1 (B). These proofs are analogous to the argument given in Vince Lyzinski et al. (2014) and Levin et al. (2017). Lemma 5 gives a concentration bound of the eigenvectors  $\mathbf{U}_{\tilde{\mathbf{P}}}^T \mathbf{U}_{\tilde{\mathbf{A}}}$  while Lemma 6 are useful Hoeffding bounds used throughout.

**Lemma 5.** (Adapted from V. Lyzinski et al. 2017, Proposition 16) Let  $\tilde{\mathbf{P}} = \mathbf{U}_{\tilde{\mathbf{P}}} \mathbf{S}_{\tilde{\mathbf{P}}} \mathbf{U}_{\tilde{\mathbf{P}}}^T - \tilde{\mathbf{U}}_{\tilde{\mathbf{P}}} \tilde{\mathbf{S}}_{\tilde{\mathbf{P}}} \tilde{\mathbf{U}}_{\tilde{\mathbf{P}}}^T$  be the eigendecomposition of  $\tilde{\mathbf{P}}$  where  $\mathbf{U}_{\tilde{\mathbf{P}}}, \tilde{\mathbf{U}}_{\tilde{\mathbf{P}}} \in \mathbb{R}^{mn \times d}$  and  $\mathbf{S}_{\tilde{\mathbf{P}}}, \tilde{\mathbf{S}}_{\tilde{\mathbf{P}}} \in \mathbb{R}^{d \times d}$  are the diagonal matrices containing the  $d$  most positive and negative eigenvalues of  $\tilde{\mathbf{P}}$ , respectively. Let  $\tilde{\mathbf{A}} = \mathbf{U}_{\tilde{\mathbf{A}}} \mathbf{S}_{\tilde{\mathbf{A}}} \mathbf{U}_{\tilde{\mathbf{A}}}^T + \tilde{\mathbf{U}}_{\tilde{\mathbf{A}}} \tilde{\mathbf{S}}_{\tilde{\mathbf{A}}} \tilde{\mathbf{U}}_{\tilde{\mathbf{A}}}^T$  be the eigendecomposition of  $\tilde{\mathbf{A}}$  where  $\mathbf{U}_{\tilde{\mathbf{A}}} \in \mathbb{R}^{mn \times d}$  and  $\mathbf{S}_{\tilde{\mathbf{A}}} \in \mathbb{R}^{d \times d}$  is the diagonal matrix containing the top  $d$  eigenvalues of  $\tilde{\mathbf{A}}$ . Lastly, let  $\mathbf{U}_{\tilde{\mathbf{P}}}^T \mathbf{U}_{\tilde{\mathbf{A}}} = \mathbf{V}_1 \tilde{\Sigma} \mathbf{V}_2^T$  be the singular value decomposition of  $\mathbf{U}_{\tilde{\mathbf{P}}}^T \mathbf{U}_{\tilde{\mathbf{A}}}$  and let  $\tilde{\mathbf{V}} = \mathbf{V}_1 \mathbf{V}_2^T$ . Then w.h.p.

$$\begin{aligned} \|\mathbf{U}_{\tilde{\mathbf{P}}}^T \mathbf{U}_{\tilde{\mathbf{A}}} - \tilde{\mathbf{V}}\|_F &\leq C \frac{dm \log nm}{n} \\ \|\tilde{\mathbf{U}}_{\tilde{\mathbf{P}}}^T \mathbf{U}_{\tilde{\mathbf{A}}}\|_F &\leq C \frac{dm \log nm}{n} \end{aligned}$$

*Proof.* Recall, by definition, that  $\tilde{\Sigma} = \text{diag}(\tilde{\sigma}_1, \dots, \tilde{\sigma}_d)$  are the singular values of the matrix  $\mathbf{U}_{\tilde{\mathbf{P}}}^T \mathbf{U}_{\tilde{\mathbf{A}}}$ . By this definition, the vector  $\Theta = (\theta_1 = \cos^{-1}(\tilde{\sigma}_1), \dots, \theta_d = \cos^{-1}(\tilde{\sigma}_d))$  contains the canonical angles between the subspace spanned by  $\mathbf{U}_{\tilde{\mathbf{P}}}$  and  $\mathbf{U}_{\tilde{\mathbf{A}}}$ . Therefore by the Davis-Kahan Theorem, as given in Yu, T. Wang, and Samworth (2014),

$$\|\mathbf{U}_{\tilde{\mathbf{A}}} \mathbf{U}_{\tilde{\mathbf{A}}}^T - \mathbf{U}_{\tilde{\mathbf{P}}} \mathbf{U}_{\tilde{\mathbf{P}}}^T\| = \max_{i \in [d]} |\sin(\theta_i)| \leq \frac{2\sqrt{d} \|\tilde{\mathbf{A}} - \tilde{\mathbf{P}}\|}{\lambda_d(\tilde{\mathbf{P}}) - \lambda_{d+1}(\tilde{\mathbf{P}})}$$

with high probability. Using the bound in Theorem 3 and the results from Lemma 4 we see that with high probability

$$\|\mathbf{U}_{\tilde{\mathbf{A}}} \mathbf{U}_{\tilde{\mathbf{A}}}^T - \mathbf{U}_{\tilde{\mathbf{P}}} \mathbf{U}_{\tilde{\mathbf{P}}}^T\| \leq C \sqrt{\frac{m \log mn}{n}}$$

With this result in mind, consider the following,

$$\begin{aligned} \|\mathbf{U}_{\tilde{\mathbf{P}}}^T \mathbf{U}_{\tilde{\mathbf{A}}} - \mathbf{V}_1 \mathbf{V}_2^T\|_F &= \|\tilde{\Sigma} - I\|_F = \sqrt{\sum_{i=1}^d (1 - \tilde{\sigma}_i)^2} \leq \sum_{i=1}^d (1 - \tilde{\sigma}_i^2) = \sum_{i=1}^d \sin^2(\theta_i) \\ &\leq d \|\mathbf{U}_{\tilde{\mathbf{A}}} \mathbf{U}_{\tilde{\mathbf{A}}}^T - \mathbf{U}_{\tilde{\mathbf{P}}} \mathbf{U}_{\tilde{\mathbf{P}}}^T\|^2 \leq Cd \frac{m \log nm}{n} \end{aligned}$$

Next, let  $\tilde{\mathbf{U}}_{\tilde{\mathbf{P}}}^T \mathbf{U}_{\tilde{\mathbf{A}}}$  have singular value decomposition  $\tilde{\mathbf{U}}_{\tilde{\mathbf{P}}}^T \mathbf{U}_{\tilde{\mathbf{A}}} = \mathbf{W}_1 \tilde{\Lambda} \mathbf{W}_2^T$ . Seeing  $\tilde{\mathbf{U}}_{\tilde{\mathbf{P}}}$  and  $\mathbf{U}_{\tilde{\mathbf{P}}}$  span orthogonal subspaces, by Property 2.1 of Zhu and Knyazev (2013),  $\tilde{\Lambda} = \text{diag}(\tilde{\lambda}_1 = \sin(\theta_d), \dots, \tilde{\lambda}_d = \sin(\theta_1))$ . Therefore, we see

$$\begin{aligned} \|\tilde{\mathbf{U}}_{\tilde{\mathbf{P}}}^T \mathbf{U}_{\tilde{\mathbf{A}}}\|_F &= \|\mathbf{W}_1 \tilde{\Lambda} \mathbf{W}_2^T\|_F = \|\tilde{\Lambda}\|_F = \sqrt{\sum_{i=1}^d \sin^2(\theta_i)} \\ &\leq \sum_{i=1}^d |\sin(\theta_i)| \leq d \|\mathbf{U}_{\tilde{\mathbf{A}}} \mathbf{U}_{\tilde{\mathbf{A}}}^T - \mathbf{U}_{\tilde{\mathbf{P}}} \mathbf{U}_{\tilde{\mathbf{P}}}^T\|^2 \leq Cd \frac{m \log nm}{n} \end{aligned}$$

□

**Lemma 6.** With the same notation above an application of Hoeffding's inequality gives with high probability

$$\begin{aligned}\|\mathbf{U}_{\tilde{\mathbf{P}}}^T(\tilde{\mathbf{A}} - \tilde{\mathbf{P}})\|_F &\leq Cm^{3/4}\sqrt{dn \log nm} \\ \|\mathbf{U}_{\tilde{\mathbf{P}}}^T(\tilde{\mathbf{A}} - \tilde{\mathbf{P}})\mathbf{U}_{\tilde{\mathbf{P}}}\|_F &\leq Cd\sqrt{m \log nm}.\end{aligned}$$

Next, we state three key Lemmas used in the proof of Theorem 1 (B). We closely follow a decomposition given in V. Lyzinski et al. (2017) and Levin et al. (2017).

**Lemma 7.** Define  $\tilde{\mathbf{V}} = \mathbf{V}_1 \mathbf{V}_2^T$  as in Lemma 5. Then with high probability

$$\begin{aligned}\|\tilde{\mathbf{V}}\mathbf{S}_{\tilde{\mathbf{A}}} - \mathbf{S}_{\tilde{\mathbf{P}}}\tilde{\mathbf{V}}\|_F &\leq Cdm \log nm \\ \|\tilde{\mathbf{V}}\mathbf{S}_{\tilde{\mathbf{A}}}^{1/2} - \mathbf{S}_{\tilde{\mathbf{P}}}^{1/2}\tilde{\mathbf{V}}\|_F &\leq C\frac{m^{3/4} \log nm}{\sqrt{n}} \\ \|\tilde{\mathbf{V}}\mathbf{S}_{\tilde{\mathbf{A}}}^{-1/2} - \mathbf{S}_{\tilde{\mathbf{P}}}^{-1/2}\tilde{\mathbf{V}}\|_F &\leq C\frac{\log nm}{n^{3/2}}\end{aligned}$$

*Proof.* First define  $\mathbf{R} = \mathbf{U}_{\tilde{\mathbf{A}}} - \mathbf{U}_{\tilde{\mathbf{P}}}\mathbf{U}_{\tilde{\mathbf{P}}}^T\mathbf{U}_{\tilde{\mathbf{A}}}$  and notice by Lemma 5 and the Davis-Kahan theorem

$$\begin{aligned}\|\mathbf{R}\|_F &= \|\mathbf{U}_{\tilde{\mathbf{A}}} - \mathbf{U}_{\tilde{\mathbf{P}}}\mathbf{U}_{\tilde{\mathbf{P}}}^T\mathbf{U}_{\tilde{\mathbf{A}}}\|_F \\ &\leq \|\mathbf{U}_{\tilde{\mathbf{A}}} - \mathbf{U}_{\tilde{\mathbf{P}}}\tilde{\mathbf{V}}\|_F + \|\mathbf{U}_{\tilde{\mathbf{P}}}(\tilde{\mathbf{V}} - \mathbf{U}_{\tilde{\mathbf{P}}}^T\mathbf{U}_{\tilde{\mathbf{A}}})\|_F \\ &\leq O\left(\sqrt{\frac{m \log mn}{n}}\right) + O\left(\frac{dm \log nm}{n}\right) \\ &= O\left(\sqrt{\frac{m \log mn}{n}}\right)\end{aligned}$$

Next, consider the following decomposition

$$\begin{aligned}\tilde{\mathbf{V}}\mathbf{S}_{\tilde{\mathbf{A}}} &= (\tilde{\mathbf{V}} - \mathbf{U}_{\tilde{\mathbf{P}}}^T\mathbf{U}_{\tilde{\mathbf{A}}})\mathbf{S}_{\tilde{\mathbf{A}}} + \mathbf{U}_{\tilde{\mathbf{P}}}^T\mathbf{U}_{\tilde{\mathbf{A}}}\mathbf{S}_{\tilde{\mathbf{A}}} \\ &= (\tilde{\mathbf{V}} - \mathbf{U}_{\tilde{\mathbf{P}}}^T\mathbf{U}_{\tilde{\mathbf{A}}})\mathbf{S}_{\tilde{\mathbf{A}}} + \mathbf{U}_{\tilde{\mathbf{P}}}^T(\tilde{\mathbf{A}} - \tilde{\mathbf{P}})\mathbf{U}_{\tilde{\mathbf{A}}} + \mathbf{U}_{\tilde{\mathbf{P}}}^T\tilde{\mathbf{P}}\mathbf{U}_{\tilde{\mathbf{A}}} \\ &= (\tilde{\mathbf{V}} - \mathbf{U}_{\tilde{\mathbf{P}}}^T\mathbf{U}_{\tilde{\mathbf{A}}})\mathbf{S}_{\tilde{\mathbf{A}}} + \mathbf{U}_{\tilde{\mathbf{P}}}^T(\tilde{\mathbf{A}} - \tilde{\mathbf{P}})\mathbf{R} + \mathbf{U}_{\tilde{\mathbf{P}}}^T(\tilde{\mathbf{A}} - \tilde{\mathbf{P}})\mathbf{U}_{\tilde{\mathbf{P}}}\mathbf{U}_{\tilde{\mathbf{P}}}^T\mathbf{U}_{\tilde{\mathbf{A}}} + \mathbf{S}_{\tilde{\mathbf{P}}}\mathbf{U}_{\tilde{\mathbf{P}}}^T\mathbf{U}_{\tilde{\mathbf{A}}}\end{aligned}$$

Rewriting this final term as  $\mathbf{S}_{\tilde{\mathbf{P}}}\mathbf{U}_{\tilde{\mathbf{P}}}^T\mathbf{U}_{\tilde{\mathbf{A}}} = \mathbf{S}_{\tilde{\mathbf{P}}}(\mathbf{U}_{\tilde{\mathbf{P}}}^T\mathbf{U}_{\tilde{\mathbf{A}}} - \tilde{\mathbf{V}}) + \mathbf{S}_{\tilde{\mathbf{P}}}\tilde{\mathbf{V}}$  we can rearrange terms and using Lemma 5 and Lemma 6 we have

$$\begin{aligned}\|\tilde{\mathbf{V}}\mathbf{S}_{\tilde{\mathbf{A}}} - \mathbf{S}_{\tilde{\mathbf{P}}}\tilde{\mathbf{V}}\|_F &\leq \|\tilde{\mathbf{V}} - \mathbf{U}_{\tilde{\mathbf{P}}}^T\mathbf{U}_{\tilde{\mathbf{A}}}\|_F(\|\mathbf{S}_{\tilde{\mathbf{A}}}\| + \|\mathbf{S}_{\tilde{\mathbf{P}}}\|) \\ &\quad + \|\mathbf{U}_{\tilde{\mathbf{P}}}^T(\tilde{\mathbf{A}} - \tilde{\mathbf{P}})\mathbf{R}\|_F \\ &\quad + \|\mathbf{U}_{\tilde{\mathbf{P}}}^T(\tilde{\mathbf{A}} - \tilde{\mathbf{P}})\mathbf{U}_{\tilde{\mathbf{P}}}\|_F\|\mathbf{U}_{\tilde{\mathbf{P}}}^T\mathbf{U}_{\tilde{\mathbf{A}}}\| \\ &\leq O(m \log n) + O\left(d^{1/2}m^{3/8} \log nm\right) + O(d\sqrt{m \log n}) \\ &= O(dm \log nm)\end{aligned}$$

Now, notice that as the  $ij$ -th entry elements of  $\tilde{\mathbf{V}}\mathbf{S}_{\tilde{\mathbf{A}}}^{1/2} - \mathbf{S}_{\tilde{\mathbf{P}}}^{1/2}\tilde{\mathbf{V}}$  can be written as

$$\tilde{\mathbf{V}}_{ij}(\lambda_i^{1/2}(\tilde{\mathbf{A}}) - \lambda_j^{1/2}(\tilde{\mathbf{P}})) = \tilde{\mathbf{V}}_{ij}\left(\frac{\lambda_i(\tilde{\mathbf{A}}) - \lambda_j(\tilde{\mathbf{P}})}{\lambda_i^{1/2}(\tilde{\mathbf{A}}) + \lambda_j^{1/2}(\tilde{\mathbf{P}})}\right)$$

Then noting that the order of the eigenvalues of  $\lambda_j^{1/2}(\tilde{\mathbf{P}})$  and  $\lambda_i^{1/2}(\tilde{\mathbf{A}})$  are of order at least  $O((n\sqrt{m})^{1/2})$ . Lastly, notice that the  $ij$ -th entry elements of  $\tilde{\mathbf{V}}\mathbf{S}_{\tilde{\mathbf{A}}}^{-1/2} - \mathbf{S}_{\tilde{\mathbf{P}}}^{-1/2}\tilde{\mathbf{V}}$  can be written as

$$\tilde{\mathbf{V}}_{ij}(\lambda_i^{-1/2}(\tilde{\mathbf{A}}) - \lambda_j^{-1/2}(\tilde{\mathbf{P}})) = \tilde{\mathbf{V}}_{ij}\left(\frac{\lambda_i^{1/2}(\tilde{\mathbf{A}}) - \lambda_j^{1/2}(\tilde{\mathbf{P}})}{-\lambda_i^{1/2}(\tilde{\mathbf{A}})\lambda_j^{1/2}(\tilde{\mathbf{P}})}\right)$$

Noting that the order of  $\lambda_i^{1/2}(\tilde{\mathbf{A}})\lambda_j^{1/2}(\tilde{\mathbf{P}})$  is at least  $O(nm^{3/4})$  concludes the proof.  $\square$

We place a bound on the remaining residual terms in Lemma 8 and Lemma 9. We do this directly following Lemma 5 in Levin et al. (2017), using Lemmas 3, 5, 6, 7 stated above. These Lemmas introduce the leading order concentration rate and the argument follows directly from the above results combined with the strategy proposed in Levin et al. 2017.

**Lemma 8.** Define  $\mathbf{R}_1 = \mathbf{U}_{\tilde{\mathbf{P}}} \mathbf{U}_{\tilde{\mathbf{P}}}^T \mathbf{U}_{\tilde{\mathbf{A}}} - \mathbf{U}_{\tilde{\mathbf{P}}} \tilde{\mathbf{V}}$ ,  $\mathbf{R}_2 = \tilde{\mathbf{V}} \mathbf{S}_{\tilde{\mathbf{A}}}^{1/2} - \mathbf{S}_{\tilde{\mathbf{P}}}^{1/2} \tilde{\mathbf{V}}$ , and  $\mathbf{R}_3 = \mathbf{U}_{\tilde{\mathbf{A}}} - \mathbf{U}_{\tilde{\mathbf{P}}} \mathbf{U}_{\tilde{\mathbf{P}}}^T \mathbf{U}_{\tilde{\mathbf{A}}} + \mathbf{R}_1$ . Then with high probability

$$\begin{aligned} \|\mathbf{R}_1 \mathbf{S}_{\tilde{\mathbf{A}}}^{1/2} + \mathbf{U}_{\tilde{\mathbf{P}}} \mathbf{R}_2\|_F &\leq \frac{Cm^{3/2} \log mn}{\sqrt{n}} \\ \|(\mathbf{I} - \mathbf{U}_{\tilde{\mathbf{P}}} \mathbf{U}_{\tilde{\mathbf{P}}}^T)(\tilde{\mathbf{A}} - \tilde{\mathbf{P}}) \mathbf{R}_3 \mathbf{S}_{\tilde{\mathbf{A}}}^{-1/2}\|_F &\leq \frac{Cm^{5/4} \log nm}{\sqrt{n}} \end{aligned}$$

**Lemma 9.** Let  $\tilde{\mathbf{P}}^{-1} = \tilde{\mathbf{U}}_{\tilde{\mathbf{P}}} \tilde{\mathbf{S}}_{\tilde{\mathbf{P}}} \tilde{\mathbf{U}}_{\tilde{\mathbf{P}}}^T \in \mathbb{R}^{nm \times nm}$  be the negative definite part of  $\tilde{\mathbf{P}}$ . Then with high probability

$$\begin{aligned} \|\tilde{\mathbf{P}}^{-1} \mathbf{U}_{\tilde{\mathbf{A}}} \mathbf{S}_{\tilde{\mathbf{A}}}^{-1/2}\|_{2,\infty} &\leq C \frac{dm \log nm}{n} \\ \|\tilde{\mathbf{P}}^{-1} \mathbf{U}_{\tilde{\mathbf{A}}} \mathbf{S}_{\tilde{\mathbf{A}}}^{-1/2}\|_F &\leq C \frac{dm^{3/2} \log nm}{\sqrt{n}} \end{aligned}$$

*Proof.* First recall that the rows of  $\tilde{\mathbf{U}}_{\tilde{\mathbf{P}}} \tilde{\mathbf{S}}_{\tilde{\mathbf{P}}}^{1/2}$  are bounded in Euclidean norm by 1. Using this fact and the fact  $\|\tilde{\mathbf{S}}_{\tilde{\mathbf{P}}}^{1/2}\| \leq C(nm)^{1/2}$  and  $\|\tilde{\mathbf{S}}_{\tilde{\mathbf{A}}}^{1/2}\| \leq C(nm)^{-1/2}$  we have

$$\|\tilde{\mathbf{U}}_{\tilde{\mathbf{P}}} \tilde{\mathbf{S}}_{\tilde{\mathbf{P}}} \tilde{\mathbf{U}}_{\tilde{\mathbf{P}}}^T \mathbf{U}_{\tilde{\mathbf{A}}} \mathbf{S}_{\tilde{\mathbf{A}}}^{-1/2}\|_{2,\infty} \leq \|\tilde{\mathbf{U}}_{\tilde{\mathbf{P}}} \tilde{\mathbf{S}}_{\tilde{\mathbf{P}}}^{1/2}\|_{2,\infty} \|\tilde{\mathbf{S}}_{\tilde{\mathbf{P}}}^{1/2}\| \|\tilde{\mathbf{U}}_{\tilde{\mathbf{P}}}^T \mathbf{U}_{\tilde{\mathbf{A}}}\| \|\mathbf{S}_{\tilde{\mathbf{A}}}^{-1/2}\| \leq C \|\tilde{\mathbf{U}}_{\tilde{\mathbf{P}}}^T \mathbf{U}_{\tilde{\mathbf{A}}}\|_F$$

Then applying Lemma 5 we have the result

$$\|\tilde{\mathbf{P}}^{-1} \mathbf{U}_{\tilde{\mathbf{A}}} \mathbf{S}_{\tilde{\mathbf{A}}}^{-1/2}\|_{2,\infty} \leq C \|\tilde{\mathbf{U}}_{\tilde{\mathbf{P}}}^T \mathbf{U}_{\tilde{\mathbf{A}}}\|_F \leq C \frac{dm \log nm}{n}.$$

We can use this result to directly establish the Frobenius norm bound.

$$\|\tilde{\mathbf{P}}^{-1} \mathbf{U}_{\tilde{\mathbf{A}}} \mathbf{S}_{\tilde{\mathbf{A}}}^{-1/2}\|_F = \sqrt{\sum_{i=1}^{nm} \|(\tilde{\mathbf{P}}^{-1} \mathbf{U}_{\tilde{\mathbf{A}}} \mathbf{S}_{\tilde{\mathbf{A}}}^{-1/2})_i\|_2^2} \leq \sqrt{nm} \|\tilde{\mathbf{P}}^{-1} \mathbf{U}_{\tilde{\mathbf{A}}} \mathbf{S}_{\tilde{\mathbf{A}}}^{-1/2}\|_{2,\infty} \leq C \frac{m^{3/2} \log nm}{\sqrt{n}}$$

$\square$

This concludes our analysis of the first moment properties of the omnibus embedding under the ESRDPG. By first studying the structure of the expected omnibus matrix  $\tilde{\mathbf{P}}$  we are able to express the omnibus embedding of  $\tilde{\mathbf{P}}$ ,  $\mathbf{Z}$ , in terms of the latent positions  $\mathbf{X}$  and the corresponding scaling matrices  $\{\mathbf{S}^{(g)}\}_{g=1}^m$  which capture the bias of the omnibus embedding. Then by demonstrating spectral bound control on the difference of  $\tilde{\mathbf{A}}$  and  $\tilde{\mathbf{P}}$  and developing a lower bound on the eigenvalues of  $\tilde{\mathbf{P}}$  we successfully employ techniques from perturbation theory, as sketched by Levin et al. (2017), to provide a uniform concentration rate of the residual term. Next, we turn our attention to the distributional properties of this residual term.

## C Second Moment

In this section we focus on the distributional properties of the residual term introduced in Theorem 1 (B). We further factor this residual into two terms, an additional residual term and a term reminiscent of the

power method. We will prove that this residual term converges in probability to 0 after being scaled by  $\sqrt{n}$ . Next, we prove that the power method term converges to a mixture of normal random variables and specify its variance explicitly. As we follow the approach introduced by Levin et al. (2017) *mutatis mutandis*, we only include proofs in which the argument was fundamentally changed by the ESRDPG model. We first prove Theorem 2; highlighting results that will be justified later in the Appendix.

*Proof of Theorem 2.* First define the second residual term  $\mathbf{R}^{(2)}$  by

$$\begin{aligned}\mathbf{R}^{(2)} &= (\tilde{\mathbf{A}} - \tilde{\mathbf{P}})\mathbf{U}_{\tilde{\mathbf{P}}} \left( \tilde{\mathbf{V}}\mathbf{S}_{\tilde{\mathbf{A}}}^{-1/2} - \mathbf{S}_{\tilde{\mathbf{P}}}^{-1/2}\tilde{\mathbf{V}} \right) - \mathbf{U}_{\tilde{\mathbf{P}}}\mathbf{U}_{\tilde{\mathbf{P}}}^T(\tilde{\mathbf{A}} - \tilde{\mathbf{P}})\mathbf{U}_{\tilde{\mathbf{P}}}\tilde{\mathbf{V}}\mathbf{S}_{\tilde{\mathbf{A}}}^{-1/2} \\ &\quad + (\mathbf{I} - \mathbf{U}_{\tilde{\mathbf{P}}}\mathbf{U}_{\tilde{\mathbf{P}}}^T)(\tilde{\mathbf{A}} - \tilde{\mathbf{P}})\mathbf{R}_3\mathbf{S}_{\tilde{\mathbf{A}}}^{-1/2} + \mathbf{R}_1\mathbf{S}_{\tilde{\mathbf{A}}}^{1/2} + \mathbf{U}_{\tilde{\mathbf{P}}}\mathbf{R}_2 - \tilde{\mathbf{U}}_{\tilde{\mathbf{P}}}\tilde{\mathbf{S}}_{\tilde{\mathbf{P}}}\tilde{\mathbf{U}}_{\tilde{\mathbf{P}}}^T\mathbf{U}_{\tilde{\mathbf{A}}}\mathbf{S}_{\tilde{\mathbf{A}}}^{-1/2}\end{aligned}$$

Then using the same decomposition we utilized in the first momement analysis we can write

$$\hat{\mathbf{L}}\mathbf{W}_n - \mathbf{L}_S = (\hat{\mathbf{L}} - \mathbf{Z}\tilde{\mathbf{V}})\tilde{\mathbf{V}}^T\tilde{\mathbf{W}}_n^T = (\tilde{\mathbf{A}} - \tilde{\mathbf{P}})\mathbf{L}_S\tilde{\mathbf{W}}_n\mathbf{S}_{\tilde{\mathbf{P}}}^{-1}\tilde{\mathbf{W}}_n^T + \mathbf{R}^{(2)}\tilde{\mathbf{V}}^T\tilde{\mathbf{W}}_n^T$$

In Lemma 10, we establish conditional on  $\{\mathbf{X}_i = \mathbf{x}_i\}$

$$\sqrt{n}[(\tilde{\mathbf{A}} - \tilde{\mathbf{P}})\mathbf{L}_S\tilde{\mathbf{W}}_n\mathbf{S}_{\tilde{\mathbf{P}}}^{-1}\tilde{\mathbf{W}}_n^T]_h | \{\mathbf{X}_i = \mathbf{x}_i\} \xrightarrow{D} N(\mathbf{0}, \Sigma_g(\mathbf{x}_i))$$

Integrating over all possible values of  $\mathbf{x}_i$  and using the Lebesgue Dominated Convergence Theorem gives for some sequence of  $\{\tilde{\mathbf{W}}_n\}_{n=1}^\infty$

$$\lim_{n \rightarrow \infty} \mathbb{P} \left[ (\tilde{\mathbf{A}} - \tilde{\mathbf{P}})\mathbf{L}_S\tilde{\mathbf{W}}_n\mathbf{S}_{\tilde{\mathbf{P}}}^{-1}\tilde{\mathbf{W}}_n^T \leq \mathbf{x} \right] = \int_{\text{supp}(F)} \Phi(\mathbf{x}; \mathbf{0}, \Sigma_g(\mathbf{y})) dF(\mathbf{y})$$

where  $\Phi(\mathbf{x}; \mu, \Sigma)$  is the normal cumulative distribution function with mean  $\mu$  and covariance matrix  $\Sigma$  evaluated at  $\mathbf{x}$  and  $\Sigma_g(\mathbf{y})$  is given in Theorem 2. As  $\tilde{\mathbf{V}}\tilde{\mathbf{W}}_n^T$  is orthogonal, it remains to show that  $\sqrt{n}\mathbf{R}_h^{(2)} \xrightarrow{\mathbb{P}} 0$ . To that end, we show each term in  $\mathbf{R}^{(2)}$  converges  $\mathbf{0}$  after being scaled by  $\sqrt{n}$  in subsequent Lemmas.

$$\begin{aligned}\sqrt{n}\mathbf{R}_h^{(n)} &= \sqrt{n}[(\tilde{\mathbf{A}} - \tilde{\mathbf{P}})\mathbf{U}_{\tilde{\mathbf{P}}}(\tilde{\mathbf{V}}\mathbf{S}_{\tilde{\mathbf{A}}}^{-1/2} - \mathbf{S}_{\tilde{\mathbf{P}}}^{-1/2}\tilde{\mathbf{V}})]_h && \text{(Lemma 11)} \\ &\quad - \sqrt{n}[\mathbf{U}_{\tilde{\mathbf{P}}}\mathbf{U}_{\tilde{\mathbf{P}}}^T(\tilde{\mathbf{A}} - \tilde{\mathbf{P}})\mathbf{U}_{\tilde{\mathbf{P}}}\tilde{\mathbf{V}}\mathbf{S}_{\tilde{\mathbf{A}}}^{-1/2}]_h && \text{(Lemma 11)} \\ &\quad + \sqrt{n}[(\mathbf{I} - \mathbf{U}_{\tilde{\mathbf{P}}}\mathbf{U}_{\tilde{\mathbf{P}}}^T)(\tilde{\mathbf{A}} - \tilde{\mathbf{P}})\mathbf{R}_3\mathbf{S}_{\tilde{\mathbf{A}}}^{-1/2}]_h && \text{(Lemma 12)} \\ &\quad + \sqrt{n}[\mathbf{R}_1\mathbf{S}_{\tilde{\mathbf{A}}}^{1/2} + \mathbf{U}_{\tilde{\mathbf{P}}}\mathbf{R}_2]_h && \text{(Lemma 11)} \\ &\quad - \sqrt{n}[\tilde{\mathbf{U}}_{\tilde{\mathbf{P}}}\tilde{\mathbf{S}}_{\tilde{\mathbf{P}}}\tilde{\mathbf{U}}_{\tilde{\mathbf{P}}}^T\mathbf{U}_{\tilde{\mathbf{A}}}\mathbf{S}_{\tilde{\mathbf{A}}}^{-1/2}]_h && \text{(Lemma 11)}\end{aligned}$$

Employing Slutsky's Theorem and combining this result with the distributional result given above concludes the proof.  $\square$

**Lemma 10.** Conditional on the event  $\{\mathbf{X}_i = \mathbf{x}_i\}$  there exists a sequence of orthogonal matrices  $\{\tilde{\mathbf{W}}_n\}_{n=1}^\infty$  such that

$$\sqrt{n}[(\tilde{\mathbf{A}} - \tilde{\mathbf{P}})\mathbf{L}_S\tilde{\mathbf{W}}_n\mathbf{S}_{\tilde{\mathbf{P}}}^{-1}\tilde{\mathbf{W}}_n^T]_h | \{\mathbf{X}_i = \mathbf{x}_i\} \xrightarrow{D} N(\mathbf{0}, \Sigma_g(\mathbf{x}_i)) \quad (7)$$

where the covariance matrix is given by

$$\Sigma_g(\mathbf{x}_i) = (\mathbf{S}^2\Delta)^{-1} \left( \left( \mathbf{S}^{(g)} + \sum_{k \neq g} \frac{1}{2}\mathbf{S}^{(k)} \right) \tilde{\Sigma}_g(\mathbf{x}_i) \left( \mathbf{S}^{(g)} + \sum_{k \neq g} \frac{1}{2}\mathbf{S}^{(k)} \right) + \frac{1}{4} \sum_{k \neq g} \mathbf{S}^{(k)} \tilde{\Sigma}_k(\mathbf{x}_i) \mathbf{S}^{(k)} \right) (\Delta\mathbf{S}^2)^{-1}$$

where  $\tilde{\Sigma}_k(\mathbf{x}_i)$  is given by

$$\tilde{\Sigma}_k(\mathbf{x}_i) = \mathbb{E} \left[ (\mathbf{x}_i^T \mathbf{C}^{(k)} \mathbf{X}_j - (\mathbf{x}_i^T \mathbf{C}^{(k)} \mathbf{X}_j)^2) \mathbf{X}_j \mathbf{X}_j^T \right]$$

*Proof.* For notational convenience, for all that follows we will condition on the event  $\{\mathbf{X}_i = \mathbf{x}_i\}$ . First notice that we can rewrite this term as follows

$$\sqrt{n}[(\tilde{\mathbf{A}} - \tilde{\mathbf{P}})\mathbf{L}_S \tilde{\mathbf{W}}_n \mathbf{S}_{\tilde{\mathbf{P}}}^{-1} \tilde{\mathbf{W}}_n^T]_h = n \tilde{\mathbf{W}}_n \mathbf{S}_{\tilde{\mathbf{P}}}^{-1} \tilde{\mathbf{W}}_n^T * \frac{1}{\sqrt{n}}[(\tilde{\mathbf{A}} - \tilde{\mathbf{P}})\mathbf{L}_S]_h$$

We will focus on each term in this product individually and then use Slutsky's Theorem to establish the result. First notice that

$$\frac{1}{n} \mathbf{L}_S^T \mathbf{L}_S = \sum_{g=1}^m \mathbf{S}^{(g)} \left( \frac{1}{n} \mathbf{X}^T \mathbf{X} \right) \mathbf{S}^{(g)}$$

By the strong law of large numbers,

$$\frac{1}{n} \mathbf{X}^T \mathbf{X} = \frac{1}{n} \sum_{j=1}^n \mathbf{X}_j \mathbf{X}_j^T = \frac{1}{n} \mathbf{x}_i \mathbf{x}_i^T + \frac{n-1}{n} * \frac{1}{n-1} \sum_{j \neq i} \mathbf{X}_j \mathbf{X}_j^T \xrightarrow{a.s.} \Delta$$

Therefore, we see that

$$\frac{1}{n} \mathbf{L}_S^T \mathbf{L}_S - \sum_{g=1}^m \mathbf{S}^{(g)} \Delta \mathbf{S}^{(g)} = \frac{1}{n} \mathbf{L}_S^T \mathbf{L}_S - \Delta \sum_{g=1}^m (\mathbf{S}^{(g)})^2 \xrightarrow{a.s.} \mathbf{0}$$

For ease of notation, let  $\mathbf{S}^2 = \sum_{g=1}^m (\mathbf{S}^{(g)})^2$ . Next, notice  $\mathbf{S}_{\tilde{\mathbf{P}}} = \mathbf{S}_{\tilde{\mathbf{P}}}^{1/2} \mathbf{U}_{\tilde{\mathbf{P}}}^T \mathbf{U}_{\tilde{\mathbf{P}}} \mathbf{S}_{\tilde{\mathbf{P}}}^{1/2} = \mathbf{Z}^T \mathbf{Z}$ . Therefore, there is a sequence of orthogonal matrices  $\{\tilde{\mathbf{W}}_n\}_{n=1}^\infty$  such that  $\tilde{\mathbf{W}}_n \mathbf{S}_{\tilde{\mathbf{P}}} \tilde{\mathbf{W}}_n^T = (\mathbf{Z} \tilde{\mathbf{W}}_n^T)^T (\mathbf{Z} \tilde{\mathbf{W}}_n^T) = \mathbf{L}_S^T \mathbf{L}_S$ . Thus, we conclude

$$\frac{1}{n} \tilde{\mathbf{W}}_n \mathbf{S}_{\tilde{\mathbf{P}}} \tilde{\mathbf{W}}_n^T - \mathbf{S}^2 \Delta \xrightarrow{a.s.} \mathbf{0}$$

Applying the continuous mapping theorem gives  $n \tilde{\mathbf{W}}_n \mathbf{S}_{\tilde{\mathbf{P}}}^{-1} \tilde{\mathbf{W}}_n^T \xrightarrow{a.s.} (\mathbf{S}^2 \Delta)^{-1}$ . Next, consider the decomposition of the power method term

$$\begin{aligned} \frac{1}{\sqrt{n}} [(\tilde{\mathbf{A}} - \tilde{\mathbf{P}})\mathbf{L}_S]_h &= \frac{1}{\sqrt{n}} \left[ \sum_{k=1}^m \left( \frac{\mathbf{A}^{(g)} - \mathbf{P}^{(g)}}{2} + \frac{\mathbf{A}^{(k)} - \mathbf{P}^{(k)}}{2} \right) \mathbf{X} \mathbf{S}^{(k)} \right]_i \\ &= \frac{1}{\sqrt{n}} \sum_{k=1}^m \mathbf{S}^{(k)} \sum_{j=1}^n \left( \frac{\mathbf{A}_{ij}^{(g)} - \mathbf{P}_{ij}^{(g)}}{2} + \frac{\mathbf{A}_{ij}^{(k)} - \mathbf{P}_{ij}^{(k)}}{2} \right) \mathbf{X}_j \\ &= \sum_{k=1}^m \mathbf{S}^{(k)} \frac{1}{\sqrt{n}} \left\{ \sum_{j \neq i} \left( \frac{\mathbf{A}_{ij}^{(g)} - \mathbf{x}_i^T \mathbf{C}^{(g)} \mathbf{X}_j}{2} + \frac{\mathbf{A}_{ij}^{(k)} - \mathbf{x}_i^T \mathbf{C}^{(k)} \mathbf{X}_j}{2} \right) \mathbf{X}_j \right\} \\ &\quad - \sum_{k=1}^m \mathbf{S}^{(k)} \frac{1}{\sqrt{n}} \left\{ \frac{\mathbf{x}_i^T \mathbf{C}^{(g)} \mathbf{x}_i}{2} + \frac{\mathbf{x}_i^T \mathbf{C}^{(k)} \mathbf{x}_i}{2} \right\} \end{aligned}$$

Notice as  $\mathbf{x}_i^T \mathbf{C}^{(g)} \mathbf{x}_i$  and  $\mathbf{x}_i^T \mathbf{C}^{(k)} \mathbf{x}_i$  are bounded by 1. Moreover, as  $\mathbf{S}^{(k)}$  is independent of  $n$  for all  $k \in [m]$

$$- \sum_{k=1}^m \mathbf{S}^{(k)} \frac{1}{\sqrt{n}} \left\{ \frac{\mathbf{x}_i^T \mathbf{C}^{(g)} \mathbf{x}_i}{2} + \frac{\mathbf{x}_i^T \mathbf{C}^{(k)} \mathbf{x}_i}{2} \right\} \xrightarrow{\mathbb{P}} \mathbf{0}$$

Focusing on this second term, notice that we can write the sum of  $n-1$  random variables as

$$\frac{1}{\sqrt{n}} \sum_{j \neq i} \left\{ \left( \mathbf{S}^{(g)} + \sum_{k \neq g} \frac{1}{2} \mathbf{S}^{(k)} \right) (\mathbf{A}_{ij}^{(g)} - \mathbf{x}_i^T \mathbf{C}^{(g)} \mathbf{X}_j) \mathbf{X}_j + \sum_{k \neq g} \frac{1}{2} \mathbf{S}^{(k)} (\mathbf{A}_{ij}^{(k)} - \mathbf{x}_i^T \mathbf{C}^{(k)} \mathbf{X}_j) \mathbf{X}_j \right\}$$

From which the the multivariate central limit theorem gives

$$\begin{aligned} \frac{1}{\sqrt{n}} \sum_{j \neq i} \left\{ \left( \mathbf{S}^{(g)} + \sum_{k \neq g} \frac{1}{2} \mathbf{S}^{(k)} \right) (\mathbf{A}_{ij}^{(g)} - \mathbf{x}_i^T \mathbf{C}^{(g)} \mathbf{X}_j) \mathbf{X}_j \right. \\ \left. + \sum_{k \neq g} \frac{1}{2} \mathbf{S}^{(k)} (\mathbf{A}_{ij}^{(k)} - \mathbf{x}_i^T \mathbf{C}^{(k)} \mathbf{X}_j) \mathbf{X}_j \right\} \xrightarrow{D} N(0, \bar{\Sigma}_g(\mathbf{x}_i)) \end{aligned}$$

where the covariance matrix is given by

$$\bar{\Sigma}_g(\mathbf{x}_i) = \left( \mathbf{S}^{(g)} + \sum_{k \neq g} \frac{1}{2} \mathbf{S}^{(k)} \right) \tilde{\Sigma}_g(\mathbf{x}_i) \left( \mathbf{S}^{(g)} + \sum_{k \neq g} \frac{1}{2} \mathbf{S}^{(k)} \right) + \frac{1}{4} \sum_{k \neq g} \mathbf{S}^{(k)} \tilde{\Sigma}_k(\mathbf{x}_i) \mathbf{S}^{(k)}$$

and  $\tilde{\Sigma}_k(\mathbf{x}_i)$  is given by

$$\tilde{\Sigma}_k(\mathbf{x}_i) = \mathbb{E} \left[ (\mathbf{x}_i^T \mathbf{C}^{(k)} \mathbf{X}_j - (\mathbf{x}_i^T \mathbf{C}^{(k)} \mathbf{X}_j)^2) \mathbf{X}_j \mathbf{X}_j^T \right]$$

Using the multivariate Slutsky's theorem then provides

$$\sqrt{n}[(\tilde{\mathbf{A}} - \tilde{\mathbf{P}}) \mathbf{L}_S \tilde{\mathbf{W}}_n \tilde{\mathbf{S}}_{\tilde{\mathbf{P}}}^{-1} \tilde{\mathbf{W}}_n^T]_h \xrightarrow{D} N(\mathbf{0}, \Sigma_g(\mathbf{x}_i))$$

where

$$\Sigma_g(\mathbf{x}_i) = (\mathbf{S}^2)^{-1} \Delta^{-1} \bar{\Sigma}_g(\mathbf{x}_i) \Delta^{-1} (\mathbf{S}^2)^{-1}$$

□

Having demonstrate the asymptotic normality of this power method term, we now turn to showing the remaining residual terms converge to zero in probability. As these Lemmas follow directly from Levin et al. (2017) and the bounds stated in Appendix B, we state then without proof and refer the reader to Levin et al. (2017).

**Lemma 11.** Let  $h = n(g-1) + i$ . Then with the notation as given in the proof of Theorem 2 we have the following convergence results.

$$\sqrt{n}[(\tilde{\mathbf{A}} - \tilde{\mathbf{P}}) \mathbf{U}_{\tilde{\mathbf{P}}} (\tilde{\mathbf{V}} \mathbf{S}_{\tilde{\mathbf{A}}}^{-1/2} - \mathbf{S}_{\tilde{\mathbf{P}}}^{-1/2} \tilde{\mathbf{V}})]_h \xrightarrow{\mathbb{P}} \mathbf{0} \quad (8)$$

$$\sqrt{n}[\mathbf{U}_{\tilde{\mathbf{P}}} \mathbf{U}_{\tilde{\mathbf{P}}}^T (\tilde{\mathbf{A}} - \tilde{\mathbf{P}}) \mathbf{U}_{\tilde{\mathbf{P}}} \tilde{\mathbf{V}} \mathbf{S}_{\tilde{\mathbf{A}}}^{-1/2}]_h \xrightarrow{\mathbb{P}} \mathbf{0} \quad (9)$$

$$\sqrt{n}[\mathbf{R}_1 \mathbf{S}_{\tilde{\mathbf{A}}}^{1/2} + \mathbf{U}_{\tilde{\mathbf{P}}} \mathbf{R}_2]_h \xrightarrow{\mathbb{P}} \mathbf{0} \quad (10)$$

$$\sqrt{n}[\tilde{\mathbf{U}}_{\tilde{\mathbf{P}}} \tilde{\mathbf{S}}_{\tilde{\mathbf{P}}} \tilde{\mathbf{U}}_{\tilde{\mathbf{P}}}^T \mathbf{U}_{\tilde{\mathbf{A}}} \mathbf{S}_{\tilde{\mathbf{A}}}^{-1/2}]_h \xrightarrow{\mathbb{P}} \mathbf{0} \quad (11)$$

**Lemma 12.** With the notation as used in the proof of Theorem 2 we have the following convergence

$$\sqrt{n}[(\mathbf{I} - \mathbf{U}_{\tilde{\mathbf{P}}} \mathbf{U}_{\tilde{\mathbf{P}}}^T) (\tilde{\mathbf{A}} - \tilde{\mathbf{P}}) \mathbf{R}_3 \mathbf{S}_{\tilde{\mathbf{A}}}^{-1/2}]_h \xrightarrow{\mathbb{P}} \mathbf{0}$$

## D Corollaries and Statistical Consequences

Included below are proofs of the Corollaries utilizing the asymptotic joint distribution of the rows of the omnibus node embeddings. These proofs largely follow direction from Theorem 1 and 2. We derive the asymptotic covariances of each set of rows explicitly as it serves as a format for the development of further estimators that utlize the rows of  $\hat{\mathbf{L}}$ .

*Proof of Corollary 1.* Define the vector  $\mathbf{R}_{r_k} = (\hat{\mathbf{L}}\tilde{\mathbf{W}}_n - \mathbf{L}_S)_{r_k} \in \mathbb{R}^d$  for a finite collection of rows indexed by  $\{r_k\}_{k=1}^K \subset [n]$ . Consider the vector

$$\mathbf{V} = [\mathbf{R}_{r_1}^T | \mathbf{R}_{r_2}^T | \dots | \mathbf{R}_{r_K}^T]^T \in \mathbb{R}^{Kd \times 1}$$

Utilizing the decomposition in the proof of Theorem 2 each  $\mathbf{R}_{r_k}$  can be written as

$$\sqrt{n}\mathbf{R}_{r_k} = \sqrt{n} \left[ (\tilde{\mathbf{A}} - \tilde{\mathbf{P}})\mathbf{L}_S \tilde{\mathbf{W}}_n \mathbf{S}_{\tilde{\mathbf{P}}}^{-1} \tilde{\mathbf{W}}_n^T \right]_{r_k} + \sqrt{n}\mathbf{R}_{r_k}^{(2)}$$

where  $\sqrt{n}\mathbf{R}_{r_k}^{(2)} \xrightarrow{\mathbb{P}} \mathbf{0}$ . Moreover, we can write the remaining term as

$$n\tilde{\mathbf{W}}_n \mathbf{S}_{\tilde{\mathbf{P}}}^{-1} \tilde{\mathbf{W}}_n^T \frac{1}{\sqrt{n}} \left[ (\tilde{\mathbf{A}} - \tilde{\mathbf{P}})\mathbf{L}_S \right]_{r_k}$$

As  $n\tilde{\mathbf{W}}_n \mathbf{S}_{\tilde{\mathbf{P}}}^{-1} \tilde{\mathbf{W}}_n^T \xrightarrow{a.s.} (\mathbf{S}^2 \Delta)^{-1}$  for each  $r_k$  we can use the multivariate Slutsky theorem as well as the distributional of the remaining term to establish the result. Suppose that each  $r_k$  can be written as  $r_k = n(g_k - 1) + i_k$  for some  $g_k \in [m]$  and  $i_k \in [n]$ . What remains is the term

$$\frac{1}{\sqrt{n}} \sum_{j=1}^n \frac{1}{2} \left\{ \left( \mathbf{S}^{(g_k)} + m\bar{\mathbf{S}} \right) (\mathbf{A}_{i_k j}^{(g_k)} - \mathbf{x}_{i_k}^T \mathbf{C}^{(g_k)} \mathbf{X}_j) \mathbf{X}_j + \sum_{\ell \neq g} \mathbf{S}^{(\ell)} (\mathbf{A}_{i_k j}^{(\ell)} - \mathbf{x}_{i_k}^T \mathbf{C}^{(\ell)} \mathbf{X}_j) \mathbf{X}_j \right\}$$

This is the term that appears in Theorem 2 and is a sum of i.i.d. mean zero random variables. Therefore, conditional on  $\{\mathbf{X}_{i_k} = \mathbf{x}_{i_k}\}$  for all  $k \in [K]$  we can apply the multivariate central limit theorem to establish asymptotic normality. The main  $d \times d$  block diagonal of this matrix is just given by variances derived in Theorem 2. Therefore, it suffices to derive the covariances off this main diagonal. Here, we need only consider the covariances when  $g_k \neq g_{k'} \in [m]$  and  $i_k \neq i_{k'}$  for  $k \neq k'$ . First, consider  $g_k \neq g_{k'}$ . The covariance for these terms are given by

$$\begin{aligned} & \mathbb{E} \left[ \text{Cov} \left( \frac{1}{2} \left\{ \left( \mathbf{S}^{(g_k)} + m\bar{\mathbf{S}} \right) (\mathbf{A}_{i_k j}^{(g_k)} - \mathbf{x}_{i_k}^T \mathbf{C}^{(g_k)} \mathbf{X}_j) \mathbf{X}_j + \sum_{\ell \neq g_k} \mathbf{S}^{(\ell)} (\mathbf{A}_{i_k j}^{(\ell)} - \mathbf{x}_{i_k}^T \mathbf{C}^{(\ell)} \mathbf{X}_j) \mathbf{X}_j \right\}, \right. \right. \\ & \quad \left. \left. \frac{1}{2} \left\{ \left( \mathbf{S}^{(g_{k'})} + m\bar{\mathbf{S}} \right) (\mathbf{A}_{i_{k'} j}^{(g_{k'})} - \mathbf{x}_{i_{k'}}^T \mathbf{C}^{(g_{k'})} \mathbf{X}_j) \mathbf{X}_j + \sum_{\ell \neq g_{k'}} \mathbf{S}^{(\ell)} (\mathbf{A}_{i_{k'} j}^{(\ell)} - \mathbf{x}_{i_{k'}}^T \mathbf{C}^{(\ell)} \mathbf{X}_j) \mathbf{X}_j \right\} \middle| \mathbf{X}_j \right) \right] \\ &= \frac{1}{4} \mathbb{E} \left[ (\mathbf{S}^{(g_k)} + m\bar{\mathbf{S}}) \mathbf{X}_j \text{Cov}(\mathbf{A}_{i_k j}^{(g_k)}, \mathbf{A}_{i_{k'} j}^{(g_{k'})} | \mathbf{X}_j) \mathbf{X}_j^T (\mathbf{S}^{(g_{k'})} + m\bar{\mathbf{S}}) \right] \\ &+ \frac{1}{4} \mathbb{E} \left[ (\mathbf{S}^{(g_k)} + m\bar{\mathbf{S}}) \mathbf{X}_j \sum_{\ell \neq g_{k'}} \text{Cov}(\mathbf{A}_{i_k j}^{(g_k)}, \mathbf{A}_{i_{k'} j}^{(\ell)} | \mathbf{X}_j) \mathbf{X}_j^T \mathbf{S}^{(\ell)} \right] \\ &+ \frac{1}{4} \mathbb{E} \left[ \sum_{\ell \neq g_k} \mathbf{S}^{(\ell)} \mathbf{X}_j \text{Cov}(\mathbf{A}_{i_k j}^{(\ell)}, \mathbf{A}_{i_{k'} j}^{(g_{k'})} | \mathbf{X}_j) \mathbf{X}_j^T (m\bar{\mathbf{S}} + \mathbf{S}^{(g_{k'})}) \right] \\ &+ \frac{1}{4} \sum_{\ell \neq g_k} \sum_{\ell' \neq g_{k'}} \mathbb{E} \left[ \mathbf{S}^{(\ell)} \mathbf{X}_j \text{Cov}(\mathbf{A}_{i_k j}^{(\ell)}, \mathbf{A}_{i_{k'} j}^{(\ell')} | \mathbf{X}_j) \mathbf{X}_j^T \mathbf{S}^{(\ell')} \right] \\ &= \frac{1}{4} (\mathbf{S}^{(g_k)} + m\bar{\mathbf{S}}) \tilde{\Sigma}_{g_k}(\mathbf{x}_{i_k}) (\mathbf{S}^{(g_k)}) + \mathbf{S}^{(g_{k'})} \tilde{\Sigma}_{g_{k'}}(\mathbf{x}_{i_k}) (m\bar{\mathbf{S}} + \mathbf{S}^{(g_{k'})}) + \frac{1}{2} \sum_{\ell \neq g_k, g_{k'}} \mathbf{S}^{(\ell)} \tilde{\Sigma}_\ell(\mathbf{x}_{i_k}) \mathbf{S}^{(\ell)} \end{aligned}$$

Therefore, we see the rows of  $\hat{\mathbf{L}}$  corresponding to vertex  $x_{i_k}$  are correlated with the above covariance pre and post multiplied by  $(\mathbf{S}^2 \Delta)^{-1}$ . Next, consider the setting where  $i_k \neq i_{k'}$  and  $g_k = g_{k'} = g$ . Then we look

to calculate the covariance

$$\begin{aligned}
& \mathbb{E} \left[ \text{Cov} \left( \frac{1}{2} \left\{ \left( \mathbf{S}^{(g)} + m\bar{\mathbf{S}} \right) (\mathbf{A}_{i_k j}^{(g)} - \mathbf{x}_{i_k}^T \mathbf{C}^{(g)} \mathbf{X}_j) \mathbf{X}_j + \sum_{\ell \neq g} \mathbf{S}^{(\ell)} (\mathbf{A}_{i_k j}^{(\ell)} - \mathbf{x}_{i_k}^T \mathbf{C}^{(\ell)} \mathbf{X}_j) \mathbf{X}_j \right\}, \right. \right. \\
& \quad \left. \left. \frac{1}{2} \left\{ \left( \mathbf{S}^{(g)} + m\bar{\mathbf{S}} \right) (\mathbf{A}_{i_{k'} j}^{(g)} - \mathbf{x}_{i_{k'}}^T \mathbf{C}^{(g)} \mathbf{X}_j) \mathbf{X}_j + \sum_{\ell \neq g} \mathbf{S}^{(\ell)} (\mathbf{A}_{i_{k'} j}^{(\ell)} - \mathbf{x}_{i_{k'}}^T \mathbf{C}^{(\ell)} \mathbf{X}_j) \mathbf{X}_j \right\} \mid \mathbf{X}_j \right) \right] \\
& = \frac{1}{4} \mathbb{E} \left[ (\mathbf{S}^{(g)} + m\bar{\mathbf{S}}) \text{Cov}(\mathbf{A}_{i_k j}^{(g)}, \mathbf{A}_{i_{k'} j}^{(g)} \mid \mathbf{X}_j) \mathbf{X}_j^T (\mathbf{S}^{(g)} + m\bar{\mathbf{S}}) \right] \\
& \quad + \frac{1}{4} \mathbb{E} \left[ (\mathbf{S}^{(g)} + m\bar{\mathbf{S}}) \mathbf{X}_j \sum_{\ell \neq g} \text{Cov}(\mathbf{A}_{i_k j}^{(g)}, \mathbf{A}_{i_{k'} j}^{(\ell)} \mid \mathbf{X}_j) \mathbf{X}_j^T \mathbf{S}^{(\ell)} \right] \\
& \quad + \frac{1}{4} \mathbb{E} \left[ \sum_{\ell \neq g} \mathbf{S}^{(\ell)} \mathbf{X}_j \text{Cov}(\mathbf{A}_{i_k j}^{(\ell)}, \mathbf{A}_{i_{k'} j}^{(g)} \mid \mathbf{X}_j) \mathbf{X}_j^T (m\bar{\mathbf{S}} + \mathbf{S}^{(g)}) \right] \\
& \quad + \frac{1}{4} \sum_{\ell \neq g} \sum_{\ell' \neq g} \mathbb{E} \left[ \mathbf{S}^{(\ell)} \mathbf{X}_j \text{Cov}(\mathbf{A}_{i_k j}^{(\ell)}, \mathbf{A}_{i_{k'} j}^{(\ell')} \mid \mathbf{X}_j) \mathbf{X}_j^T \mathbf{S}^{(\ell')} \right] \\
& = 0
\end{aligned}$$

Therefore, we see that rows of  $\hat{\mathbf{L}}$  that correspond to different vertices are asymptotically independent. These two covariance results characterize the joint distribution of the rows of  $\hat{\mathbf{L}}$ .  $\square$

*Proof of Corollary 2.* Utilizing the same decomposition as in Theorem 2, we can write

$$\begin{aligned}
\sqrt{n} [\bar{\mathbf{X}} \mathbf{W}_n - \mathbf{X} \bar{\mathbf{S}}]_i &= \sqrt{n} \frac{1}{m} \sum_{g=1}^m \left( \hat{\mathbf{X}}_{\text{Omn}}^{(g)} \mathbf{W}_n - \mathbf{X} \mathbf{S}^{(g)} \right)_i \\
&= \frac{1}{m} \sum_{g=1}^m \left\{ \sqrt{n} \left[ (\tilde{\mathbf{A}} - \tilde{\mathbf{P}}) \mathbf{L}_S \tilde{\mathbf{W}}_n \mathbf{S}_{\tilde{\mathbf{P}}}^{-1} \tilde{\mathbf{W}}_n^T \right]_{i+n(g-1)} \right\} \\
&\quad + \frac{1}{m} \sum_{g=1}^m \sqrt{n} \mathbf{R}_{i+n(g-1)}^{(2)}
\end{aligned}$$

From the proof of Theorem 2,  $\sqrt{n} \mathbf{R}_{i+n(g-1)}^{(2)} \xrightarrow{\mathbb{P}} \mathbf{0}$ . Expanding the remaining term, we have

$$\frac{1}{m} \sum_{g=1}^m \left\{ \sqrt{n} \left[ (\tilde{\mathbf{A}} - \tilde{\mathbf{P}}) \mathbf{L}_S \tilde{\mathbf{W}}_n \mathbf{S}_{\tilde{\mathbf{P}}}^{-1} \tilde{\mathbf{W}}_n^T \right]_{i+n(g-1)} \right\} = n \tilde{\mathbf{W}}_n \mathbf{S}_{\tilde{\mathbf{P}}}^{-1} \tilde{\mathbf{W}}_n^T \frac{1}{m} \sum_{g=1}^m \left\{ \frac{1}{\sqrt{n}} \left[ (\tilde{\mathbf{A}} - \tilde{\mathbf{P}}) \mathbf{L}_S \right]_{i+n(g-1)} \right\}$$

From our proof of Theorem 2,  $n \tilde{\mathbf{W}}_n \mathbf{S}_{\tilde{\mathbf{P}}}^{-1} \tilde{\mathbf{W}}_n^T \xrightarrow{a.s.} (\mathbf{S}^2 \Delta)^{-1}$ . All that remains is analyzing this sum of power method terms. As we did above, condition on the event  $\{\mathbf{X}_i = \mathbf{x}_i\}$ .

$$\begin{aligned}
\frac{1}{m} \sum_{g=1}^m \left\{ \frac{1}{\sqrt{n}} \left[ (\tilde{\mathbf{A}} - \tilde{\mathbf{P}}) \mathbf{L}_S \right]_{i+n(g-1)} \right\} &= \frac{1}{m} \sum_{g=1}^m \frac{1}{\sqrt{n}} \left\{ \sum_{\ell=1}^m \mathbf{S}^{(\ell)} \sum_{j=1}^n \left( \frac{\mathbf{A}_{ij}^{(g)} - \mathbf{P}_{ij}^{(g)}}{2} + \frac{\mathbf{A}_{ij}^{(\ell)} - \mathbf{P}_{ij}^{(\ell)}}{2} \right) \mathbf{X}_j \right\} \\
&= \frac{1}{\sqrt{n}} \sum_{j \neq i} \left\{ \frac{1}{m} \sum_{g=1}^m \sum_{\ell=1}^m \mathbf{S}^{(\ell)} \left( \frac{\mathbf{A}_{ij}^{(g)} - \mathbf{x}_i^T \mathbf{C}^{(g)} \mathbf{X}_j}{2} + \frac{\mathbf{A}_{ij}^{(\ell)} - \mathbf{x}_i^T \mathbf{C}^{(\ell)} \mathbf{X}_j}{2} \right) \mathbf{X}_j \right\} \\
&\quad - \frac{1}{\sqrt{n}} \left\{ \frac{1}{m} \sum_{g=1}^m \sum_{\ell=1}^m \mathbf{S}^{(\ell)} \left( \frac{\mathbf{x}_i^T \mathbf{C}^{(g)} \mathbf{x}_i}{2} + \frac{\mathbf{x}_i^T \mathbf{C}^{(\ell)} \mathbf{x}_i}{2} \right) \mathbf{x}_i \right\}
\end{aligned}$$

Letting  $n \rightarrow \infty$ , we see this second term converges in probability to zero. That is

$$-\frac{1}{\sqrt{n}} \left\{ \frac{1}{m} \sum_{g=1}^m \sum_{\ell=1}^m \mathbf{S}^{(\ell)} \left( \frac{\mathbf{x}_i^T \mathbf{C}^{(g)} \mathbf{x}_i}{2} + \frac{\mathbf{x}_i^T \mathbf{C}^{(\ell)} \mathbf{x}_i}{2} \right) \mathbf{x}_i \right\} \xrightarrow{\mathbb{P}} \mathbf{0}$$

Rearranging terms in the remaining terms we have

$$\begin{aligned} & \frac{1}{\sqrt{n}} \sum_{j \neq i} \left\{ \frac{1}{m} \sum_{g=1}^m \sum_{\ell=1}^m \mathbf{S}^{(\ell)} \left( \frac{\mathbf{A}_{ij}^{(g)} - \mathbf{x}_i^T \mathbf{C}^{(g)} \mathbf{X}_j}{2} + \frac{\mathbf{A}_{ij}^{(\ell)} - \mathbf{x}_i^T \mathbf{C}^{(\ell)} \mathbf{X}_j}{2} \right) \mathbf{X}_j \right\} \\ &= \frac{1}{\sqrt{n}} \sum_{j \neq i} \left\{ \sum_{g=1}^m \left( \frac{1}{2m} \sum_{\ell \neq g} \mathbf{S}^{(\ell)} + \frac{m+1}{2m} \mathbf{S}^{(g)} \right) (\mathbf{A}_{ij}^{(g)} - \mathbf{x}_i^T \mathbf{C}^{(g)} \mathbf{X}_j) \mathbf{X}_j \right\} \end{aligned}$$

This is a sum of  $n-1$  random variables which by the multivariate central limit theorem gives implies this sum converges in distribution to a normal random variable with variance given by

$$\begin{aligned} & \text{Var} \left( \sum_{g=1}^m \left( \frac{1}{2m} \sum_{\ell \neq g} \mathbf{S}^{(\ell)} + \frac{m+1}{2m} \mathbf{S}^{(g)} \right) (\mathbf{A}_{ij}^{(g)} - \mathbf{x}_i^T \mathbf{C}^{(g)} \mathbf{X}_j) \mathbf{X}_j \right) \\ &= \mathbb{E} \left[ \text{Var} \left( \sum_{g=1}^m \left( \frac{1}{2m} \sum_{\ell \neq g} \mathbf{S}^{(\ell)} + \frac{m+1}{2m} \mathbf{S}^{(g)} \right) (\mathbf{A}_{ij}^{(g)} - \mathbf{x}_i^T \mathbf{C}^{(g)} \mathbf{X}_j) \mathbf{X}_j \mid \mathbf{X}_j \right) \right] \\ &= \sum_{g=1}^m \left( \frac{1}{2m} \sum_{\ell \neq g} \mathbf{S}^{(\ell)} + \frac{m+1}{2m} \mathbf{S}^{(g)} \right) \tilde{\Sigma}_g(\mathbf{x}_i) \left( \frac{1}{2m} \sum_{\ell \neq g} \mathbf{S}^{(\ell)} + \frac{m+1}{2m} \mathbf{S}^{(g)} \right) \end{aligned}$$

□

*Proof of Corollary 3.* Conditional on a vertices community under the RDPG is equivalent with conditioning on a community's latent vector. Conditional on this event, the event  $\{\mathbf{X}_i = \mathbf{x}_i\}$ , the distribution of  $\mathbf{X}_i$  reduces to a point mass over  $\mathbf{x}_i$ . Therefore, when integrating in the final step of the proof of Theorem 2 is equivalent to evaluating the normal cumulative distribution at  $\mathbf{x}_i$ . This is the statement given in Corollary 3. □

*Proof of Corollary 4.* Utilizing the same decomposition as in Theorem 2, we can write

$$\begin{aligned} \sqrt{n}(\hat{\mathbf{L}}\mathbf{W}_n - \mathbf{L}_S)_{r_g} - \sqrt{n}(\hat{\mathbf{L}}\mathbf{W}_n - \mathbf{L}_S)_{r_k} &= \sqrt{n} \left[ (\tilde{\mathbf{A}} - \tilde{\mathbf{P}})\mathbf{L}_S \tilde{\mathbf{W}}_n \mathbf{S}_{\tilde{\mathbf{P}}}^{-1} \tilde{\mathbf{W}}_n^T \right]_{r_g} \\ &\quad - \sqrt{n} \left[ (\tilde{\mathbf{A}} - \tilde{\mathbf{P}})\mathbf{L}_S \tilde{\mathbf{W}}_n \mathbf{S}_{\tilde{\mathbf{P}}}^{-1} \tilde{\mathbf{W}}_n^T \right]_{r_k} \\ &\quad + \sqrt{n}\mathbf{R}_{r_g}^{(2)} - \sqrt{n}\mathbf{R}_{r_k}^{(2)} \end{aligned}$$

From the proof of Theorem 2,  $\sqrt{n}\mathbf{R}_{r_g}^{(2)} \xrightarrow{\mathbb{P}} \mathbf{0}$  and  $\sqrt{n}\mathbf{R}_{r_k}^{(2)} \xrightarrow{\mathbb{P}} \mathbf{0}$ . Expanding the remaining term, we have

$$\sqrt{n} \left[ (\hat{\mathbf{L}}\mathbf{W}_n - \mathbf{L}_S)_{r_g} - (\hat{\mathbf{L}}\mathbf{W}_n - \mathbf{L}_S)_{r_k} \right] = n \tilde{\mathbf{W}}_n \mathbf{S}_{\tilde{\mathbf{P}}}^{-1} \tilde{\mathbf{W}}_n^T \frac{1}{\sqrt{n}} \left\{ \left[ (\tilde{\mathbf{A}} - \tilde{\mathbf{P}})\mathbf{L}_S \right]_{r_g} - \left[ (\tilde{\mathbf{A}} - \tilde{\mathbf{P}})\mathbf{L}_S \right]_{r_k} \right\}$$

From our proof of Theorem 2,  $n \tilde{\mathbf{W}}_n \mathbf{S}_{\tilde{\mathbf{P}}}^{-1} \tilde{\mathbf{W}}_n^T \xrightarrow{a.s.} (\mathbf{S}^2 \Delta)^{-1}$ . All that remains is analyzing this difference of power method terms. As we did in the proof of Theorem 2, condition on the event  $\{\mathbf{X}_i = \mathbf{x}_i\}$  and consider

the following

$$\begin{aligned}
& \frac{1}{\sqrt{n}} \left\{ \left[ (\tilde{\mathbf{A}} - \tilde{\mathbf{P}}) \mathbf{L}_S \right]_{r_g} - \left[ (\tilde{\mathbf{A}} - \tilde{\mathbf{P}}) \mathbf{L}_S \right]_{r_k} \right\} \\
&= \frac{1}{\sqrt{n}} \sum_{j=1}^n \left\{ \left( \sum_{\ell=1}^m \mathbf{S}^{(\ell)} \right) \left( \frac{\mathbf{A}_{ij}^{(g)} - \mathbf{x}_i^T \mathbf{C}^{(g)} \mathbf{X}_j}{2} - \frac{\mathbf{A}_{ij}^{(k)} - \mathbf{x}_i^T \mathbf{C}^{(k)} \mathbf{X}_j}{2} \right) \right\} \\
&= \frac{1}{\sqrt{n}} \sum_{j \neq i} \left\{ \left( \sum_{\ell=1}^m \mathbf{S}^{(\ell)} \right) \left( \frac{\mathbf{A}_{ij}^{(g)} - \mathbf{x}_i^T \mathbf{C}^{(g)} \mathbf{X}_j}{2} - \frac{\mathbf{A}_{ij}^{(k)} - \mathbf{x}_i^T \mathbf{C}^{(k)} \mathbf{X}_j}{2} \right) \mathbf{X}_j \right\} \\
&\quad - \frac{1}{\sqrt{n}} \left\{ \left( \sum_{\ell=1}^m \mathbf{S}^{(\ell)} \right) \left( \frac{\mathbf{x}_i^T \mathbf{C}^{(g)} \mathbf{x}_i}{2} - \frac{\mathbf{x}_i^T \mathbf{C}^{(k)} \mathbf{x}_i}{2} \right) \mathbf{x}_i \right\}
\end{aligned}$$

Letting  $n \rightarrow \infty$ , we see this second term converges in probability to zero. That is

$$-\frac{1}{\sqrt{n}} \left\{ \left( \sum_{\ell=1}^m \mathbf{S}^{(\ell)} \right) \left( \frac{\mathbf{x}_i^T \mathbf{C}^{(g)} \mathbf{x}_i}{2} - \frac{\mathbf{x}_i^T \mathbf{C}^{(k)} \mathbf{x}_i}{2} \right) \mathbf{x}_i \right\} \xrightarrow{\mathbb{P}} \mathbf{0}$$

Considering the remaining terms, we see that

$$\frac{1}{\sqrt{n}} \sum_{j \neq i} \left\{ \left( \sum_{\ell=1}^m \mathbf{S}^{(\ell)} \right) \left( \frac{\mathbf{A}_{ij}^{(g)} - \mathbf{x}_i^T \mathbf{C}^{(g)} \mathbf{X}_j}{2} - \frac{\mathbf{A}_{ij}^{(k)} - \mathbf{x}_i^T \mathbf{C}^{(k)} \mathbf{X}_j}{2} \right) \mathbf{X}_j \right\}$$

is a sum of  $n-1$  random variables which by the multivariate central limit theorem implies this sum converges in distribution to a normal random variable with variance given by

$$\begin{aligned}
& \text{Var} \left( \left( \sum_{\ell=1}^m \mathbf{S}^{(\ell)} \right) \left( \frac{\mathbf{A}_{ij}^{(g)} - \mathbf{x}_i^T \mathbf{C}^{(g)} \mathbf{X}_j}{2} - \frac{\mathbf{A}_{ij}^{(k)} - \mathbf{x}_i^T \mathbf{C}^{(k)} \mathbf{X}_j}{2} \right) \mathbf{X}_j \right) \\
&= \left( \sum_{\ell=1}^m \mathbf{S}^{(\ell)} \right) \mathbb{E} \left[ \text{Var} \left( \left( \frac{\mathbf{A}_{ij}^{(g)} - \mathbf{x}_i^T \mathbf{C}^{(g)} \mathbf{X}_j}{2} - \frac{\mathbf{A}_{ij}^{(k)} - \mathbf{x}_i^T \mathbf{C}^{(k)} \mathbf{X}_j}{2} \right) \mathbf{X}_j \middle| \mathbf{X}_j \right) \right] \left( \sum_{\ell=1}^m \mathbf{S}^{(\ell)} \right) \\
&= \left( \sum_{\ell=1}^m \mathbf{S}^{(\ell)} \right) \left[ \frac{\tilde{\Sigma}_g(\mathbf{x}_i) + \tilde{\Sigma}_k(\mathbf{x}_i)}{4} \right] \left( \sum_{\ell=1}^m \mathbf{S}^{(\ell)} \right)
\end{aligned}$$

Therefore, we see that the full variance is given by

$$\Sigma_D(\mathbf{x}_i) = (\mathbf{S}^2 \Delta)^{-1} \left( \sum_{\ell=1}^m \mathbf{S}^{(\ell)} \right) \left[ \frac{\tilde{\Sigma}_g(\mathbf{x}_i) + \tilde{\Sigma}_k(\mathbf{x}_i)}{4} \right] \left( \sum_{\ell=1}^m \mathbf{S}^{(\ell)} \right) (\mathbf{S}^2 \Delta)^{-1}$$

Integrating over all possible values of  $\mathbf{x}_i$  gives the result.  $\square$

*Proof of Theorem 3.* Theorem 1 and Theorem 2 establish the asymptotic distribution of the rows of  $\hat{\mathbf{L}}$

$$(\hat{\mathbf{L}} \mathbf{W}_n)_h = \mathbf{S}^{(g)} \mathbf{X}_i + [(\tilde{\mathbf{A}} - \tilde{\mathbf{P}}) \mathbf{L}_S \tilde{\mathbf{W}}_n \mathbf{S}_{\tilde{\mathbf{P}}}^{-1} \tilde{\mathbf{W}}_n^T]_h + \mathbf{W}_n \mathbf{R}_h^{(2)}.$$

Define  $\mathbf{N}_h = [(\tilde{\mathbf{A}} - \tilde{\mathbf{P}}) \mathbf{L}_S \tilde{\mathbf{W}}_n \mathbf{S}_{\tilde{\mathbf{P}}}^{-1} \tilde{\mathbf{W}}_n^T]_h = \tilde{\mathbf{W}}_n \mathbf{S}_{\tilde{\mathbf{P}}}^{-1} \tilde{\mathbf{W}}_n^T [(\tilde{\mathbf{A}} - \tilde{\mathbf{P}}) \mathbf{L}_S]_h$  and express the statistic  $\hat{\mathbf{D}}_i = (\hat{\mathbf{X}}_{\text{Omn}}^{(1)})_i - (\hat{\mathbf{X}}_{\text{Omn}}^{(2)})_{n+i}$  as

$$(\hat{\mathbf{D}} \mathbf{W}_n)_i = (\mathbf{S}^{(1)} - \mathbf{S}^{(2)}) \mathbf{X}_i + (\mathbf{N}_i - \mathbf{N}_{n+i}) + \mathbf{W}_n (\mathbf{R}_i^{(2)} - \mathbf{R}_{n+i}^{(2)}).$$

Corollary 4 establishes that the asymptotic distribution of  $\sqrt{n}[\hat{\mathbf{D}}\mathbf{W}_n - \mathbf{X}(\mathbf{S}^{(1)} - \mathbf{S}^{(2)})]_i$  is a mixture of normal random variables with covariance given by  $\Sigma_D(\mathbf{X}_i)$ . This inspires the test statistic  $W_i = \hat{\mathbf{D}}_i^T \Sigma_D^{-1}(\mathbf{X}_i) \hat{\mathbf{D}}_i$ . Under  $H_0$ ,  $\mathbf{S}^{(1)} = \mathbf{S}^{(2)}$  and  $W_i$  takes the form

$$\begin{aligned} W_i &= \mathbf{W}_n^T W_i \mathbf{W}_n = (\mathbf{N}_i - \mathbf{N}_{n+i})^T \Sigma_D^{-1}(\mathbf{X}_i) (\mathbf{N}_i - \mathbf{N}_{n+i}) \\ &\quad + 2(\mathbf{N}_i - \mathbf{N}_{n+i})^T \Sigma_D^{-1}(\mathbf{X}_i) (\mathbf{R}_i^{(2)} - \mathbf{R}_{n+i}^{(2)}) \\ &\quad + (\mathbf{R}_i^{(2)} - \mathbf{R}_{n+i}^{(2)})^T \Sigma_D^{-1}(\mathbf{X}_i) (\mathbf{R}_i^{(2)} - \mathbf{R}_{n+i}^{(2)}). \end{aligned}$$

Corollary 4 establishes that  $\sqrt{n}(\mathbf{N}_i - \mathbf{N}_{n+i})$  converges in distribution to a mixture of normal random variables. Moreover, results in Appendix C establishes  $\sqrt{n}\mathbf{R}_i^{(2)} \xrightarrow{\mathbb{P}} 0$ . These results, the fact that  $\Sigma_D^{-1}(\mathbf{X}_i)$  is bounded in  $n$ , and Slutsky's Theorem gives

$$\begin{aligned} n \left[ 2(\mathbf{N}_i - \mathbf{N}_{n+i})^T \Sigma_D^{-1}(\mathbf{X}_i) (\mathbf{R}_i^{(2)} - \mathbf{R}_{n+i}^{(2)}) \right] &\xrightarrow{\mathbb{P}} 0 \\ n \left[ (\mathbf{R}_i^{(2)} - \mathbf{R}_{n+i}^{(2)})^T \Sigma_D^{-1}(\mathbf{X}_i) (\mathbf{R}_i^{(2)} - \mathbf{R}_{n+i}^{(2)}) \right] &\xrightarrow{\mathbb{P}} 0. \end{aligned}$$

All that remains is analyzing the behaviour of  $[\sqrt{n}\Sigma_D^{-1/2}(\mathbf{X}_i)(\mathbf{N}_i - \mathbf{N}_{n+i})]^T [\sqrt{n}\Sigma_D^{-1/2}(\mathbf{X}_i)(\mathbf{N}_i - \mathbf{N}_{n+i})]$ . Corollary 4 establishes that  $\sqrt{n}\Sigma_D^{-1/2}(\mathbf{X}_i)(\mathbf{N}_i - \mathbf{N}_{n+i}) \xrightarrow{D} N(0, \mathbf{I})$ . Therefore, by the second order Delta Method,

$$n(\mathbf{N}_i - \mathbf{N}_{n+i})^T \Sigma_D^{-1}(\mathbf{X}_i) (\mathbf{N}_i - \mathbf{N}_{n+i}) \xrightarrow{D} \chi_d^2$$

Under the alternative hypothesis,  $\mathbf{C}^{(1)} \neq \mathbf{C}^{(2)}$  and by Proposition B.1  $\mathbf{S}^{(1)} \neq \mathbf{S}^{(2)}$ . Following a similar analysis as above, the results from Appendix B and Appendix C with Slutsky's Theorem and Corollary 4 gives

$$\begin{aligned} &\lim_{n \rightarrow \infty} \mathbb{P} \left[ \sqrt{n}(W_i - \mathbf{X}_i^T (\mathbf{S}^{(1)} - \mathbf{S}^{(2)})^T \Sigma_D^{-1}(\mathbf{X}_i) (\mathbf{S}^{(1)} - \mathbf{S}^{(2)}) \mathbf{X}_i) \leq x \right] \\ &= \lim_{n \rightarrow \infty} \mathbb{P} \left[ \sqrt{n}(2\mathbf{X}_i^T (\mathbf{S}^{(1)} - \mathbf{S}^{(2)})^T \Sigma_D^{-1}(\mathbf{X}_i) (\mathbf{N}_i - \mathbf{N}_{n+i})) \leq x \right] \\ &= \int_{\text{supp}(F)} \Phi(x; 0, 4\mathbf{y}^T (\mathbf{S}^{(1)} - \mathbf{S}^{(2)})^T \Sigma_D^{-1}(\mathbf{y}) (\mathbf{S}^{(1)} - \mathbf{S}^{(2)}) \mathbf{y}) dF(\mathbf{y}). \end{aligned}$$

□